Intrinsic heterogeneity in the survival and proliferation capacities of naïve CD8$^+$ T cells

by

Vinay Subhash Mahajan

M.B.B.S, All India Institute of Medical Sciences (2002)

Submitted to the Department of Biological Engineering
in partial fulfillment of the requirements for the degree of

Doctor of Philosophy in Applied Biosciences

at the

MASSACHUSETTS INSTITUTE OF TECHNOLOGY

June 2009

Author .....
Department of Biological Engineering
May 15, 2009

Certified by .....
Darrell J. Irvine
Associate Professor
Thesis Supervisor

Certified by .....
Jianzhu Chen
Professor
Thesis Supervisor

Accepted by .....
Alan Grodzinsky
Chairman, Department Committee on Graduate Theses

Intrinsic heterogeneity in the survival and proliferation capacities of naïve CD8$^+$ T cells

by

Vinay Subhash Mahajan

Submitted to the Department of Biological Engineering
on May 15, 2009, in partial fulfillment of the
requirements for the degree of
Doctor of Philosophy in Applied Biosciences

Abstract

This thesis describes the identification and characterization of a novel 'layer' of intrinsic non-genetic functional heterogeneity within the seemingly homogeneous naïve CD8$^+$ T cell population in their survival and proliferation capacities. This heterogeneity is predictably marked by the surface level of CD5. Naïve CD8$^+$ T cells that are also CD5^{hi} have a greater intrinsic capacity to proliferate both in response to IL7 alone or identical stimulation of the TCR pathway (same dose of PMA/ionomycin) as compared to CD5^{lo} cells. In contrast, CD5^{lo} cells survive better in conditions of cytokine deprivation. The selective proliferation in response to IL7 as well as the relative CD5 level is preserved even after several rounds of activation-induced proliferation and differentiation into memory-like cells *in vitro*, suggesting that the relative CD5 level could be used as a lineage marker to predict the proliferation capacity of CD8$^+$ T cells. Microarray analysis of two naïve TCR transgenic CD8$^+$ T cells, from the same genetic background, but with marked differences in CD5 levels, namely OT-1 and F5 Rag$^{-/-}$ T cells, revealed consistent differerences in their cell survival, proliferation and metabolic pathways. Analysis of upstream regulatory networks suggests that the E2A family of transcription factors and miR-181 are likely involved in setting the proliferation and survival capacities of naïve T cells, possibly during thymic development. Our estimates of spMHC-induced signals in OT-1 (CD5^{hi}) and F5 (CD5^{lo}) cells, based on cytosolic Ca^{2+} influx measurements, suggest that the differences in their lymphophenia-induced proliferation, which were previously attributed to putative corresponding differences in their strength of interaction with self-peptide MHC, may also largely be a result of intrinsic differences in their proliferation capacities in response to IL7. Further, the potential of exogenous IL7 therapy to skew the CD8$^+$ T cell repertoire towards the CD5^{hi} phenotype was demonstrated with *in vivo* studies in mice. Conversely, antibody-mediated depletion of IL7 has the opposite result.

Thesis Supervisor: Darrell J. Irvine
Title: Associate Professor

Thesis Supervisor: Jianzhu Chen
Title: Professor

Acknowledgments

I am extremely grateful to my advisors Jianzhu Chen and Darrell Irvine for their patience, encouragement and support in advising me throughout the ups and downs of my graduate work. I have greatly benefited from Jianzhu's thorough approach to research problems and am very grateful to him for encouraging me to pursue my interests wherever they led. Darrell was always enthusiastic about discussing ideas about immunology with me even when I went to his office with no data in hand. I have been especially fortunate to learn about biomaterials from him, which was a completely new field to me. I don't have enough words to express my sincere gratitude to Herman Eisen for his mentorship, generosity and for always keeping his door open for my naïve questions. His relentless personal quest for a quantitatively accurate description of T cell biology of will forever be an inspiration for me. Both Jianzhu and Herman took personal interest in all our lab journal club presentations and taught us how to critically interpret scientific literature in immunology. My thesis committee, Doug Lauffenburger and Dane Wittrup have been instrumental in steering my project in a practical direction at a critical juncture when their input was needed most. I am especially grateful to Doug for making it possible for me to pursue a collaborative project between two departments as a graduate student in the Department of Biological Engineering.

I am extremely thankful to Megan Palmer of the Lauffenburger lab, for a very productive collaboration over the past three years. I have learnt a great deal from her about systems biology and this thesis would not be possible without her support and understanding especially during the last few months. I am very indebted to Grace Yuen, a UROP student, who was very much my right hand in the last two years. Her enthusiasm to learn and the amount of time she spent in lab was very unusual for any undergraduate. Her thoughtfulness and wit is highly appreciated. Patrick Stern, from the Hynes lab, generously shared reagents with me and taught me about the nuances of lentiviral vectors.

I am very grateful to Ching-Hung Shen, my bay-mate every since I joined the lab,

and who has borne my idiosyncrasies more than anyone else in the lab. He has kindly shared his insights into the intricate subtleties of the biology of T cell memory and virology. I regard him, next to my advisors, as my guru. I am very thankful to Adam Drake for always being willing to discuss immunology with me whenever I approached him, and for the valuable input he has had in my research. Senior graduate students and postdocs my labs, in particular, Ailin Bai, Qing Ge, Brian Haines, Brendan Jones and Siddhartha Jain, helped me get started on my research and I am grateful for their advice from time to time. My fellow graduate students, Lily Trajman, Ilya Leskov, Mobolaji Olurinde, Eileen Higham, Carol Koh and Oezcan Talay, made my years in the Chen lab, where I spent most of my time, a lot of fun. I am very thankful to Ashok Prasad and Jayajit Das, both theoretical immunologists, for sharing their ideas on theoretical biology with me. Mimi, Kristyn and Zhuyan provided valuable technical support. I was fortunate to be the Chen and Irvine labs, which were filled with both graduate student and post-doc colleagues with extremely varied backgrounds.

An endeavor like a PhD thesis is not possible without the support of friends and family. I have dedicated this thesis to my parents who have strived to make it possible for me to get the best opportunities throughout their lives. My brother, Yogesh, has been an immense source of support. He also helped me with the interpretation of the microarray data and was always available to answer technical questions, even when he was busy writing his own PhD thesis. My uncle, Anil, [PhD '85, MIT], has been a constant source of advice and inspiration, and I wish to thank his family and Dr. Dhirendra Bana for their help in my transition to MIT. I would like to thank my cousins, Shantanu, Swati and Kshitij for their encouragement. I have been extremely fortunate to have friends like Manas, Ananya, Priyank, Puneeta, Taro, Rishi, Ramya, Siddhartha, Viji, Anoop, Ajit and Bhargavi who have made my stay at MIT and Boston so much more fun. There isn't enough space to acknowledge everyone and I apologize for any omissions.

Dedicated to my loving parents.

Contents

List of Figures

List of Tables

List of Abbreviations

2-ME	β-mercapto-ethanol
BMDC	Bone-marrow-derived dendritic cell
C10	Complete medium
CDR	Complementarity determining region
CFSE	Carboxy-fluorescein succinimidyl ester
DC	Dendritic cell
FC	Fold change
FCS	Fetal bovine serum
GM-CSF	Granulocyte-Monocyte Colony Stimulating Factor
GO	Gene ontology
GSEA	Gene set enrichment analysis
HBSS	Hank's Balanced Salt Solution
i.p.	intra-peritoneal
i.v.	intra-venous
LIP	Lymphopenia-induced proliferation
MHC	Major histocompatibility complex
miRNA	microRNA
MSigDB	Molecular Signature Database
ORF	Open reading frame
pMHC	peptide-MHC

s.c.	sub-cutaneous
SNR	Signal-to-noise ratio caculated as $\frac{\mu_A - \mu_B}{\sigma_A + \sigma_B}$
spMHC	self-peptide-MHC
TCR	T cell receptor
TCR	T cell receptor
TFBS	Transcription factor binding sites

Chapter 1

Highlights of this thesis

The naïve T cell repertoire is extremely vast and is estimated to comprise of over a trillion specificities in humans. This is critical for us to be able to detect a very broad array of foreign antigens. T cell diversity is solely generated in the thymus by a combinatorial process called VDJ recombination. Unlike B cells, T cells do not diversify their repertoire any further by somatic hypermutation in the periphery, likely making the preservation of T cell diversity generated in the thymus especially important. While the thymic generation of a diverse repertoire of T cells has been extensively studied, limited work has been done to study the efficient physiological maintenance of the diversity of the mature T cell repertoire. This thesis delves into this area and presents novel findings related to the characterization of a previously undescribed 'layer' of functional heterogeneity in T cells that likely arises as a consequence of the heterogeneity in the strength of thymic selection and deconstructs possible transcriptional networks that may determine these subtle but imprinted functional differences within the naïve $CD8^+$ T cell population.

1.1 Homeostasis of T cell diversity

Homeostasis refers to the tendency of the body to preserve its internal steady state, allowing it to return to a normal set point following perturbation. The term was first used by the American physiologist Walter Cannon in his seminal work, *Wisdom*

of the Body, in 1932. He emphasized the dynamic nature of homeostasis, stating that while it ensures stability of the organism, homeostasis *does not imply something set and immobile, a stagnation.* This dynamism is evident in the homeostasis of mature T cells where rapid fluctuations in the number, diversity, and function of T lymphocytes occur during immune responses. Yet, for the efficient function of the immune system, the population and activation states of T cells need to remain relatively stable in the long term. The term T cell homeostasis has been used to refer to the maintenance of T cell numbers as well as the maintenance of T cell diversity [125, 31]. Increasing evidence suggests that the homeostasis of both T cell number and diversity is regulated through competition for limiting resources, including self-peptide-MHC complexes (spMHC) and cytokines such as IL7 and IL15 [43].

The specificity of a T cell for antigen is determined by the binding of its T cell receptor (TCR) to peptide-MHC (pMHC). Most TCRs that strongly bind self-peptide MHC (spMHC) are eliminated during thymic selection. Successful T cell development in the thymus requires favorable TCR binding to spMHC in the thymus. Interaction with spMHC inevitably continues in lymphoid organs in the periphery as circulating naïve T cells actively seek out rare foreign antigens on the surface of antigen-presenting cells. In contrast to the sustained and strong TCR signaling induced by foreign peptides (agonists), TCR signaling from self-peptides is transitory and weak. Yet, naïve T cells depend upon such 'tickling' of their TCRs by self-peptides for their survival and maintenance. They also need IL7, a common gamma-chain cytokine, for their survival in the periphery. But it is not immediately obvious how the 'Homeostasis of naïve T cell diversity' presents a research problem. It would certainly not be viewed as a research problem if all T cells that are generated in the thymus have an equal chance of survival in the periphery and the homeostasis of T cell diversity is solely determined by a stable thymic output. However, the picture is more complex as it is thought that T cells have a varying ability to respond to spMHC in the periphery depending on the specificity of the TCR. This view is largely supported by the observation that the rates of lymphopenia-induced proliferation (LIP) of TCR transgenic T cells bearing different TCRs are variable and depend upon the specificity of

their TCRs. This view presents a problem sometimes referred to as the 'competition-diversity paradox'. If indeed, the homeostasis of T cell diversity is maintained by competition for spMHC and IL7, and T cells respond identically to IL7 and variably to spMHC, then the diversity of the peripheral repertoire would gradually decrease if T cells bearing TCRs with a higher avidity for spMHC selectively gain a survival advantage. However, this prediction does not bear out in practice. To explain this discrepancy, the signaling in $CD8^+$ T cells due to spMHC and IL7 were independently studied in vitro. Unexpectedly, this led to the identification of an entirely novel 'layer' of heterogeneity within the seemingly homogeneous population of naïve $CD8^+$ T cells in their responsiveness to IL7.

1.2 Characterization of functional intrinsic heterogeneity within the naïve $CD8^+$ T cell pool

A number of studies of LIP of TCR transgenic T cells bearing different TCRs have been interpreted with the implicit assumption that naïve $CD8^+$ T cells bearing different TCRs respond equally to pro-survival cytokines such as IL7. This thesis suggests an alternative view and presents novel evidence for intrinsic differences in the cytokine signaling networks of mature T cells and in their survival and proliferation capacities even within a seemingly homogeneous population of naïve $CD8^+$ T cells. This novel 'layer' of functional intrinsic heterogeneity in T cells likely arises during thymic development as a result of variability in the strength of selection of different TCRs. This heterogeneity is marked by the surface level of CD5 and is also observable even among T cells bearing the same TCR. We speculate that this intrinsic fine tuning of T cell signaling networks is critically important for the maintenance of T cell diversity as well as T cell tolerance in the periphery. This thesis considers the possible origins of the observed functional heterogeneity in the survival and proliferation capacities of $CD8^+$ T cells, which have the same genetic makeup with the sole exception of their TCR that is generated by VDJ recombination. This functional heterogeneity could

arise from either of the following possibilities.

Extrinsic The heterogeneity could reflect the effect of possibly heterogeneous spMHC or IL7 signaling in the periphery among T cells bearing different TCRs. This is also the prevailing view and is based on the implicit assumption that these functional differences would disappear when the T cells are removed from the heterogeneous spMHC and IL7 stimuli in their environment *in vivo*.

Intrinsic The heterogeneity is independent of ongoing TCR signals in the periphery and could reflect intrinsic properties of the cells.

My results are in strong support of a predominantly intrinsic mechanism of heterogeneity arising out of intrinsic differences in both the IL7 and TCR signaling pathways. T cells from the same TCR transgenic mouse respond variably to IL7 in a manner predicted by the surface levels of CD5. CD5 levels were shown to be differentially imprinted among $CD8^+$ T cells and may be used as a marker for a spectrum of correlated intrinsic functional differences among naïve $CD8^+$ T cells. As CD5 is a negative regulator of TCR signaling, it also reflects intrinsic differences in the TCR signaling pathway among $CD8^+$ T cells. Differences in the intrinsic responsiveness to IL7 are preserved even after T cell activation and differentiation into memory-like cells despite dramatic physiological changes in cell physiology as well as multiple rounds of cell division that occur during T cell activation.

Live video microscopy to study T:DC co-cultures was used to measure spMHC-induced TCR signaling in naïve T cells bearing different TCRs from two different TCR transgenic mice (OT-1 and F5 $Rag^{-/-}$ mice). Surprisingly, the Ca^{2+} influx induced by spMHC on dendritic cells was comparable in OT-1 and F5 cells, although the same dendritic cells induced dramatically different rates of proliferation in the T cells. Further, identical downstream triggers of the TCR pathway that bypass the TCR specificity, such as PMA/ionomycin, as well as the same dose of IL7, induced different rates of proliferation in T cells marked by different surface levels of CD5. These results suggest an intrinsic difference in the ability of T cells to proliferate. Similarly,

we identified baseline differences in IL7R levels, which are unmasked when cells are removed from IL7, suggesting an intrinsic difference involving the IL7 pathway itself.

In order to better understand the extent of the intrinsic heterogeneity in cellular processes in $CD5^{hi}$ and $CD5^{lo}$ cells and the underlying molecular mechanisms, a microarray expression profiling approach was undertaken. Pathway analysis studies revealed putative transcriptional factor and miRNA networks that underlie these differences. The origin of intrinsic differences in the T cell transcriptional networks is also discussed in the context of thymic development. We believe that these differences likely arise during thymic development but further work is necessary to characterize how they originate and become imprinted in T cells.

By demonstrating that naïve T cells bearing different TCRs respond differentially to IL7 rather than spMHC, the problems posed by the 'competition-diversity paradox' are not resolved but the focus of this paradox is merely shifted to IL7 responsiveness. However, a careful consideration of the physiological levels of IL7 suggests how this paradox may be avoided in vivo. Estimation of IL7 levels in vivo shows that IL7 is not too high to avoid selective proliferation of high-avidity T cells and not too low to avoid survival of low-avidity T cells. As predicted, artificially raising the levels of IL7 in vivo causes selective proliferation of high-avidity T cells and a reduction in the levels of IL7 in vivo causes selective survival of low avidity T cells. Finally, the immunological and biological implications of these findings are discussed in a broader pathophysiological context.

1.3 Outline of chapters

Chapter two reviews IL7 signaling and spMHC-induced TCR signaling in the periphery in the context of T cell homeostasis.

Chapter three discusses the attempts of this thesis to quantify spMHC-mediated TCR signaling in naïve $CD8^+$ T cells bearing different TCRs, and presents evidence for intrinsic differences in TCR signaling among naïve T cells in the periphery.

Chapter four presents novel findings of this thesis related to intrinsic heterogeneity in T cells in their ability to survive and proliferate in response to IL7.

Chapter five delves into the molecular mechanism driving the intrinsic heterogeneity in mature T cells and identifies putative transcriptional networks that could explain the observed phenomena.

Chapter six considers the above findings in a pathophysiologic context.

Chapter seven discusses the broader implications of these novel findings and suggests directions for future research.

Chapter 2

Homeostasis of T cell diversity

Some sections of this chapter have been previously published as a part of two review articles co-authored by me for Cellular and Molecular Immunology [74, 92].

T cell homeostasis commonly refers to the maintenance of relatively stable T cell numbers in the peripheral lymphoid organs. Among the large numbers of T cells in the periphery, T cells exhibit structural diversity, i.e., the expression of a diverse repertoire of T cell receptors (TCRs), and functional diversity, i.e., T cells of different lineages and developmental stages. Although the homeostasis of T cell numbers has been extensively studied, investigation of the mechanisms underlying the maintenance of structural and functional diversity of T cells is still at an early stage. The fundamental feature throughout T cell development is the interaction between the TCR and either self or foreign peptides in association with MHC molecules. It is suggested that the homeostasis of T cells (both number and diversity) is mediated through competition for limiting resources. The number of T cells is maintained through competition for limiting cytokines, whereas the diversity of T cells is thought to be maintained by competition for diverse cognate self-peptide-MHC complexes [74].

2.1 Lymphocyte homeostasis

Competition for extraneous and limited resources that are required for the survival and proliferation of T cells emerges as a central theme in the regulation of lymphocyte homeostasis. In contrast to other known biological systems in which population

	Cytokines	Self-peptide MHC
Naïve	IL7 is needed for survival of both $CD4^+$ and $CD8^+$ T cells. IL7 is essential for LIP of naïve T cells.	Interaction with spMHC is necessary for survival of naïve $CD4^+$ and $CD8^+$ T cells and for LIP. IL15 is needed for basal proliferation.
Memory	IL7 or IL15 can support acute LIP of memory T cells.	spMHC are not required for memory T cell survival but are necessary for the maintenance of memory cell function.

Table 2.1: **Factors needed for the homeostasis of $\alpha\beta$ T cells.**

numbers are regulated, such as quorum sensing in bacteria [80] and community effect in *Xenopus* embryonic mesoderm[44, 45], T cell homeostasis does not involve competition for autocrine ligands produced by the T cells themselves but for extraneous factors such as cytokines and spMHC that are produced by dendritic cells and stromal cells in the lymphoid tissues. These limited and limiting resources, which are often referred to as 'space', set the limits on the numbers and the diversity of an individual T cell population. Table 2.1 summarizes the factors for which $\alpha\beta$ T cells compete [115]. These factors include both pro-survival cytokines as well as spMHC. The major pro-survival cytokines, IL7 and IL15, are produced constitutively by dendritic cells and stromal cells in the lymphoid tissues [40, 131]. spMHC is also expressed at high levels by dendritic cells, which are believed to be the most important source of spMHC for T cells.

Because recognition of particular spMHC depends on TCR specificity, whereas interactions between cytokines and their receptors is thought to be independent of T cell specificity, it is believed that the pro-survival cytokines regulate total T cell numbers while spMHC regulates the T cell repertoire (see Figure 2-1). The homeostasis of T cell numbers and diversity is brought about through a balance of generation, proliferation, survival, death and differentiation of T cells [36]. T cells are generated in the thymus and the naïve T cell compartment is primarily replenished by thymic output. At the extremes of life, i.e., in neonates and in old age, the thymic output is not adequate to fill the peripheral T cell compartment. Under these circumstances, increased survival and proliferation of T cells in the periphery is believed to compensate in a

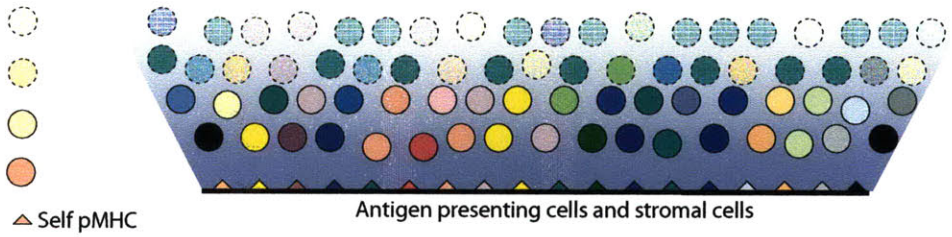

Figure 2-1: **Homeostasis of T cell numbers and diversity** This figure schematically depicts our current understanding of the homeostasis of T cell numbers and diversity. The circles of different colors represent T cells of different specificities and triangles of a particular color represent the set of spMHC displayed in steady-state conditions on the surface of APCs that can be recognized by T cells of the corresponding specificity. The gradient of blue represents the limiting availability of survival cytokines, IL-7 and IL-15, that are constitutively produced by antigen presenting cells and stromal cells in the lymphoid tissues. T cells are driven to occupy the available space and the T cells that do not have adequate access to space consequently die out (represented by broken circles). While interaction with spMHC is TCR specific, signaling by cytokines does not depend on the TCR specificity.

manner that maintains the total number of T cells. This highlights the importance of peripheral mechanisms such as proliferation, survival, death and differentiation in the regulation of T cell homeostasis under normal physiological conditions. T cells in different compartments turnover at different rates. For example, naïve T cells rarely proliferate while, in contrast, memory T cells undergo a slow but steady proliferation that depends on availability of IL15 [39]. Naïve T cells require both IL7 and spMHC for survival [123, 62]. However, spMHC are not required for the survival of both $CD8^+$ and $CD4^+$ memory T cells [88, 110], but rather are needed for the maintenance of their function [57]. The lack of dependence of memory T cells on spMHC probably ensures the long-term maintenance of memory cells that are selected by a particular antigen experience, without being subjected to possible skewing effects of the self-peptide repertoire. Pro-survival cytokines such as IL7 and IL15 increase the levels of anti-apoptotic factors such as Bcl-2 and Bcl-xL in T cells, while the lack of access to survival cytokines results in their apoptotic death [1]. Upregulation of anti-apoptotic

factors such as Bcl-2 is especially important in the long-term maintenance of memory T cells [42]. Competition for limiting pro-survival factors, which becomes especially pronounced in densely crowded lymphoid organs, is a key mechanism for maintaining T cell homeostasis. Rapid proliferation of naïve T cells can occur under two circumstances and in both cases it is accompanied by concomitant phenotypic change or differentiation into effector or memory cells. When stimulated by antigens, naïve T cells are activated and undergo rapid proliferation and concomitant differentiation into effector cells and subsequently into memory cells. Naïve T cells also proliferate in a lymphopenic setting, but in this case they differentiate directly into memory phenotype cells by a process that is dependent on IL7 and spMHC [18]. These memory phenotype cells are indistinguishable from conventional antigen-induced memory cells based on a variety of functional and molecular assays [38]. LIP also occurs under physiological conditions, as in neonates when the thymic output has yet to fill the peripheral space with mature T cells [81]. It is also believed to be important in old age when lymphopenic conditions may be present due to a severe decline in thymic output or other physiological changes. LIP is often equated with homeostatic proliferation by some investigators. We prefer not to use this term because LIP of naïve T cells does not result in the replenishment of the naïve T cell compartment even in the long term [34]. Rather LIP results in differentiation of naïve T cells into memory cells and therefore contributes to homeostasis of the memory compartment. Thus, T cell numbers and diversity are maintained throughout life through a balance of generation, proliferation, survival, death and differentiation.

2.2 T cell diversity

The diversity of a population refers to both the variety and abundance of the constituent individuals or in the case of T cells, the constituent clones. Two common measures of diversity are defined in Table 2.2. A diverse repertoire of T cells is selected by a diverse array of cognate spMHC in the thymus. Similar spMHC complexes continue to engage with TCRs in in the periphery, where they are thought

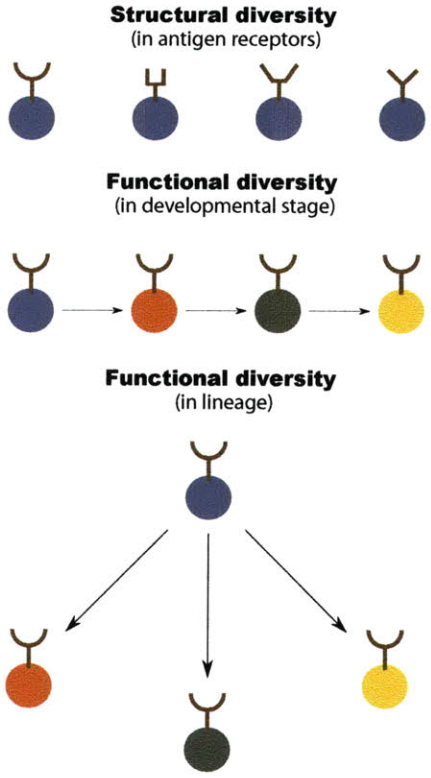

Figure 2-2: **Structural and functional diversity of T cells.** Structural diversity of T cells refers to the diversity in antigen receptors. Functional diversity in T cells can arise from differences in developmental stage or lineage. See Table 2.3 for specific examples.

to keep a diverse population of naïve T cells alive and poised to respond to foreign antigen [119, 9, 116]. It has been estimated that in both mice and humans, more than 10^{15} different TCRs can be generated in the thymus but only about 1 to 30 in a 100 (i.e.,$\sim 10^{13}$) can survive thymic selection [22, 89]. However there is space in the periphery of a mouse for only about 10^8 T cells and in humans for about 10^{12} T cells [25, 4]. Thus, selection for certain TCR specificities is likely to occur in the periphery due to competition for specific spMHC. The homeostasis of T cell numbers and diversity is interrelated in the sense that both processes involve competition for resources. While the homeostasis of T cell numbers involves competition for resources that are shared among all T cells, the maintenance of T cell diversity is believed to result from competition for access to a diverse set of cognate peripheral self-peptides.

While T cell diversity usually refers to the vast repertoire of antigenic specificities

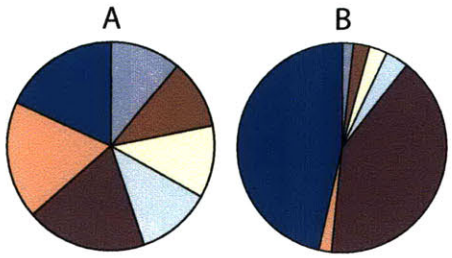

Index of Diversity	Expression	Definition
Simpson's index	$D^s = \frac{\sum_{i=1}^{S} n_i(n_i-1)}{N(N-1)}$	This index measures the probability that any two individuals in the population are different. It gives less importance to rare species.
Shannon-Weaver index	$D^{sw} = \sum_{i=1}^{S} s_i \ln s_i$	This index is based on information theory and is a measure of information contained. Rare species are better accounted for by this index.

n_i is the number of individuals of a particular species, N is the total number of individuals, s_i is the frequency of an individual species, and S is the total number of species.

Table 2.2: **Indices of diversity.** Shannon-Weaver index and Simpson's index are two two commonly used indices of population diversity. Population A and B are each comprised of seven clones but in different proportions. Population A is considered to be more diverse in terms of both the variety of the clones present as well as their relative abundance.

in an animal, T cells are also diverse in their function (see Figure 2-2). Functional diversity refers to T cells with different specialized function. It arises from differences in T cell lineage or developmental stage. For examples of each, see Table 2.3). Each lineage of T cells may be found at multiple developmental stages which have distinct functions. Indeed, a similar pattern of functional diversity is observed with other lymphocytes such as B cells or NK cells. B cells have variable BCR repertoire, are seen in different lineages (B1, MZB, and B2) and in different developmental stages (naïve, plasma, and memory). NK cell subsets also express different combinations of NK receptors and like T or B cells, and they also undergo activation and proliferation. This thesis describes an entirely 'novel' layer of functional heterogeneity within a seemingly homogeneous population of naïve $\alpha\beta$ $CD8^+$ T cells.

Experiments involving adoptive transfer of naïve TCR transgenic T cells into syngeneic wild-type mice suggest that 20-200 naïve T cells of a particular specificity can

Type	Varying factor	Examples
Structural diversity	Antigen receptor	T cells with different TCRs and thereby different antigenic and self specificities.
Functional diversity	Lineage	**Restricted by MHC-I/II:** $CD4^+$, $CD8^+$, natural T_{reg} **Restricted by non-classical MHC:** NKT (CD1d restricted), MAIT (MR1 restricted)
	Developmental stage	**Mature:** naïve, effector, memory, exhausted, tolerized, induced T_{reg} **Immature:** DN1, DN2, DN3, DN4, DP

Table 2.3: **Types of T cell diversity.**

survive long term and increasing the number of transferred cells resulted in progressive decline in their half-life in vivo [47]. This observation is thought to be reflective of the precursor frequency of antigen-specific T cells. The precursor frequency of antigen specific T cells has been directly measured and is found to be slightly higher for $CD8^+$ than $CD4^+$ T cells [84, 90]. These data are in agreement with previous estimates based on indirect approaches [11]. The failure of a large number of T cells of a single specificity to survive *in vivo* for long periods suggests that T cells recognize specific and limited cognate spMHC ligands. However, a transferred polyclonal population of T cells can persist *vivo* for significantly longer periods of time [47]. This suggests that there is a mechanism for maximizing the diversity of the T cell population and one way how this could be achieved is that the T cells compete for their specific cognate spMHC ligands and the diversity of the spMHC repertoire maintains a correspondingly diverse T cell repertoire in the periphery.

2.3 Diversity of self-peptides

The diversity of the self-peptide repertoire has been estimated and some quantitative estimates are presented below for the class I spMHC repertoire and similar arguments can be made for the class II spMHC repertoire. From a total of 30,000 distinct proteins present in the mouse or human with an average length of 400 amino acids, it can be

calculated that nearly 10^7 peptides of 8-9 amino acids in length can be generated. This estimate assumes no preference for specific protease cleavage sites. For a peptide to be presented on class I MHC it needs to be (i) generated by proteases, (ii) transported by TAP into the endoplasmic reticulum, and (iii) bound by an MHC molecule. When a sequence corresponding to a naturally occurring epitope is inserted anywhere into a protein, it is nearly always displayed on the cell surface but at widely varying levels depending on its flanking sequences unless the epitope carries an obligate protease cleavage site [102]. There may be some selection for transport of particular peptides occurring at the level of TAP [63] but the major bottleneck for display of a peptide on the surface lies in its ability to form stable peptide MHC complexes. Evidence suggests that the *a priori* probability for any random peptide to bind relatively stably to MHC is about 1% [12]. This leaves only around 10^5 of a total of 10^7 peptides that can be generated in the animal to be presented on the surface of APCs as peptide-MHC complexes per MHC allele. Experiments suggest that majority of the self-peptides on class I MHC are derived from abundant housekeeping proteins such as ribosomal proteins, N-terminal leader sequences, histones and heat shock proteins [52]. The $\sim$30,000 distinct proteins expressed in the mouse or human are present in widely varying quantities in the body. Since there are only around 100,000 MHC class I molecules expressed by each APC, equal representation of peptides on MHC class I molecules from each of these proteins is not possible [142]. It has been found that the population of MHC class I molecules on uninfected cells simultaneously displays about 1,000 to more than 10,000 different 'naturally processed' peptides with a broad range of copy number. A few of these peptides are present at 10,000 copies per cell, whereas the remaining are presented at less than ten to a couple of hundred copies per cell [27]. Thus, assuming a mean of 100 copies per peptide, a single APC presents about 10^3 different self-peptides albeit in widely varying quantities. In comparison, the total number of *distinct* spMHC complexes in an animal can be estimated to be about 10^5 (see above) which is many orders of magnitude smaller than the TCR diversity. This disparity implies that the spMHC molecules are shared among different TCRs, highlighting the degree of competition for the same spMHC that can occur among T

cells expressing different TCRs.

Type of pMHC complex	Induced T cell response	Specificity for a given TCR
Agonist	Full activation of T cell; cytokine secretion; T-cell proliferation; CTL effector function	++++
Antagonist	Inhibits activation by agonist; does not induce activation on its own	++
Weak agonist	Same as agonist, but requires a higher dose for the same degree of activation; slower activation kinetics	++
Partial agonist	Induces some, but not all, effects of agonist (e.g., cytokine secretion but not proliferation)	++
Null	No detectable activation	Not TCR specific

Table 2.4: **Types of peptides.** Classification of peptide MHC based on T cell response.

From a single TCR perspective, cognate self-peptides can be divided on the basis of their biological activity into agonist peptides, weak agonists, partial agonists, antagonists or null peptides (see Table 2.4). However, these are not all present in identical proportions (see Figure 2-3). Peptides that are null (non-cognate) are likely to be the most abundant. Agonist peptides for a given TCR are likely to be the least abundant because they are most TCR specific and because T cells that strongly recognize self-peptides are negatively selected in the thymus. It seems counterintuitive that $\alpha\beta$ T cells specific for any agonist self-peptides can survive negative selection under the physiological conditions. Not all self-antigens are expressed in the thymus at adequate levels to allow strict negative selection. Such T cells could recognize self-antigens as agonists in the periphery and are potentially autoreactive but are kept in check by various mechanisms of peripheral tolerance [96]. Nevertheless, in the self-peptide repertoire, the fraction of agonist peptides for a given TCR is likely to be extremely small. For any given TCR found in the periphery, a slightly larger fraction of the self-peptide repertoire could be intermediate affinity ligands such as

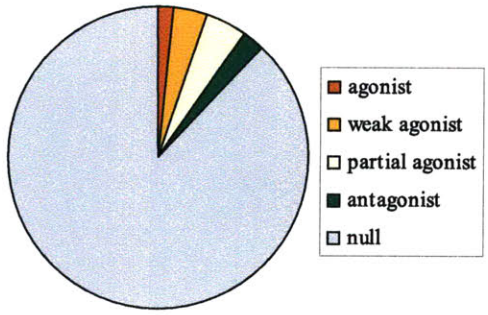

Figure 2-3: **Hypothetical proportions of the types of self-peptides in the periphery seen from the perspective of a single TCR.** From a single TCR perspective, null peptides are likely to be the most abundant since they are not TCR specific. High affinity agonist peptides among spMHC are likely to be the least abundant because T cells that strongly recognize self-peptides are negatively selected in the thymus. For any given TCR found in the periphery, an intermediate fraction of the self-peptide repertoire could be low affinity ligands such as weak or partial agonists or even antagonists because there is likely to be higher cross-reactivity among low affinity ligands for a given TCR than for high affinity ligands. A similar argument can be made from a single spMHC perspective that majority of the TCR specificities will see it as a null peptide; a very small fraction of TCRs will recognize it as an agonist and an intermediate fraction of TCRs will recognize any particular spMHC complex as a low affinity ligand such as a weak agonist, partial agonist or an antagonist.

weak or partial agonists or even antagonists. They are likely to be more abundant than agonist peptides not only because T cells are positively selected on such low affinity ligands in the thymus which are presumably also be found in the periphery but also because there is a higher cross-reactivity among low affinity ligands for a single TCR. From a single spMHC perspective, a similar argument can be made that any given spMHC will be seen as a null peptide by a majority of the TCR specificities. A very small fraction of TCRs will recognize a given spMHC as an agonist and an intermediate fraction of TCRs will recognize any particular spMHC complex as a low affinity ligand such as a weak agonist, partial agonist or an antagonist. Although it is interesting to speculate on the nature of single TCR-spMHC interactions, it should be emphasized that when a T cell interacts with a single dendritic cell, $\sim 10^5$ TCRs on the T cell interact with a diverse set of spMHC on the surface of the APC, which in combination, give rise to a TCR signal.

2.4 Identity of the self-peptides that regulate T cell homeostasis

The identity of cognate self-peptides that regulate the homeostasis of T cell diversity in the periphery is still not clear. Competition between clones expressing different TCRs during LIP suggests that cognate self-peptides are present in limiting amounts in the periphery. The low affinity self-peptides, rather than agonist peptides, are likely to drive LIP because of the lack of concurrent observable T cell activation. Studies with $CD4^+$ cells selected in H2-$M^{-/-}$ mice, which express mostly the CLIP peptide (class II-associated invariant chain peptide) in the periphery, suggest that the positively selecting ligands in the thymus are responsible for LIP in the periphery [28]. However, this does not entirely rule out the possibility that agonist self-peptides play a role in LIP. Weak agonist peptides may be able to drive LIP without resulting in conventional activation either because they are present in extremely low amounts or because they stimulate T cells in the absence of costimulation or by cooperating with other (null) spMHC. Regardless whether agonist peptides or low affinity peptides or both support lymphocyte homeostasis, given that the amount of these peptides is small, it is natural that competition for these peptides contributes to the homeostasis of TCR diversity in the periphery.

A majority of the naturally occurring cognate self-peptides that have been characterized so far arise from abundantly expressed self-proteins.This could be because the detection of rare but functional naturally occurring cognate self-peptides for any particular TCR may be limited by the sensitivity of the peptide purification and biological assays used in their identification. It is quite likely that there are many cognate self-peptides that are recognized by the above TCRs and regulate their homeostasis but too rare to be detected by current biochemical assays. Further, the spMHC-mediated signaling that is responsible for T cell survival in the periphery is neither well understood nor easy to measure directly. Therefore, the biological assays used for the detection of naturally occurring cognate self-peptides such as CTL killing or co-receptor dulling in DP cells, which are often used with excess concentration of

test peptides may not be truly representative of physiological homeostatic spMHC-mediated TCR signaling that has been referred to as peripheral 'TCR tickling' by some authors. Given that null peptides are most abundant, it is certainly possible that they could also contribute to the TCR signal required for lymphocyte homeostasis. It should be emphasized that the definition of a null peptide-MHC complex (pMHC) is only related to its lack of potential to induce any grade of activation in a T cell. It does not mean that null pMHCs are biochemically null in terms of interacting with a TCR. A TCR contacts pMHC at its three complementarity determining regions (CDR1, CDR2 and CDR3). The CDR1 and CDR2 regions of the TCR primarily interact with the MHC portion of the pMHC complex and the CDR3 interacts with the presented peptide. If the peptide in the pMHC complex is a null peptide it is conceivable that a stable TCR-pMHC complex is not formed but the CDR1 and CDR2 can still interact weakly with the MHC alone, perhaps giving rise to short-lived 'TCR-null pMHC' complex. Such transient interactions, wherein the peptide plays a minimal contributory role, may become cumulatively significant because of the abundance of null peptides and may provide a homeostatic signal to T cells. Furthermore, it is also conceivable that spMHC-TCR interactions only increase the duration of contact with dendritic cells and other uncharacterized ligands on the surface of dendritic cells may also provide a survival signal to T cells and future research is likely to shed light on these areas.

2.5 spMHC-mediated TCR signaling

A schematic of TCR signaling is presented in Figure 2-4 [68]. Full-blown TCR stimulation by a foreign agonist pMHC results in a naïve T cell results in the sustained activation of multiple downstream TCR pathways as described below. However, spMHC alone can also trigger partial activation of especially the proximal components of the TCR signaling cascade. Both $CD4^+$ and $CD8^+$ T cells are thought to receive a tonic signal from spMHC in vivo and they have a reduced lifespan when deprived of contact with MHC [122, 124]. Stimulation of the TCR by antigenic pMHC triggers the

activation of the Src family kinase, Lck. Lck is present in both as a soluble factor and bound to the co-receptor (CD4 or CD8). Binding to pMHC induces co-localization of TCR and the co-receptor, which helps bring Lck in close proximity to the CD3 complex. The CD3 ϵ, δ, γ and ζ subunits are critical components of the TCR complex and contain a number of ITAMs (immunotryosine-based activation motifs) which are phosphorylated by Lck, which in turn recruit ZAP70 to the TCR signaling complex. In the presence of agonist pMHC, ZAP70 phosphorylates its substrates LAT and SLP-76 which which through many intermediaries trigger (i) calcium influx into the cytosol, (ii) activation of the Ras pathway, and (iii) cytoskeletal remodeling. Partial phosphorylation of CD3ζ chains and recruitment of ZAP70 is also seen in freshly isolated T cells and is thought to reflect tonic signaling from spMHC in vivo [116].

The recruitment of PLCγ1 (Phospholipase Cγ1) to the membrane by LAT causes hydrolysis of PIP_2 (phosphatidyl-inositol 4,5 bis-phosphate) into IP_3 (inositol 1,4,5 triphosphate) and DAG (diacyl glycerol). IP_3 is a critical second messenger that triggers calcium influx into the cytosol, which is a hallmark of TCR signaling. Ca^{2+} influx initially occurs from the ER which leads to the opening of the CRAC (Ca^{2+} release activated Ca^{2+}) channels in the plasma membrane and a rush of extracellular Ca^{2+} into the cytosol. The extracellular Ca^{2+} concentration is 10,000-fold higher than intracellular levels, allowing the rapid influx of Ca^{2+} through the CRAC channels and activation of calcineurin, which in turn dephosphorylates the transcription factor, NFAT, causing its translocation to the nucleus. Cytosolic Ca^{2+} influx is also seen during spMHC-mediated TCR signaling but it is brief and intermittent unlike the sustained Ca^{2+} influx seen upon agonist pMHC-mediated stimulation of the TCR [24].

Activation of the Ras pathway is critical for TCR signaling. RasGRP, a guanine exchange factor, is activated by DAG. RasGRP and PKC trigger the activation of Ras pathway, which is comprised of a signaling cascade of kinases that leads to the activation of MAP kinases Erk1/2, JNK and p38. These MAP kinases activate the heterodimeric transcription factor AP-1. This is conventionally referred to as the 'first signal'. Production of IL2 during T cell activation requires the release of tran-

scription factor NF-κB from IκB. This is dependent on the 'second signal', provided by co-stimulatory pathways (e.g. CD28). CD28 leads to Akt and MAPKKK activation, which activate IKK and consequent phosphorylation of IκB, which marks it for ubiquitin-mediated degradation.

During antigen recognition by the TCR, a rearrangement of a number of surface molecules in addition to the TCR:pMHC complexes is observed at the T-APC cell interface. This supra-molecular clustering of TCRs, adhesion, signaling and cytoskeletal molecules, has been termed the 'immunological synapse' [41]. Extensive cytoskeletal remodeling and reorientation of the T cell microtubule organizing center towards the APC, which is triggered upon TCR signaling, may also be involved in synapse formation. A 'mature' immunological synapse normally seen in the context of agonist pMHC-driven signaling has a supramolecular activation cluster (cSMAC) enriched in TCR, CD2 and CD28, which is surrounded by a peripheral SMAC (pSMAC), enriched in LFA-1 (lymphocyte functionassociated antigen-1) [41, 83]. The formation of immunological synapses has also been reported in T cells interacting with dendritic cells even in the absence of agonist peptides [106]. Such agonist antigen-independent synapse formation is driven by spMHC even in the absence of agonist pMHC, and is also tightly associated with brief weak Ca^{2+} responses. The formation of the immunological synapses induced by spMHC is also not sustained and may result in unusual synapse morphologies.

CD5 is a type I transmembrane protein of the group B of scavenger receptor cysteine-rich (SRCR) superfamily. The CD5 ectodomain interacts with conserved fungal cell wall components and protects from zymosan-induced septic shock-like syndrome [128]. It also has a large cytoplasmic tail with numerous conserved tryosine as well as serine/threonine phosphorylation sites, which is critical for modulating TCR signaling. The cytoplasmic domain is critical for the modulatory effects of the TCR and is highly conserved (see Figure 2-6). The mechanism by which CD5 modulates TCR signaling is shown in Figure 2-5. CD6 is a closely related molecule of the same family, which also associates with the TCR and CD5, and is closely linked to CD5 on chromosome 19 in mouse and chromosome 11 in humans [37]. It is possible that

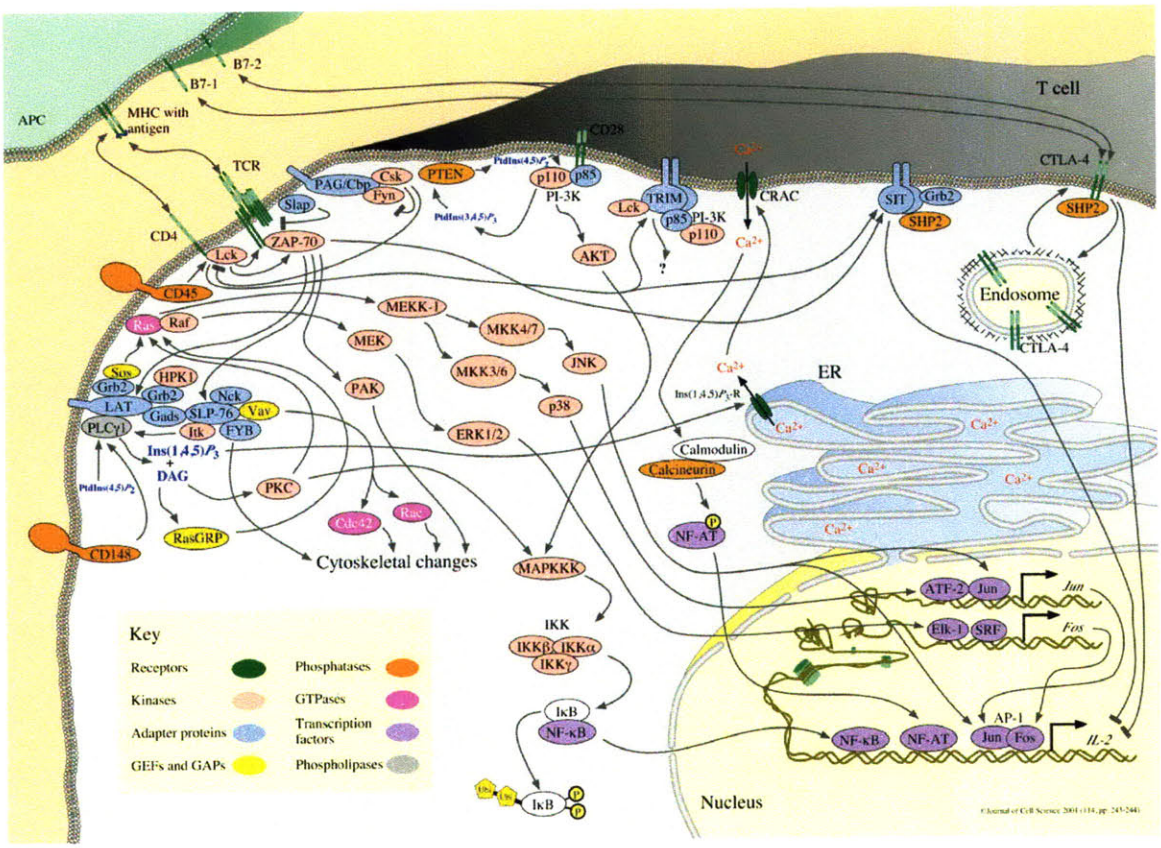

Figure 2-4: **TCR signaling network.** This is a detailed schematic of TCR signaling involved in T cell activation and selection, as prepared by Joseph Lin and Arthur Weiss [68]. The details of spMHC-mediated homeostatic TCR signaling are poorly understood, but the upstream molecules are likely to be shared and involve partial phosphorylation of CD3ζ chains and the recruitment of ZAP70 to the TCR complex, as well as brief spikes of cytosolic Ca^{2+} influx. However, sustained activation of the downstream TCR pathways depicted above is not triggered in resting T cells by spMHC.

they arose from genomic duplication but have significant differences in their cytosolic domains. CD5 associates with the TCR signaling complex and modulates T cell activation and differentiation [72]. Cross-linking of CD5 with antibodies has suggested that CD5 can positively impact TCR signaling but the physiological significance of these results is unclear [72]. However, genetic studies, using CD5 knockouts suggest that CD5 has an inhibitory role [6]. CD5 inhibits the extent of tyrosine phosphorylation at the synapse as well as the amplitude of calcium responses induced by antigen recognition without interfering in synapse formation [13]. CD5 is developmentally regulated in the thymus and is upregulated during positive selection [7]. In the pe-

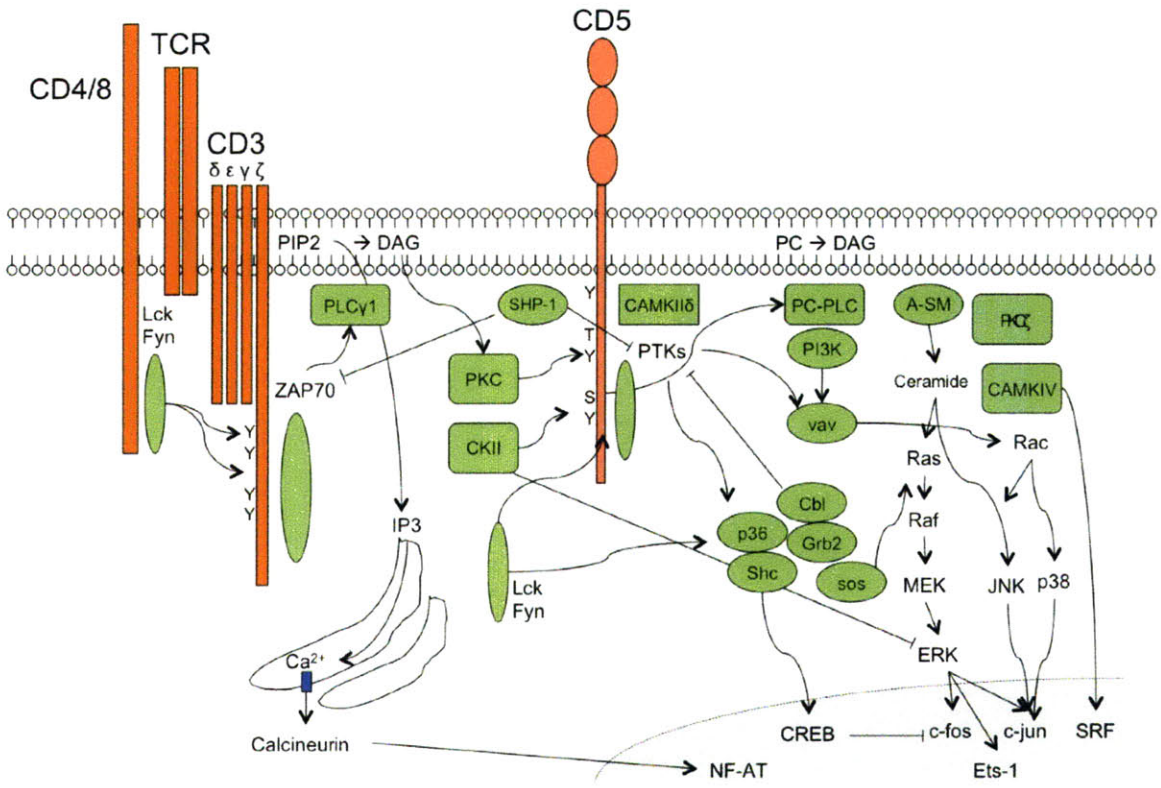

Figure 2-5: **CD5 signaling network.** The intra-cellular domain of CD5 is rich in phosphorylation sites and it can recruit a number of signaling mediators that impact TCR signaling. Genetic studies suggest that CD5 is a negative regulator of TCR signaling. SHP-1, which interferes with proximal TCR signaling, is a major component of this inhibitory interaction.

riphery, the level of CD5 is thought to be maintained by engagement with spMHC and therefore, the levels of CD5 on mature T cells is often used as an indicator of the strength of spMHC-induced TCR signaling in the periphery [113]. The transcription of CD5 is positively regulated by the Ets family transcription factors and inhibited by the E2A family transcription factor, E47 [3, 138].

2.6 IL7 signaling network

IL7 is produced primarily by fibroblastic reticular cells in the T cell zone in lymphoid organs [69] and binds to the IL7 receptor complex, a heterodimer consisting of the IL7Rα chain (IL7R) and the common gamma (γc) chain [78]. While IL7 shares pro-

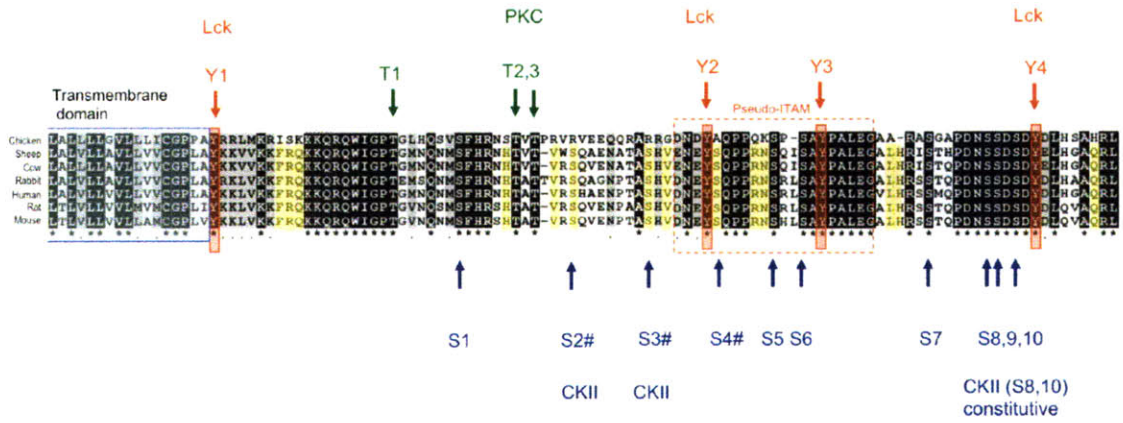

Figure 2-6: **Conservation of CD5 signaling domain.** CD5 intracellular alignment with ClustalW is shown above with putative serine, threonine and tyrosine phosphorylation sites. The sites of phosphorylation by casein-kinase II and protein kinase C and the pseudo-ITAM domain are indicated above.

survival and proliferative capacities with related interleukin family members, it also plays non-redundant roles in T cell development and homeostasis [53]. IL7R is also expressed on pro-B cells, dendritic cells (DCs) and monocytes, suggesting a possible role for IL7 in multiple hematopoietic lineages [104]. IL7 is bound to the extracellular matrix and is likely displayed in a matrix-associated form in sites near the sites of production, like other cytokines which bind the common γ chain [136]. Naïve T cells continuously recirculate between IL7-rich lymphoid organs and blood and it is speculated that IL7 consumption occurs primarily in the secondary lymphoid organs but not while in transit in the lymph and blood [120]. Indeed, the survival of T cells is found to be impaired in mice that lack secondary lymphoid organs [21].

In lymphocytes, IL7R signaling results in survival, proliferation and differentiation, depending on the developmental stage of the lymphocyte. In dendritic cells, IL7R signaling has an immunomodulatory role, especially in the context of thymic stromal lymphopoietin (TSLP), which also signals through the IL7R in a heterodimeric complex with the TSLP receptor (TSLPR). Both IL7 and IL7R knockout mice have been studied. IL7 knockout mice are deficient in T cells, B cells, NK cells, and NKT cells as well as intra-epithelial lymphocytes [129]. Similarly, mice lacking IL7R have a similar but more severe phenotype than IL7 knockout mice [95], possibly

because TSLP signaling is also abrogated in the IL7R knockout mice. Binding of TSLP to the IL7R:TSLPR complex can activate at least some of the signaling cascades normally activated by IL7, but it also triggers some unique signaling pathways involving the Tec kinases [51, 70].

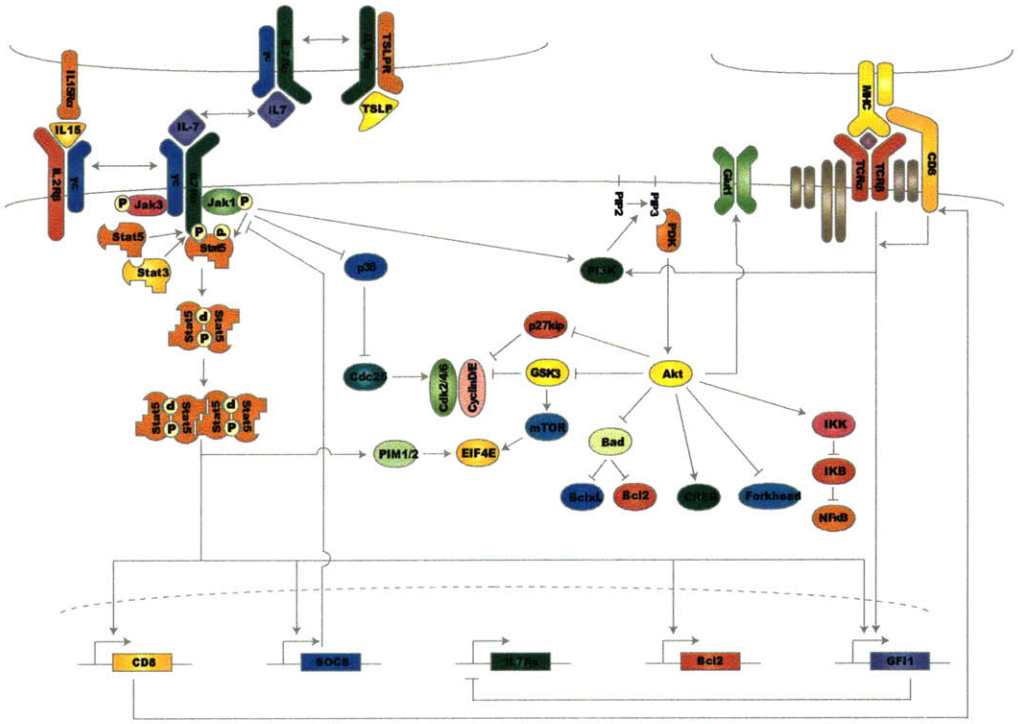

Figure 2-7: **IL7 signaling network.** A schematic diagram of the IL7R signaling network and its connectivity with interacting signaling networks, including TSLP, IL15 and the TCR.

Major signaling cascades activated by the binding of IL7 to IL7R include the Jak-Stat and PI3K-Akt pathways (see Figure 2-7) [53, 120]. IL7 binding to IL7R/γc complex causes activation of Jak1 (bound to IL7R) and Jak3 (bound to the γc chain). They phosphorylate Stat5a/b which causes migration of the phosphorylated Stat5 dimers to the nucleus and gene transcription. Deletion of Il7R, Jak3, γc chain, or a combined deletion of Stat5a and Stat5b causes severe lymphopenia as a result of defective T cell development and survival [65]. Simultaneous deletion of Stat5a and

Stat5b in mature T cells results in a severe depletion of mature T cells, suggesting the critical role of IL7 signaling in mature T cell survival [139]. IL7 signaling prevents the mitochondrial pathway of apoptosis. Bcl2 and Mcl1 play a dominant role in naïve T cells because other anti-apoptotic molecules are not expressed at high levels in naïve T cells. Bcl2 and Mcl1 interfere with the pro-apoptotic molecules Bax and Bak, which can induce the mitochondrial pathway of apoptosis by inducing the release of cytochrome c from mitochondria [59]. Bcl2 and Mcl1 can also inhibit multiple BH3-only family members such as Bim, Bid, PUMA and Bad which activate Bax and Bak [17]. $Bcl2^{-/-}$ mice can be rescued from premature death by crossing them onto a $Bim^{+/-}$ background ($Bcl2l11^{+/-}$). Although $CD8^{+}$ T cell development is near normal in these mice, the survival in the periphery is highly impaired. This defect can be further rescued in $Bcl2^{-/-}$ $Bcl2l11^{-/-}$ mice where the naïve T cell numbers are mostly restored [134]. This suggests that Bcl2l11 is a key mediator of T cell death. Excess IL7, as seen in lymphopenia, can induce the spontaneous proliferation of naïve T cells, without inducing activation. IL7-mediated proliferation requires the PI3K pathway, and Gsk3 and $p27^{kip1}$ are key mediators of the IL7-induced progression of cell cycle from the G to S phase (see Figure 2-7). IL7 signaling is also known to induce a number of feedback suppression loops. IL7 signaling suppressed the transcription of IL7R, via a feedback loop involving the transcription factor Gfi1b. SOCS1 (suppressor of cytokine signaling 1) is yet another feedback suppressor of IL7 signaling that is also induced by IL7 signaling.

In addition to the balance between pro-apoptotic and anti-apoptotic pathways, autophagy is another highly conserved mechanism that promotes the survival of naïve T cells during nutrient deprivation. Autophagy was shown to be critical for maintaining the survival of IL3-dependent cell lines after cytokine withdrawal [73]. A role for autophagy in T cell survival and proliferation has been shown in vivo using lethally irradiated mice repopulated with hematopoietic cells from fetal livers of $Atg5^{-/-}$ mice [100]. $Atg5^{-/-}$ T cells develop normally in the recipient thymus, but fail to repopulate the periphery due to a dramatic defect in cell survival. It is speculated that T cells, on exit from the thymus, become exposed to nutritional stress owing to limited access to

pro-survival factors and require autophagy to sustain them in the periphery. It is not known if T cells require a basal level of autophagy to maintain their survival in the periphery but autophagosomes have been reported in freshly isolated mouse T cells [100]. Similar results are seen with $Atg7^{-/-}$ mice. Superfluous mitochondria, which could be a source of toxic ROS, are also consumed by autophagy and eliminated. This may be an additional function of autophagy in T cell development.

2.7 Competition-diversity paradox

The 'competition-diversity paradox' refers to the idea that competition among peripheral lymphocytes for *in vivo* survival factors would ultimately result in the domination of the repertoire by T cell clones with the best ability to compete for the survival factors [23, 30]. This is likely to be applicable for T cells, as they require spMHC for survival and it is currently believed that there is a widespread variation in the strengths of spMHC signals received by T cells bearing different TCRs. Differential responsiveness to survival factors among T cells can also occur as a result of variable access or responsiveness to IL7 (see Figure 2-8).

It is currently believed that the differences in the levels of CD5, IL7R and CD8α among $CD8^+$ T cells are extrinsic, i.e. the differences would disappear upon withdrawal from the heterogeneous sources of spMHC or IL7 in their physiological environment. Variable strengths of interaction with cognate spMHC among TCRs of different specificities, is thought to be responsible for the differences in CD5 levels. It is worth noting the terms 'spMHC avidity' and 'spMHC signal' have sometimes used interchangeably. However, this thesis draws a distinction between them and I have used the terms to refer to the biochemical interaction with the TCR and the signal transduced through the TCR respectively. In this thesis, the spMHC-mediated TCR signal has been operationally defined in terms of the degree of cytosolic calcium influx in T cells.

There are at least two mechanisms that cause variability in the responsiveness of $CD8^+$ T cells to IL7 (see Figures 2-8b and c). (i) $CD8^+$ T cells that are recently sig-

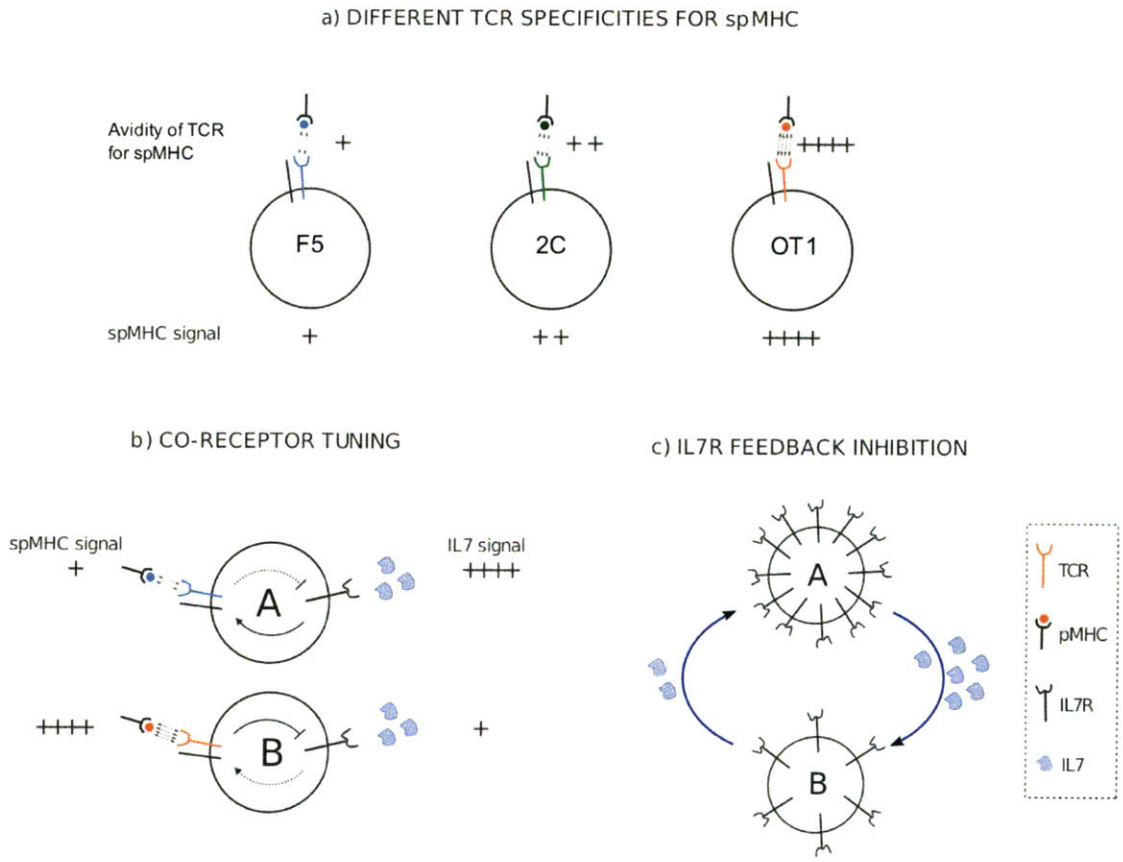

Figure 2-8: **Extrinsic diversity Extrinsic diversity in T cells.** Three potential sources of extrinsic heterogeneity in T cells are shown above. Note that all these extrinsic differences would be expected to disappear once the T cells are isolated from the respective extrinsic modulator of their signaling networks. (a) **Different levels of CD5**. The TCRs of OT-1, 2C and F5 cells are thought to have different avidities for their cognate spMHC. This is believed to result in correspondingly different CD5 levels on the T cells as well as different spMHC-induced TCR signals. (b) **Co-receptor tuning**. This model proposes that the spMHC-mediated TCR signal inhibits the IL7 signaling pathway and conversely, IL7 signaling enhances the TCR signal by increasing the transcription of CD8α. Thus two cells with different responsiveness to spMHC would be predicted to have extrinsic differences in both the TCR and IL7 pathways. (c) **'Altruistic' downregulation of IL7R**. Recently signaled T cells are thought to 'altruistically' downregulate the transcription of IL7R to allow optimal utilization of IL7 from the perspective of the entire population. Thus, recently signaled T cells would be expected to have an extrinsic difference in their IL7 signaling pathway. T cells are thought to be exposed to a spatially heterogeneous IL7 environment in vivo.

naled by IL7 downregulate the levels of IL7R, resulting in a heterogenous population of T cells with varying IL7R levels, which has been considered to be an 'altruistic' way of maximizing IL7 utilization among $CD8^+$ T cells [93]. (ii) Cross-wiring of the TCR and IL7 signaling networks called 'co-receptor tuning' is thought to result in the dampening of IL7 signaling in T cells that receive stronger TCR signals [94]. Such feedback, cross-inhibiting and amplifying loops could result in the maximization of the cumulative signal in T cells from both spMHC and IL7 [92] (see Figure 2-8). However, further quantitative analysis needs to be done to determine their impact on the trade-off between T cell competition and their diversity.

Chapter 3

spMHC-induced TCR signaling

The differences in LIP among TCR transgenic mice are believed to be due to their receiving spMHC signals of correspondingly different strengths. This is supported by the strong correlation between CD5 levels and the rate of LIP for any given T cell. However, direct measurements of spMHC responsiveness in TCR transgenic T cells with variable rates of LIP have not been performed to rigorously test this hypothesis. This chapter details our efforts in this direction. We have focused on naïve $CD8^+$ T cells as we had ready access to a panel of TCR transgenic $Rag1^{-/-}$ T cells, namely OT-1, 2C and F5, all of which are selected into the $CD8^+$ lineage, in an identical MHC background (C57/BL6, $H\text{-}2^b$). These TCR transgenic T cells exhibit different rates of LIP upon adoptive transer into the same syngeneic $Rag^{-/-}$ background. In particular, we focused on $CD8^+$ T cells obtained from OT-1 and F5 $Rag1^{-/-}$ mice (hereafter referred to as just OT-1 or F5 cells), as they were expected to show the maximum difference in spMHC-mediated signaling based on a comparison of their CD5 levels and rates of LIP [33].

3.1 An in vitro co-culture system to study LIP

LIP can be recapitulated *in vitro* using a T-cell:DC co-culture system with a sufficiently high DC:T-cell ratio[33]. We surveyed the ability of the following syngeneic dendritic cells derived from various sources for their ability to support LIP of OT-

1 T cells *in vitro*: (i) Splenic DCs were magnetically enriched ($CD11c^+$ selection) from the spleens of B6 mice, which had been implanted with GMCSF-producing B16 melanoma cells (see Appendix A.2). (ii) BMDCs were differentiated from B6 bone marrow precursors with GMCSF treatment for seven days (see Appendix A.2). (iii) DC2.4 is a cell line originally derived from the oncogenic transformation of B6 bone marrow dendritic cells [111]. These three DC types were co-cultured with CFSE labeled naïve OT-1 cells in a 1:1 ratio for seven days, and T cell proliferation was assessed (see Figure 3-1). To prevent proliferation of DC2.4 cells, they were gamma-irradiated with 500 Rads using a ^{137}Cs irradiation source. DC2.4 cells were best able to support the LIP of OT-1 T cells. The proliferation was dependent on MHC-I in all cases. Splenic DCs derived from $\beta_2m^{-/-}$ mice did not support the proliferation of OT-1 cells. In the absence of MHC-I, BMDCs and DC2.4 cells could not even support the survival of OT-1 cells as evident from co-culture of OT-1 cells with BMDCs from $\beta_2m^{-/-}$ mice and the addition of 10µg of anti-K^b antibody (B8.24.3) to the co-culture with DC2.4 cells completely. This is consistent with previous studies showing that OT-1 cells are selected on K^b and likely recognize spMHC presented on K^b in the periphery [107]. Therefore, DC2.4 cells were chosen for further analysis.

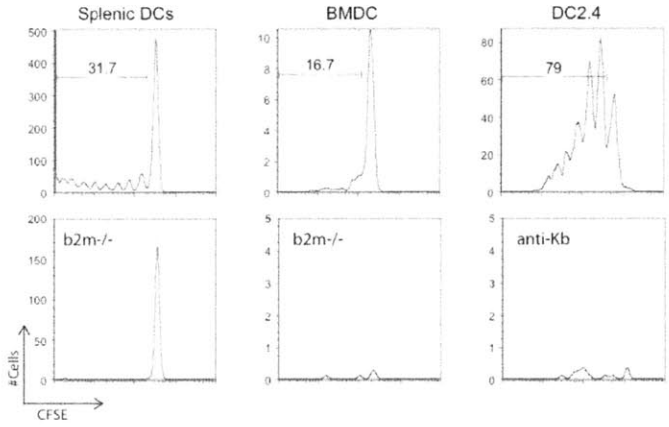

Figure 3-1: ***In vitro* lymphopenia-induced proliferation induced by dendritic cells from different sources.** Splenic DCs, BMDCs or irradiated DC2.4 cells were co-cultured with CFSE-labeled OT-1 cells in a 1:1 ratio for seven days and OT-1 cell proliferation was assessed by CFSE dilution.

To test if the relative differences in the rates of LIP seen *in vivo* can be recapitu-

lated in this *in vitro* system, CFSE-labeled naïve OT-1 and F5 T cells were co-cultured with DC2.4 cells for three days in a 1:1 ratio (see Figure 3-2). OT-1 T cells proliferated for up to four divisions. The proliferating OT-1 cells also showed a progressive upregulation of CD44 and no change in CD69 levels, as observed *in vivo* during LIP. In contrast, F5 T cells did not undergo any divisions in this *in vitro* LIP co-culture system. These results are consistent with the differences in LIP observed following transfer of OT-1 and F5 T cells into syngeneic $Rag^{-/-}$ mice, suggesting that this T:DC co-culture system using DC2.4 cells could be used to explore the mechanisms underlying the differential rates of LIP among T cells bearing different TCRs.

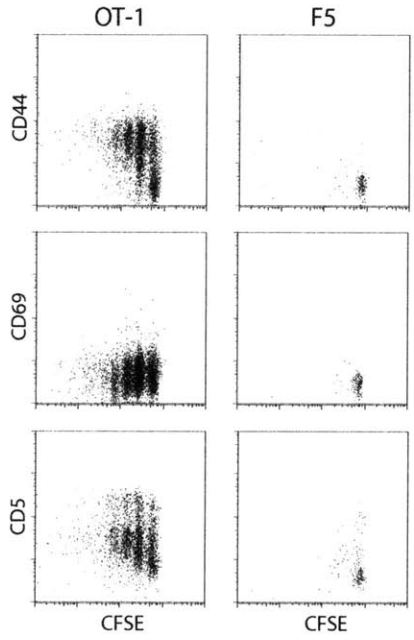

Figure 3-2: ***In vitro* lymphopenia-induced proliferation of naïve OT-1 and F5 $Rag^{-/-}$ T cells.** CFSE labeled naïve OT-1 and F5 T cells were co-cultured with DC2.4 cells in a 1:1 ratio for 3 days. CFSE profiles of live $CD8^{+}$ at day 3 are shown.

3.2 Measurement of spMHC-induced signaling

Cytosolic calcium influx is an early and sensitive indicator of TCR-mediated signaling and can be induced even by a single agonist pMHC [50]. Even in the absence of agonist pMHC, spMHCs on DCs can also induce an observable but transitory influx

of cytosolic calcium in naïve T cells [24]. We reasoned that calcium flux measurements in T cells using live video-microscopy could be used to make a direct comparison of the intensity of proximal spMHC-mediated signaling by the same syngeneic dendritic cells in OT-1 and F5 T cells. As spMHC-dependent calcium signals in T cells interacting with DCs in the absence of foreign antigen are weak, transitory and unsynchronized, a large number of T:DC pairs need to be imaged at a high frequency. DC2.4 cells were particularly suited for this as they induce robust *in vitro* LIP of OT-1 T cells such that a large fraction of T cells respond to spMHC (see Figure 3-1) and also have a dramatically different effect on OT-1 and F5 T cells (see Figure 3-2).

OT-1 and F5 T cells were labeled with a calcium-sensitive dye (Fura 2AM) and co-cultured with DC2.4 cells at 100% confluence in a 1:1 ratio, causing all the T cells to be in contact with at least one dendritic cell. 100 to 200 T:DC pairs were were imaged every 15 seconds at $400\times$ magnification for up to 60 minutes to limit possible phototoxicity from repeated UV excitation (see Appendix A.4). Imaging for longer periods was also prohibited by the gradual loss of Fura dye from the T cell cytoplasm due to sequestration into intra-cellular compartments. The fluorescence excitation ratio of Fura dye at 340:380 nm, which is linearly correlated with cytosolic calcium levels, was analyzed in individual T cells. When the T cells were cultured by themselves, the Fura ratio in $> 99\%$ of the cells remained below 0.6 for the entire duration of tracking. Therefore, a Fura ratio of > 0.6 was considered to be indicative of TCR-induced calcium flux in this system.

Although all imaged T cells were in contact with dendritic cells, calcium flux above background was detectable in only $\sim 50\%$ of the T cells in the case of both OT-1 and F5 cells, (see Figure 3-4). Similar data have been previously described for polyclonal naïve $CD8^+$ or $CD4^+$ cells or TCR-transgenic HNT T cells but a comparison between T cells bearing different TCRs has not yet been reported [24]. Both OT-1 and F5 cells instantly showed a comparably strong and sustained calcium flux on exposure to agonist peptides (see Figure 3-5), confirming that there was no inherent defect in proximal TCR signaling in either of these T cells. However, there were no obvious differences in calcium influx between OT-1 and F5 T cells during the first 30 minutes

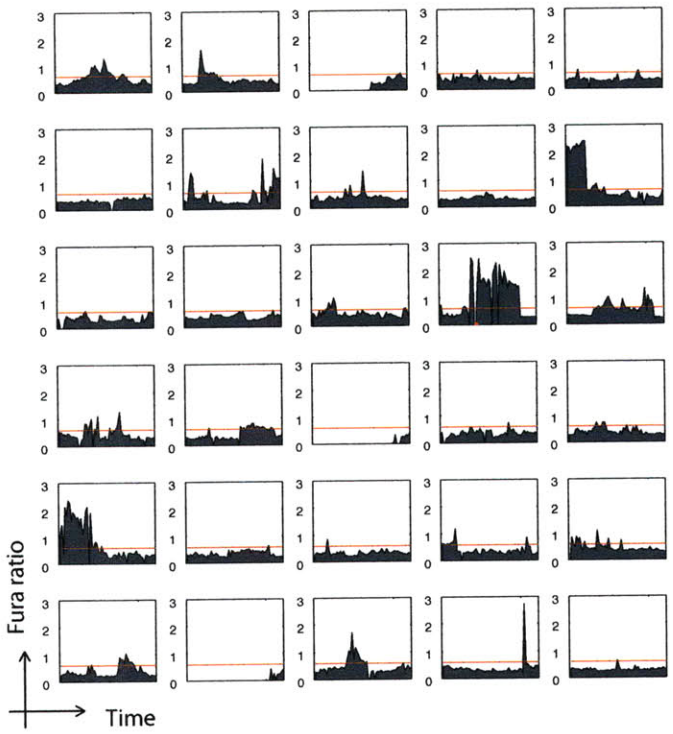

Figure 3-3: **Calcium flux traces of OT-1 cells co-cultured with DC2.4.** Fura-labeled OT-1 were co-cultured with DC2.4 cells in a 1:1 ratio at 100% confluence, such that all the T cells were in contact with DCs. Fluorescence excitation was recorded for every 15 seconds for 30 minutes and the Fura ratios in tracked T cells were used to estimated calcium influx. Representative traces of cytosolic calcium signal (represented by Fura ratio) for 30 randomly picked OT-1 cells are shown. The horizontal red line indicates the background level (Fura ratio = 0.6) of calcium flux seen when OT-1 cells are cultured by themselves.

of T:DC co-culture. This was in stark contrast to the difference in LIP between OT-1 and F5 T cells observed at three days after co-culture with the same dendritic cells in nearly identical conditions (see Figure 3-2). It is conceivable that there may still be some subtle differences in spMHC-mediated TCR signaling between OT-1 and F5 cells, which are undetectable in the short timescales of proximal TCR signaling leading to calcium influx, but which, cumulatively, could result in differential proliferation over longer timescales.

Some naturally occurring self-peptides presented on murine K^b, which are recognized by the OT-1 TCR, have been identfied [107]. Among these, two peptides,

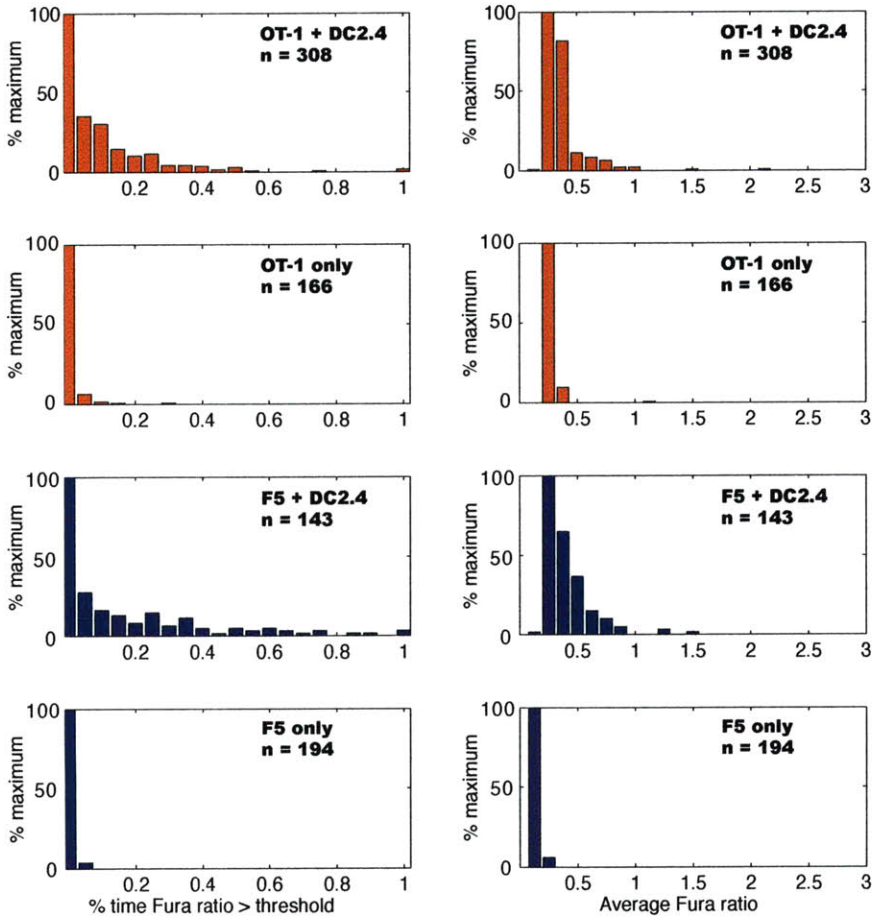

Figure 3-4: **Comparison of calcium flux in OT-1 and F5 T cells induced by the same spMHC repertoire.** Fura-labeled OT-1 (top two panels) or F5 (bottom two panels) T cells were co-cultured with DC2.4 cells and calcium influx was estimated as shown in Figure 3-3. Histograms of the fraction of of time the cells fluxed calcium above background, i.e. Fura ratio > 0.6 (left panel) and histograms of the average Fura ratio recorded for the entire duration of the tracking (right panel) are plotted.

RTYTYEKL and ISFKFDHL, can induce positive selection of OT-1 T cells in fetal thymic organ cultures. OT-1 T cells were co-cultured with BMDCs derived from syngeneic B6 TAP$^{-/-}$ mice in the presence of 5 μM of these positively selecting peptides and T cell calcium influx was recorded (see Figure 3-5). Calcium influx was very close to background in the absence of any additional peptide. ISFKFDHL induced a mild increase in average Fura ratio in each cell while the pattern of calcium influx induced by RTYTYEKL was comparable to endogenous self-peptides presented by wild-type

B6 BMDCs. Indeed, RTYTYEKL is more potent than ISFKFDHL in the co-receptor dulling assay for positive selection using DP OT-1 cells [107]. The agonist peptide, SIINFEKL (1 μM) induced a very strong calcium influx in majority of the OT-1 cells. This further confirms that the degree of calcium influx observed in this assay system is consistent with the known strength of interaction of a given TCR with different spMHC and may be used to interpret differences in the responsiveness of OT-1 and F5 T cells to spMHCs presented on dendritic cells.

3.3 Differential imprinting of baseline CD5 levels

While it was surprising that OT-1 and F5 cells exhibited similar Ca^{2+} influx in response to the same spMHC repertoire presented on DCs, we wondered if this could be due to the fact that freshly isolated OT-1 have higher levels of CD5 than F5 cells as CD5 is a known negative regulator ofproximal TCR signaling. The level of CD5 is maintained by engagement with spMHC in the periphery but the levels can be restored to a baseline after culturing the cells in vitro in the absence of spMHC [113]. Therefore, we cultured OT-1 and F5 cells in vitro in order to allow their CD5 levels to equalize. The cells were cultured in the presence IL7 to maintain their viability. As expected, the levels of CD5 in OT-1 and F5 cells steadily decreased in both the cell types after withdrawal from spMHC but surprisingly, the differences between OT-1 and F5 persisted throughout the duration of the experiment, such that the CD5 levels decayed to *different* 'baselines' (see Figure 3-6). We confirmed that this was not due IL7 as varying the concentration of IL7 did not impact the rate of CD5 decay. The experiment could not be extended beyond five days because of substantially reduced viability of cells in conditions with low concentrations of IL7. This suggests that neither TCR nor IL7 signals are required to maintain the *differences* in CD5 levels between OT-1 and F5 cells. Furthermore, the fractional decrease in CD5 levels was comparable in OT-1 and F5 cells. This suggests that both OT-1 and F5 T cells receive sufficient spMHC-mediated signals to maintain their surface levels of CD5 a little over 50% above baseline in vivo.

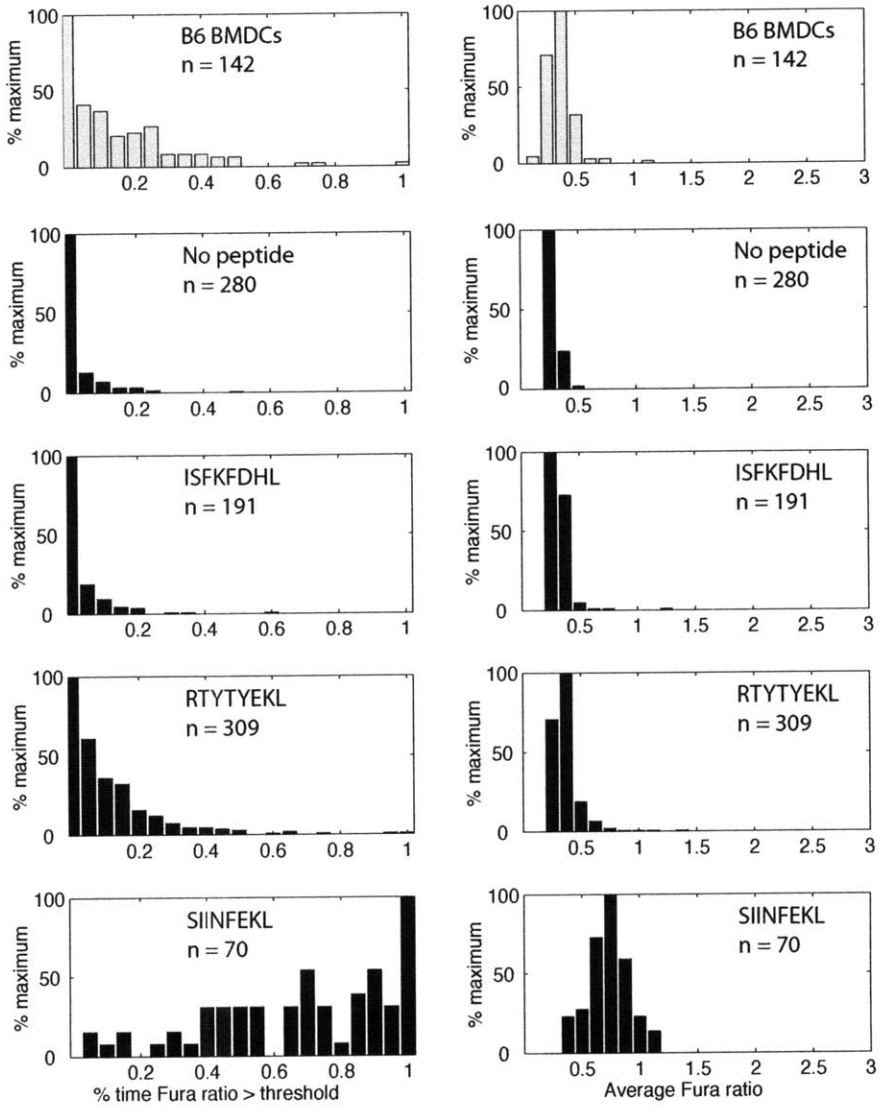

Figure 3-5: **Calcium flux induced in OT-1 cells by positively selecting spMHC.** Histograms of the fraction of of time the cells fluxed calcium above background, i.e. Fura ratio > 0.6 (left panel) and histograms of the average Fura ratio recorded for the entire duration of the tracking (right panel) are plotted. The top panel shows the analysis of calcium flux in OT-1 cells co-cultured with B6 BMDCs. The lower panels show OT-1 cells co-cultured with B6.TAP$^{-/-}$ BMDCs co-cultured with no peptide, ISFKFDHL (5 μM), RTYTYEKL (5 μM) and SIINFEKL (1 μM).

Given that the 'baseline' levels of CD5 appear to be differentially imprinted in OT-1 and F5 T cells, we tested if the differences in CD5 levels are maintained even after T cell activation and differentiation into 'memory-like' cells in vitro. OT-1 and F5 T cells were activated with an identical dose of PMA/ionomycin, and cultured in

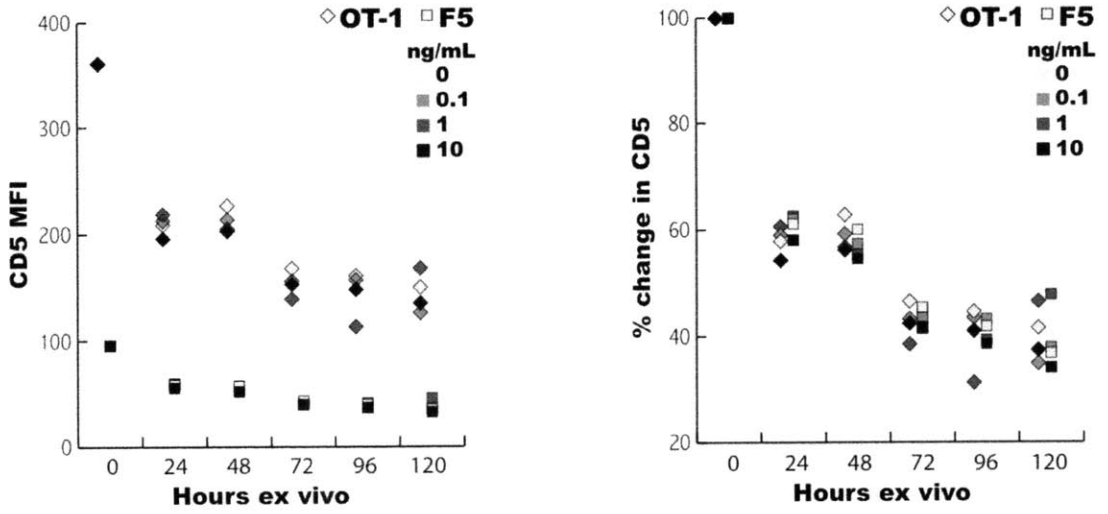

Figure 3-6: **Differences in 'baseline' levels of CD5.** OT-1 and F5 cells were cultured in vitro in varying concentrations of IL7 for five days and CD5 levels were assayed daily. The levels of CD5 decrease in both cell types upon withdrawal of spMHC signaling but do not equalize.

200 U/mL of IL2 for three days, and rested in 10 ng/mL of IL7 for an additional four days. Even after T cell activation and several rounds of proliferation, the differences in CD5 level were still found to persist (see Figure 3-7). This strongly suggests that the relative CD5 level is an intrinsic or imprinted property of T cells. The intrinsic differences in CD5 expression, a negative regulator of TCR signaling, suggests that the TCR signaling network itself may be intrinsically different among $CD8^+$ T cells.

3.4 Positive selection of OT-1 and F5 T cells occurs at different strengths

The lack of any obvious difference in proximal TCR signaling in OT-1 and F5 cells is surprising and may be due to the compensatory effects of differences in their CD5 levels. However, OT-1 cells are predicted to have a higher avidity for their cognate spMHC than F5 cells, given that developmental upregulation of the CD5 level during thymic selection is thought to parallel the avidity of the positively selecting TCR:spMHC interaction [7, 6]. Therefore, we measured the CD5 profiles of DP OT-1

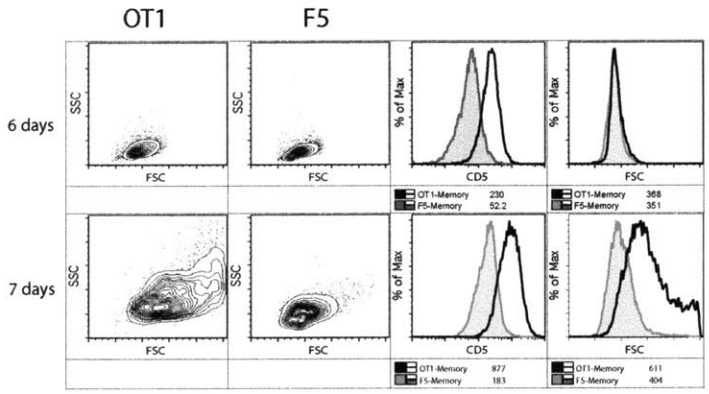

Figure 3-7: **Differences in CD5 levels and selective IL7 responsiveness persist after differentiation into memory-like cells in vitro.** OT-1 and F5 cells were differentiated into memory-like cells after activation with PMA/ionomycin and culture in IL2 (200 U/mL) for three days, followed by culture in IL7 (10 ng/mL) for a additional three days. The FSC in OT-1 and F5 cells were comparable at this stage (top panel). FSC was assayed again after 24 hrs of IL7 treatment (lower panel). The relative differences in CD5 levels between OT-1 and F5 cells persisted throughout the experiment.

and F5 T cells. A direct comparison of the CD5 profiles in these two DP cells is not possible as the CD5 profiles of OT-1 and F5 T cells are strikingly different, with only OT-1 DP cells resembling that of non-transgenic B6 mice. The CD5 profile of DP cells in F5 thymi is consistent with a significant accumulation of DP cells at the $CD5^{hi}$ stage of maturation, suggestive of a partial block in the maturation of F5 DP $CD5^{hi}$ cells into SP $CD8^{+}$ cells (see Figure 3-9). This was tested using competitive reconstitution of the naïve T cell compartment in B6.$Rag^{-/-}$ mice with a 1:1 mix of bone marrow progenitors obtained from OT-1 and F5 $Rag^{-/-}$ mice (see Appendix A.7). Strikingly, $> 95\,\%$ of the DP T cells in the thymus were of F5 origin, although the numbers of OT-1 and F5 T cells in the periphery were almost equal. This supports the notion that a majority of F5 T cells are indeed arrested in the DP $CD5^{hi}$ stage and accumulate until they die by neglect, presumably due to low abundance of appropriate positively selecting cognate spMHC for the F5 TCR in the thymic epithelium. Thus, F5 T cells that do make it through positive selection may experience a weaker positively selecting signal than OT-1 T cells. These results suggest that the F5 TCR

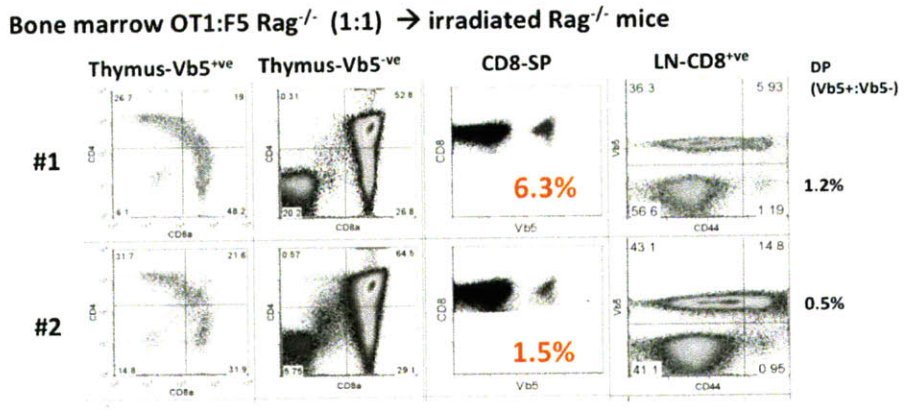

(a) Mixed bone marrow chimeras

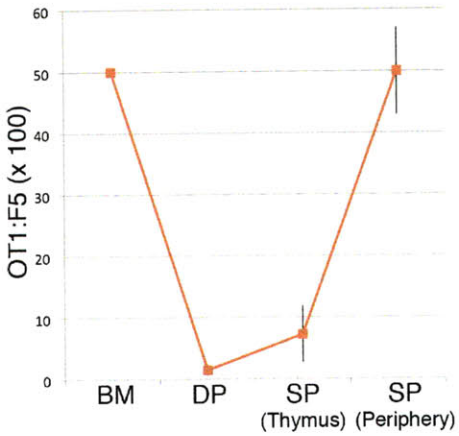

(b) Competitive reconstitution

Figure 3-8: **Analysis of OT-1 and F5 mixed hematopoietic chimeras.** (a) OT-1/F5 mixed hematopoietic chimeras were generated after reconstitution of sublethally irradiated Rag1$^{-/-}$ mice with a 1:1 mixture of donor OT-1 and F5 bone marrow cells. Reconstitution of T cells in the thymus and periphery was analyzed six weeks after reconstitution. The DP cells (Vβ5^{-ve}) and SP CD8^{+} cells in the thymi of these mice are predominantly of F5 origin. In contrast, the reconstitution of the periphery is equivalent for OT-1 and F5 cells. FACS profiles from two representative mice are shown. (b) Plot of the ratio of OT-1:F5 cells in the donor cells (BM) and at each stage of development (DP, SP-Thymus and SP-Periphery) in the reconstituted mice (n=4).

may indeed have a lesser avidity for its cognate spMHC than the OT-1 TCR that results in weak positive selection of the F5 TCR and the death by neglect of a majority of the F5 DP CD5^{hi} cells .

In our model system, OT-1 and F5 TCR transgenes are in a background with limited negative selection. Therefore, we hypothesized that the thymic output could

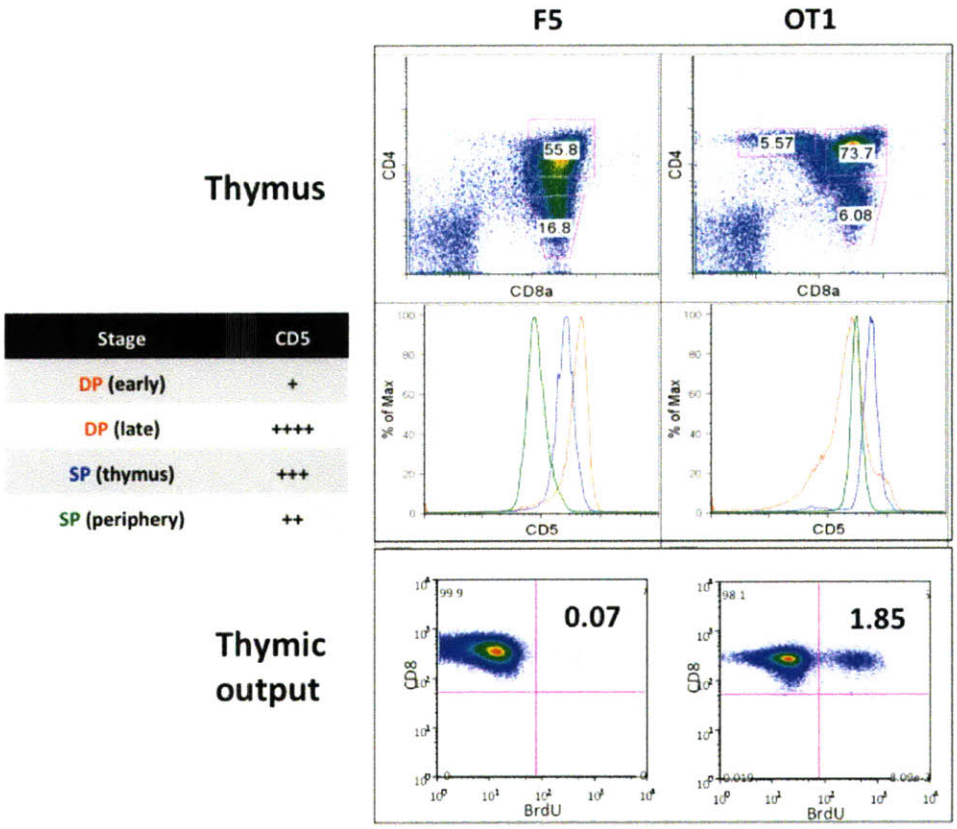

Figure 3-9: **Differences in the strength of selection of OT-1 and F5 mice.** The CD4 vs. CD8 profiles of the thymi of OT-1 and F5 mice are shown in the top panel. The middle panel shows the CD5 levels in DP (red), SP $CD8^+$ cells from the thymus (blue), and $CD8^+$ cells from the periphery (green). The relative levels of CD5 in these cells from WT mice is shown in the corresponding table. Thymic output in OT-1 and F5 mice, as assessed by BrdU staining of peripheral naïve T cells at 48 hrs after BrdU injection is shown in the lowest panel.

also be used as a surrogate measure of the strength of the positively selecting signal received by OT-1 and F5 TCRs. BrdU was injected i.p. into OT-1 and F5 mice and the percentage of naïve $BrdU^+$ $CD8^+$ cells was measured in the periphery after 24 and 48 hrs (see Appendix A.5). As naïve OT-1 or F5 cells are not in cell cycle in the periphery, BrdU is incorporated only into the rapidly proliferating immature T cells in the thymus and the percentage of $BrdU^+$ T cells in the periphery reflects the rate of thymic output. Our results suggest that the thymic output is about 10-fold higher in OT-1 mice (see Figure 3-9). This also supports the conclusion that the F5 T cells receive a weaker TCR signal during positive selection as compared to OT-1 cells.

3.5 Differences in proliferative capacity among $CD8^+$ cells

Given that the spMHC-induced calcium influx studies revealed no obvious differences in proximal TCR signaling between OT-1 and F5 T cells, and yet they exhibited markedly different proliferation responses to the same spMHCs presented on dendritic cells, we considered the possibility that the two T cells had intrinsically different proliferative capacities that may be manifest even upon receiving the *same* proximal TCR signal. We assayed the response of OT-1 and F5 cells to saturating doses of agonist peptides. CFSE-labeled OT-1 and F5 splenocytes were cultured in a saturating level of IL2 (200 U/mL) with up to 5 μM of their respective agonist pMHC (see Figure 3-10). Both OT-1 and F5 cells completely diluted their CFSE at 48 hrs, indicating that there was no intrinsic defect in the proliferation capacity of either cell type. However, OT-1 and F5 T cells respond to different agonist pMHCs, i.e. SIINFEKL/K^b and ASNENMDAM/D^b, respectively. The differences in the affinities of these agonist pMHC complexes for their respective TCRs and possible differences in the stability of these pMHC complexes make it difficult to devise a pMHC-based system, whereby a genuinely 'identical' TCR stimulus is delivered to OT-1 and F5 cells. Instead, we pulsed OT-1 and F5 cells as well as sorted naïve $CD8^+$ $CD5^{hi}$ and $CD5^{lo}$ cells for four hours with PMA (10 ng/mL) and ionomycin (500 ng/mL), which activate the downstream TCR pathways independent of TCR specificity, and measured their proliferation upon culture with a saturating concentration of IL2 (200 U/mL). OT-1 cells and polyclonal $CD5^{hi}$ cells had a slightly higher rate of division but all cells eventually diluted their CFSE completely by 2-3 days (see Figure 3-11) regardless of their CD5 levels. This suggests that $CD5^{hi}$ cells have an intrinsic capacity to proliferate *faster* than $CD5^{lo}$ cells even when they receive the same stimulation of the TCR pathway.

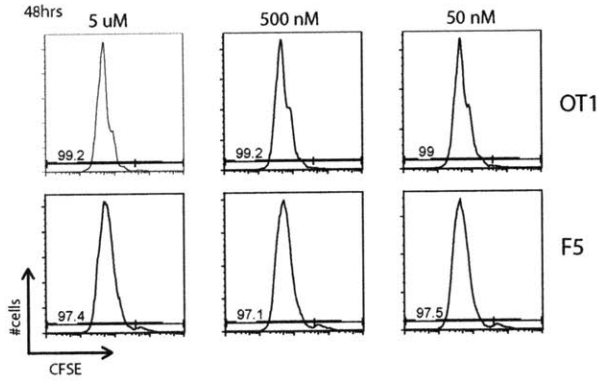

Figure 3-10: **Proliferation of OT-1 and F5 T cells induced by agonist peptides.** 10^5 CFSE labeled OT-1 and F5 splenocytes were cultured in 5 to 0.05 µM of agonist peptides (SIINFEKL and ASNENMDAM respectively)for 48 hrs with 200 U/mL of IL2. The CFSE profiles of $CD8^+$ T cells at 48 hours are shown above.

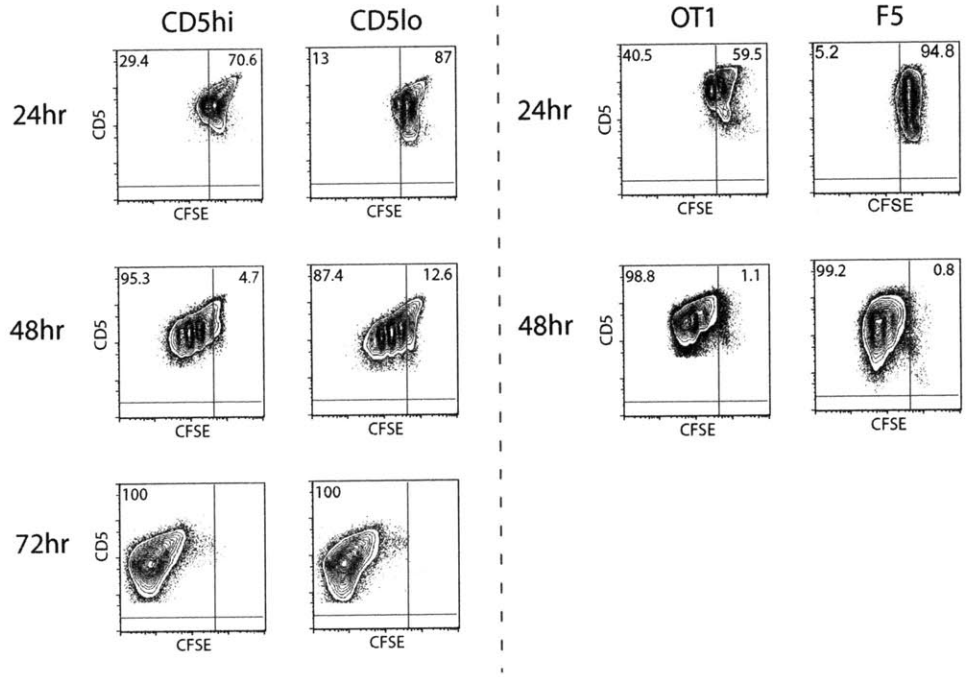

Figure 3-11: **Proliferation of $CD5^{hi}$ and $CD5^{lo}$ cells stimulated with PMA/Ionomycin.** Naïve $CD8^+$ $CD5^{hi}$ and $CD5^{lo}$ cells or OT-1 and F5 T cells were stimulated with PMA and ionomycin and subsequently cultured in IL2 (200 U/mL) for 3 days. Proliferation at 24, 48, and 72 hrs is shown.

Chapter 4

Intrinsic heterogeneity in T cells

Estimation of proximal TCR signaling events by cytosolic calcium influx induced by the same syngeneic spMHC repertoire in OT-1 and F5 T cells did not reveal an appreciable difference. Thus, differences in the rates of LIP between OT-1 and F5 cells in the same MHC background may not be due to differences in their strengths of interaction with spMHC. Alternatively, evidence for *intrinsic* differences in the $CD8^+$ T cell response to IL7 is presented in this chapter.

4.1 Heterogeneity in IL7-mediated proliferation

As the TCR and IL7 signaling pathways are interlinked and both pathways are involved in LIP [92], we determined if the differences in LIP of $CD5^{hi}$ and $CD5^{lo}$ naïve $CD8^+$ T cells could be due to *instrinsic* differences in IL7 signaling. CFSE labeled OT-1 and F5 T cells were co-cultured in the same well in vitro in the presence of 10 ng/mL of IL7 for seven days at a low density (5×10^4 cells/mL) to minimize cell-cell contacts, as well as possible TCR-spMHC interactions. OT-1 cells were observed to preferentially proliferate (see Figure 4-1a). Unlike LIP, there was no change in CD44, CD25 or CD69 levels but only an increase in cell size. This IL7-dependent proliferation of naïve $CD8^+$ T cells occured only at doses of IL7 greater than 1 ng/mL (see Figure 4-1b). Similarly, when congenically marked $CD5^{hi}$ and $CD5^{lo}$ subsets of B6 polyclonal naïve $CD8^+$ T cells were cultured in the same well with 10 ng/mL of

IL7, $CD5^{hi}$ cells were observed to proliferate preferentially (see Figure 4-2). To exclude the possibility that some concomitant spMHC-induced TCR signaling was also present in this system, because $CD8^+$ T cells do express low levels of class I MHC, we repeated the same experiment using $CD8^+$ $TAP^{-/-}$ T cells, which lack class-I MHC (see Figure 4-2). As $CD8^+$ T cells are not selected in $TAP^{-/-}$ mice, they were generated in hematopoietic chimeras of bone marrow from B6.$TAP^{-/-}$ mice implanted in B6.$Rag^{-/-}$ recipients (see Appendix A.7). When sorted $CD5^{hi}$ and $CD5^{lo}$ fractions of $CD8^+$ $TAP^{-/-}$ T cells were cultured in the presence of 10 ng/mL IL7 as above, $CD5^{hi}$ cells were still found to preferentially proliferate (see Figure 4-2). Thus, a high CD5 level appears to mark the ability of naïve $CD8^+$ cells to proliferate in response to high doses of IL7 alone. In all the above experiments, the relative differences in CD5 levels were maintained even after seven days in culture with IL7 alone (see Figures 4-1a and 4-2) in the absence of spMHC-induced TCR signaling. This also suggests that the CD5 level in OT-1 and F5 cells may be differentially imprinted in the two cell types.

4.2 Differences in IL7 response persist after memory differentiation

Naïve T cells do not express receptors for IL2, namely IL2Rα and IL2Rβ. However memory cells have high levels of IL2Rβ and proliferate in response to IL2 and IL15. We tested if the differential ability to proliferate in response to IL7 was preserved after differentiation into memory-like cells. After differentiation into memory-like cells, OT-1 and F5 T cells were cultured in the presence of IL2, IL7 or IL15 (see Figure 4-3). OT-1 cells retain their ability to selectively proliferate in response to IL7 even after multiple rounds of activation-induced proliferation. This suggests that the selective responsiveness to IL7 in OT-1 cells is imprinted and is an intrinsic feature of these T cells. As F5 cells can proliferate in response to IL2 and IL15, it further confirms that there is no global defect in cell proliferation in F5 cells.

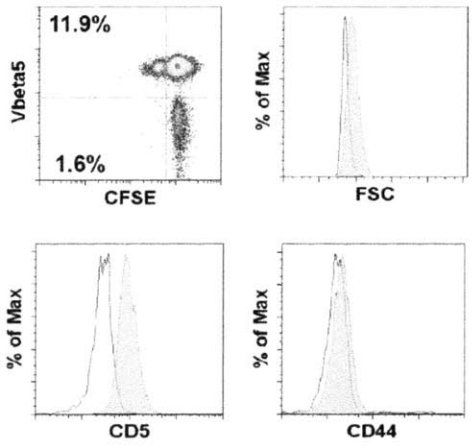

(a) CFSE vs CD5

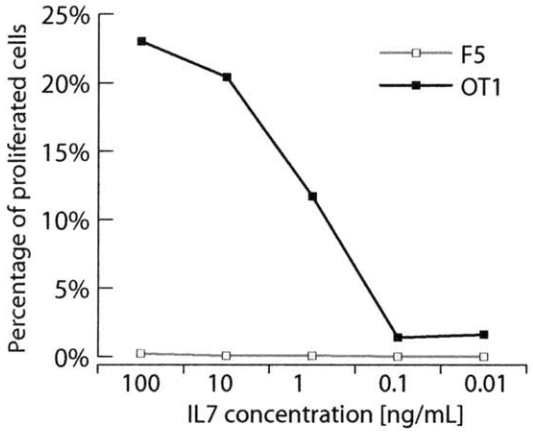

(b) Proliferation in different IL7

Figure 4-1: **Proliferation of OT-1 and F5 T cells in response to IL7 alone.** (a) 1×10^5 CFSE labeled OT-1 and F5 T cells were cultured in the same well with 10 ng/mL of IL7 in vitro for seven days with medium changes every third day. OT-1 cells were distinguished by presence $V\beta5^+$ staining. (b) Proliferation of naïve OT-1 and F5 cells is assessed in varying concentrations of IL7.

4.3 Differences in 'baseline' IL7R levels

IL7R is under chronic feedback suppression due to IL7 signaling in vivo [93]. Therefore, the levels of surface IL7R in freshly isolated OT-1 and F5 cells were compared after cytokine withdrawal following overnight culture in medium with no IL7 (see Figure 4-4). While freshly isolated cells showed a modest difference in IL7R, culture of OT-1 and F5 T cells in vitro in the absence of IL7 unmasked a significant difference in the 'baseline' level of IL7R. IL7R levels were completely suppressed in the presence

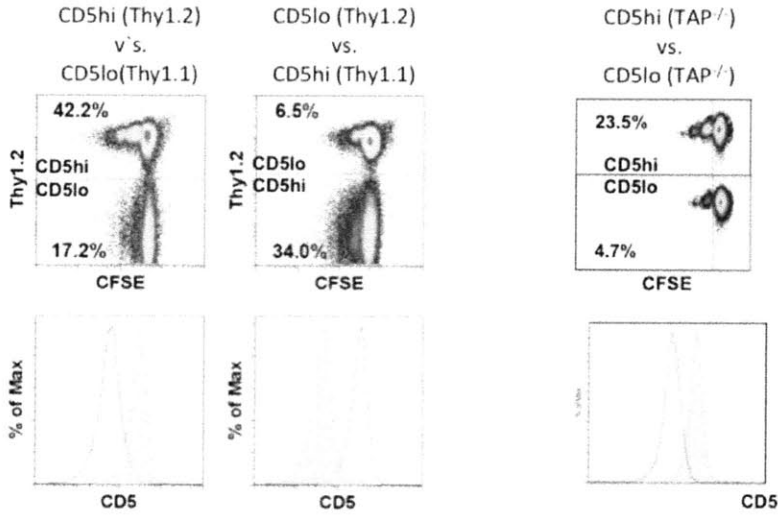

Figure 4-2: **Proliferation of CD5^{hi} and CD5^{lo} cells in IL7 alone.** 10^5 CFSE-labeled naïve CD8$^+$ CD5^{hi} and CD5^{lo} T cells, congenically marked with Thy1.1 and Thy1.2 respectively (and vice versa), were cultured in the same well in 10 ng/mL of IL7 in vitro for seven days with medium changes every third day. Similarly, TAP$^{-/-}$ CD5^{hi} and CD5^{lo} cells were treated in the same manner. The lower panel shows the CD5 levels after seven days in culture in the absence of spMHC stimuli.

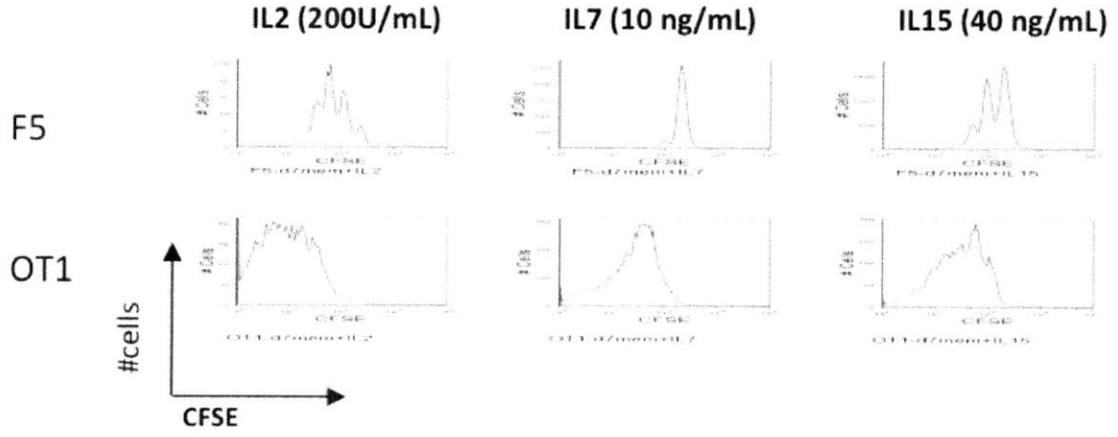

Figure 4-3: **Differences in responsiveness of OT-1 and F5 cells to gamma-chain cytokines after differentiation into memory-like cells in vitro.** OT-1 and F5 cells were differentiated into memory-like cells as before and labeled with CFSE. CFSE dilution was assayed after treatment with IL2 (200 U/mL), IL7 (10 ng/mL) and IL15 (40 ng/mL).

of 10 ng/mL of IL7 in both OT-1 and F5 cells (see Figure 4-4). Polyclonal CD5^{hi} and CD5^{lo} cells showed concordant differences in IL7R levels, suggesting that there could be an intrinsic difference in the IL7 pathway itself that is marked by differences in

CD5 levels.

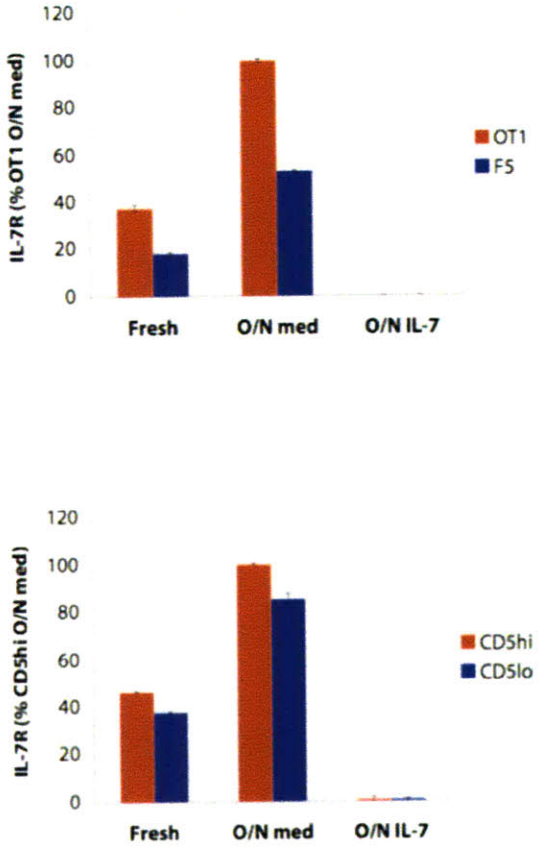

Figure 4-4: **Differences in IL7R levels between CD5^{hi} and CD5^{lo} cells.** The surface levels of IL7R levels in naïve polyclonal CD5^{hi} and CD5^{lo} cells as well as OT-1 and F5 cells were measured under the following conditions: (i) freshly isolated (ii) overnight rested in medium alone (iii) overnight rested in medium with 10 ng/mL IL7.

4.4 Differences in IL7 signaling

To identify molecular differences in the IL7 signaling pathway we measured IL7-induced phosphorylation of Stat5 and Gsk3 and increase in Bcl2 and CD8α levels in OT-1 and F5 T cells as well as naïve polyclonal CD5^{hi} and CD5^{lo} cells by flow cytometry. T cells were rested overnight to eliminate any effects of possible heterogeneous TCR or IL7 signaling received in vivo before measuring the intermediates of IL7

signaling. This also restores the IL7R level to its baseline uninhibited state. Phosphorylation of Stat5 and GSK3 was measured at 20 minutes and 24 hrs respectively after treatment with 10 ng/mL of IL7 (see Figure 4-5). A higher level of phosphorylation of Stat5 and GSK3, was seen in OT-1 and polyclonal $CD5^{hi}$ cells. The induction of Bcl2 and CD8α at 24 hrs after exposure to IL7 10 ng/mL, was also higher in OT-1 and polyclonal $CD5^{hi}$ cells (see Figure 4-5). This shows that the differences in baseline IL7R levels between $CD5^{hi}$ and $CD5^{lo}$ cells are functional or could imply that there are additional intrinsic differences within the IL7 pathway in cells marked by different levels of CD5. These results are in apparent contradiction to the predictions of the 'co-receptor tuning' model proposed by Park et al [94]. In their model system, $CD8^+$ T cells with a high avidity for spMHC (T cells from male HY mice) require a period of overnight rest before the IL7 pathway is relieved of spMHC-mediated suppression. However, the IL7-pathway does not appear to be under spMHC-mediated suppression in both OT-1 and F5 cells and robust pStat5 induction is observable in both freshly isolated OT-1 and F5 cells (see Figure 4-6).

4.5 Variation in the metabolic states of cells with different levels of CD5

We found a strong correlation between CD5 level and forward angle light scatter by flow cytometry for both polyclonal and TCR-transgenic naïve $CD8^+$ T cells (see Figure 4-7). Forward scatter is well correlated with cell size as determined by light microscopy. Cell growth and proliferation are intimately linked and it is suggested that a cell needs to attain a minimum size before it can divide [54]. The differences in cell size between naïve OT-1 and F5 Tcells or polyclonal $CD8^+$ $CD5^{hi}$ and $CD5^{lo}$ cells could partially explain the differences in their kinetics of proliferation in response to identical doses of PMA and ionomycin. We also identified differences in the uptake of glucose in OT-1 and F5 cells, as measured using the uptake of a fluorescent analog of glucose, 2-NBDG (see Figure 4-8). F5 T cells consistently uptake more glucose than

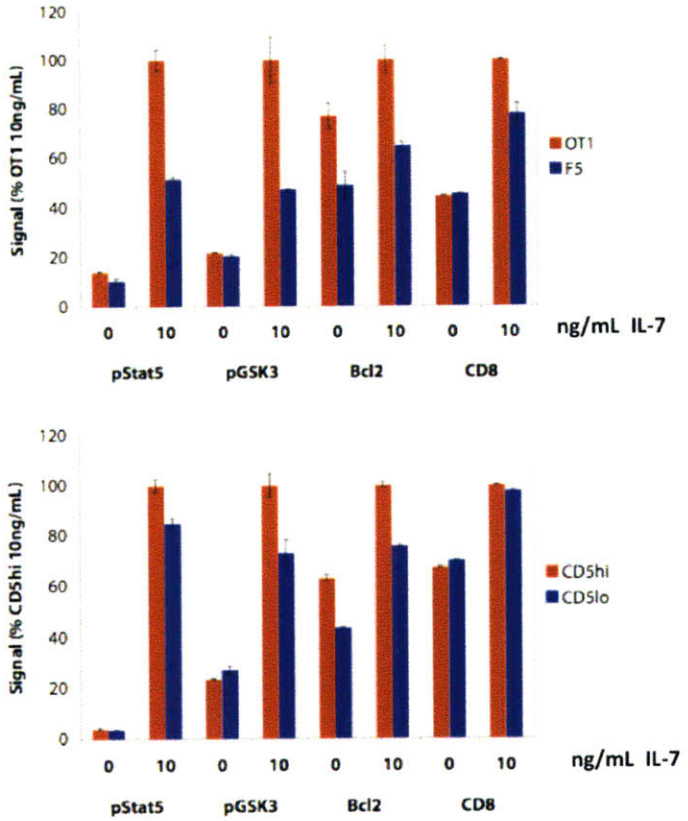

Figure 4-5: **Differences in IL7 signaling between CD5^{hi} and CD5^{lo} T cells.** OT-1 and F5 cells or polyclonal naïve CD8^{+} CD5^{hi} and CD5^{lo} cells were rested overnight in medium without any IL7 to allow any residual IL7 and spMHC-mediated signals to dissipate. They were then treated with or without 10 ng/mL IL7 and the levels of pStat5, Gsk3, Bcl2 and CD8α were measured at 24 hrs except for pStat5 which was measured at 20 minutes.

OT-1 cells. There is a modest increase in glucose uptake following IL-7 treatment but the difference between OT-1 and F5 cells persists. F5 cells as well as CD5^{lo} cells have a better ability to survive in low concentrations of IL7 in vitro as compared to CD5^{hi} cells. This suggests that there is a spectrum of metabolic differences between OT-1 and F5 cells which could also contribute to their differential survival and proliferation capacities.

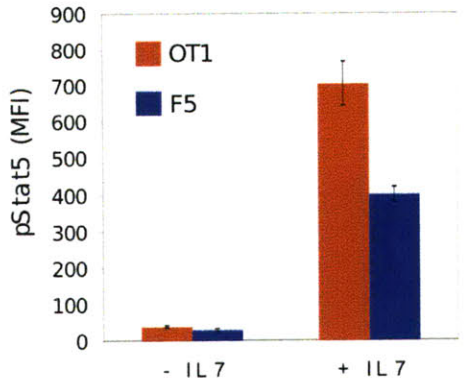

Figure 4-6: **IL7-mediated pStat5 induction in freshly isolated naïve OT-1 and F5 T cells.** The levels of pStat5 were measured by intracellular staining in freshly isolated OT-1 and F5 T cells treated with or without 1 ng/mL IL7 for 20 minutes.

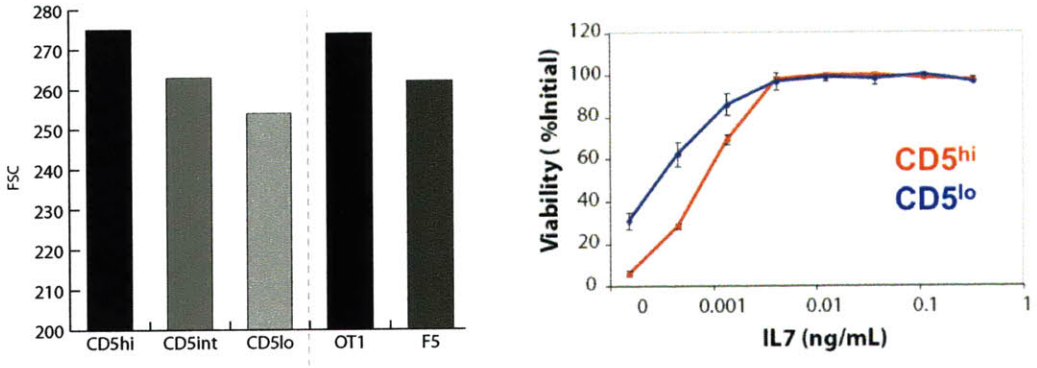

(a) Cell size

(b) Cell survival

Figure 4-7: **Intrinsic heterogeneity in cell size and in survival under conditions of cytokine deprivation.** (a) Variation in cell size as estimated by forward scatter (FSC) in freshly isolated T cells is shown above. Polyclonal $CD8^+$ cells were divided equally into three fractions of CD5 high, intermediate and low populations for this comparison. Cell size is positively correlated with the level of CD5 on both naïve polyclonal and TCR transgenic T cells. (b) Cell survival of naïve $CD5^{hi}$ and $CD5^{lo}$ $CD8^+$ T cells at 72 hours after ex vivo culture in varying concentrations of IL7.

4.6 Intraclonal heterogeneity among T cells expressing the same TCR

A small variation in CD5 levels is seen even among T cells from a single TCR transgenic mouse. To see if this variation in CD5 levels, despite its low magnitude, reflects

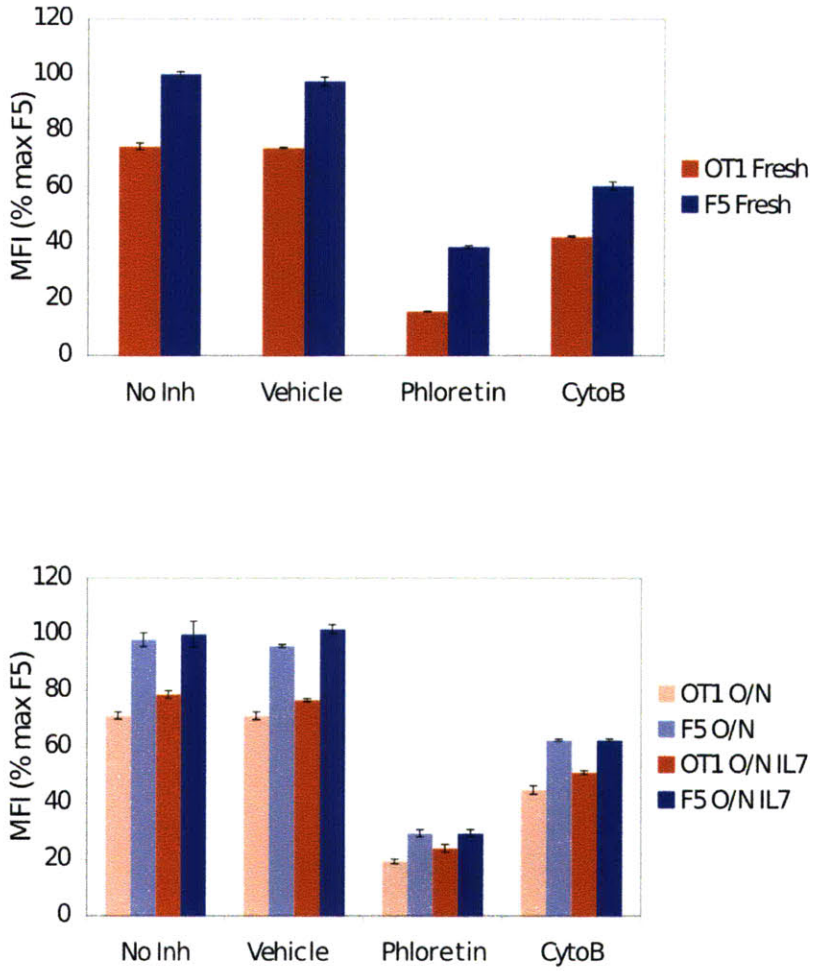

Figure 4-8: **Glucose uptake in OT-1 and F5 cells measured by NBDG fluorescence.** Glucose uptake in OT-1 and F5 was estimated by culturing cells in 100 μM NBDG for 1 hour in glucose-free medium and measuring the fluorescence of live cells using a flow cytometer. Reduced uptake of NBDG was seen in the presence of phloretin (100 μM) and cytochalasin B (10 μM), which are known inhibitors of glucose uptake. The NBDG uptake seen in freshly isolated (upper panel) and overnight rested (lower panel) OT-1 and F5 cells are shown above.

a functional intra-clonal heterogeneity among T cells selected by an identical TCR within the same animal, we sorted naïve T cells from either OT-1 or F5 $Rag^{-/-}$ mice into $CD5^{hi}$ and $CD5^{lo}$ populations. To increase the specificity of sorting, the CD5 antigen was simultaneously stained with two anti-CD5 antibodies labeled with different fluorochromes. This allowed simultaneous detection of CD5 in two different channels on the FACS instrument, while minimizing measurement and staining errors that can adversely impact the flow sorting of a narrow population of cells. The

sorted cells were treated in the same way as in Figures 4-1a and 4-2. Culture in 10 ng/mL of IL7 showed that naïve $CD5^{hi}$ OT-1 T cells had a modestly higher rate of proliferation than $CD5^{lo}$ OT-1 cells. No proliferation was seen with either $CD5^{hi}$ or $CD5^{lo}$ F5 T cells (see Figure 4-9). We also tested if the CD5 level is imprinted in T cells after differentiation into memory-like cells after in vitro activation. Differences in the level of CD5 in sorted populations of $CD5^{hi}$ and $CD5^{lo}$ cells from OT-1 and F5 mice were observed to persist after activation and differentiation into memory-like cells in vitro. This shows CD5 level is indeed an intrinsic property of T cells and could be used analogous to a lineage marker for determining the proliferation capacity of naïve $CD8^+$ T cells, independent of their response to TCR or IL7 signaling. Strikingly, the differences in rates of proliferation could be discerned even when sorted OT-1^+ $CD5^{hi}$ FSC^{hi} and $CD5^{lo}$ FSC^{lo} cells were transferred into into $Rag^{-/-}$ mice and assayed by a CFSE dilution assay at five days post transfer (see Figure 4-10). Thus, even in the presence of the same spMHC, T cells expressing the same TCR can have different rates of IL7-induced proliferation both in vitro and in vivo. This further supports the notion that intraclonal variation among T cells is non-genetic.

Our demonstration of intra-clonal heterogeneity within the same TCR transgenic mice suggest that the differences in the 'baseline' CD5 levels among naïve $CD8^+$ T cells are non-genetic and robustly imprinted even if small in magnitude. This suggests that this heterogeneity is the outcome of differential imprinting, possibly of multiple loci, in T cells. We believe that such imprinting arises from a robust one-time epigenetic remodeling event rather than by continuous weak signaling in the periphery by spMHC, whose effects (such as partial phosphorylation of CD3ζ, recruitment of ZAP70 to the CD3 complex, or the upregulation of CD5 levels above baseline) have a tendency to dissipate upon withdrawal from continued spMHC stimuli. A major differentiation program involving the epigenetic remodeling of multiple loci is implemented during lineage commitment of T cells in the thymus [16, 126] and it is likely that variation in this one-time epigenetic remodeling event may be responsible for the functional intrinsic heterogeneity in the periphery. As thymic selection is directed by stochastic TCR:spMHC interactions, it is conceivable that the epigenetic

remodeling events of lineage commitment are subject to variation on account of the spatio-temporally variable repertoire of cognate spMHCs in the thymus. Indeed, we have shown than the only a small fraction of F5 thymocytes can successfully complete positive selection while a majority die by neglect, supporting the possibility that the F5 thymocytes that do get selected may have received variable strengths of selecting signals in the thymus (see Figure 3-8).

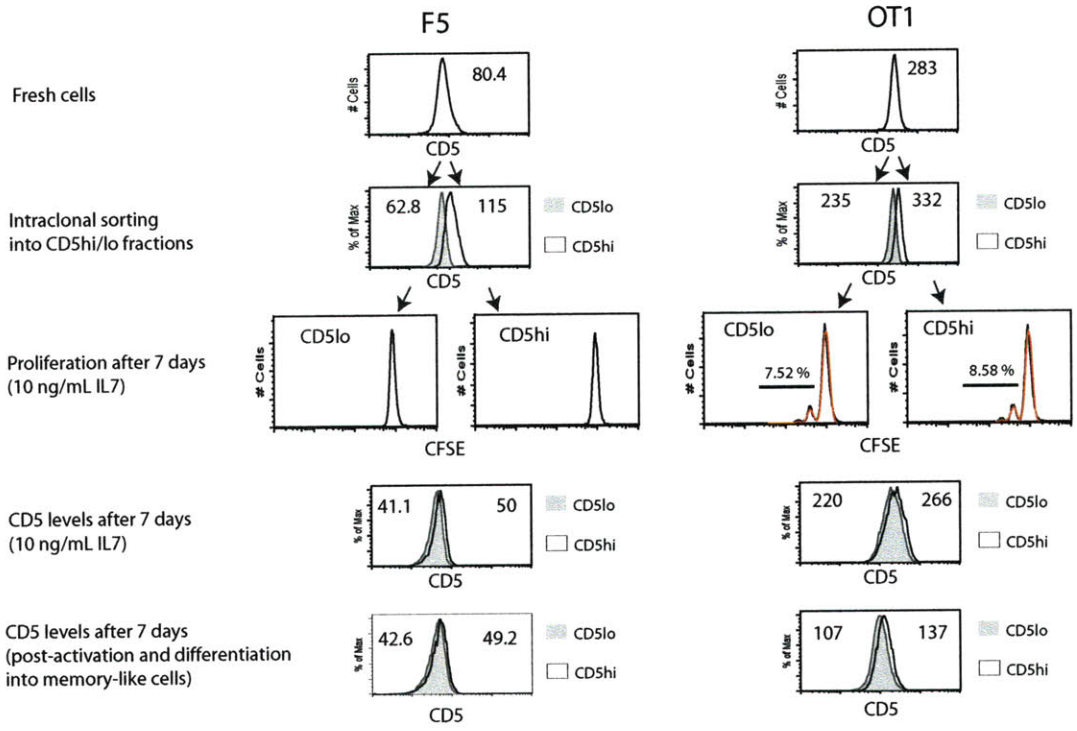

Figure 4-9: **Functional intraclonal heterogeneity within OT-1 and F5 cells.** Naïve OT-1 and F5 T cells were sorted into $CD5^{hi}$ and $CD5^{lo}$ fractions after CD5 staining in two channels. 5×10^5 sorted cells were labeled with CFSE and cultured in 10 ng/mL of IL7 for 7 days, with medium changes every third day and proliferation was assayed at 7 days. The CD5 level at 7 days was also measured. A separate aliquot of 1×10^5 unlabeled cells was activated with PMA/ionomycin for 4 hrs, cultured in 200 U/mL for 3 days, and subsequently transferred into medium containing 10 ng/mL of IL7 for an additional 4 days. The levels of CD5 were assayed in these post-activation memory-like cells at day 7.

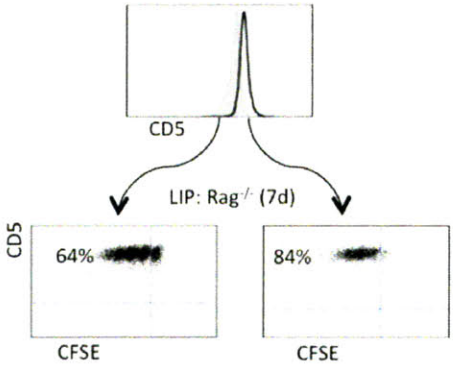

Figure 4-10: **Differences in LIP between CD5^{hi} and CD5^{lo} OT-1 T cells.** Naïve OT-1 cells were sorted into CD5^{hi} FSC^{hi} and CD5^{lo} FSC^{lo} fractions, labeled with CFSE and transferred into syngeneic Rag1$^{-/-}$ mice. CFSE dilution of donor CD8^{+} cells was assayed in cells recovered from the spleens of recipient mice after five days.

Chapter 5

Molecular basis of intrinsic heterogeneity in T cells

The novel 'layer' of intrinsic functional diversity in survival and proliferation capacities among naïve $CD8^+$ T cells has to ultimately arise from the differences in the TCR itself as it is the *only* genetic difference among these cells. Furthermore, similar intrinsic differences, which are marked by the levels of CD5, are also seen among naïve $CD8^+$ T cells within the *same* TCR transgenic mouse. This suggests that this intrinsic functional heterogeneity may be *non-genetic* and may be imprinted as a result of heterogeneous spMHC interactions in the thymus during their CD4 vs. CD8 lineage commitment. Given that naïve T cells from $CD5^{-/-}$ mice and $CD5^{tg}$ mice are reported to be otherwise normal except for subtly altered T cell selection, we believe that CD5 is unlikely to directly mediate these functional differences but is rather just a 'marker' of a spectrum of closely correlated functional differences [6, 127]. Instead, the CD5 level may be determined by intermediary 'master regulators', which also determine the correlated intrinsic differences in survival, proliferation and metabolic capacities of $CD8^+$ T cells. The activity of these potential 'master regulators', may ultimately be imprinted during T cell development by the strength of thymic selection, and regulate both (i) the developmental imprinting of CD5 [7] as well as (ii) the imprinting of proliferative capacities in response to IL7 that persist even after T cell activation (see Figure 7-1). In order to better understand both the extent of the

intrinsic heterogeneity in gene expression across the entire genome among $CD8^+$ T cells, and ultimately, the molecular mechanisms underlying this phenomenon, a whole genome transcription profiling approach was applied. Putative molecular pathways that may be responsible for these differences are discussed in this chapter.

5.1 Whole genome expression analysis

The Affymetrix 430.2 expression array platform was used for the comparison of whole genome expression profiles of naïve $CD8^+$ $CD44^{lo}$ T cells obtained from age and sex-matched OT-1 or F5 mice (see Appendix A.6). After normalization using default parameters of the Affymetrix MAS5.0 algorithm, the whole genome expression profiles yielded data for 21689 distinct genes whose probe intensities were above background on all the gene chips (see Figure 5-1). The difference in the expression of each gene between OT-1 and F5 cells is represented as a ratio or fold-change (FC) in the mean probe intensity of each gene in the expression arrays for *OT-1 over F5* throughout this chapter. The statistical significance of differential expression was assessed using Student's t-test (see Figure 5-2). The distribution of differentially expressed genes is summarized in Table 5.1. Only 169 genes (0.8 % of total) were found to have at least a 2-fold difference in intensities between OT-1 and F5 with $p < 0.05$. The top 20 genes with highest relative expression in OT-1 or F5 cells and $p < 0.05$ are listed in Table 5.2. As expected, the differences in the expression of CD5 (FC=3.5, $p=2.24 \times 10^{-6}$), IL7R (FC=1.48, $p=4.4 \times 10^{-6}$) and Bcl2 (FC=1.48, p=0.047) were higher in OT-1 cells than F5 cells, and are concordant with observations made in Chapters 3-4. Given that CD5, IL7R and Bcl2 are primarily transcriptionally regulated, this could be considered to independently validate of the data from the microarray experiment.

Only subtle differences were expected from the comparison between naïve OT-1 and F5 cells as they are both $CD8^+$ cells at the same developmental stage and are selected in the same genetic background. Indeed, the gene expression profiles of OT-1 and F5 cells are very similar (see Figure 5-1). This calls for greater stringency in identifying gene subsets with statistically significant differences in expression that are

also biologically meaningful. To be conservative, genes with probe intensities below the 50^{th} percentile intensity rank in *both* OT-1 and F5 cells have been excluded from the analysis presented in this chapter although genes with statistically significant differences ($p < 0.5$) are seen at all intensity values (see Figure 5-3). The 50^{th} percentile probe intensity rank corresponds to a mean intensity that is $\sim$ 1000-fold lower than the maximum and $\sim$ 10-fold higher than the minimum in either cell type. Furthermore, there appears to be an inflexion point in the probe intensity vs. percentile rank plot around the 50^{th} percentile mark (see Figure 5-4), which may correlate with a shift away from background-associated non-specific hybridization kinetics.

Table 5.1: **Summary of microarray data** The distribution of differentially expressed genes in freshly isolated naïve $CD8^+$ OT-1 and F5 cells is summarized. Only 169 genes (0.8% of total) have at least a 2-fold difference between OT-1 and F5 cells.

OT-1/F5	All genes		$p < 0.05$		$p < 0.01$	
$\log_2$(ratio)	Count	%	Count	%	Count	%
>2	7	0.03	7	0.21	7	0.46
1.5 to 2	10	0.05	10	0.30	10	0.66
1 to 1.5	53	0.24	48	1.46	41	2.72
0.5 to 1	315	1.45	251	7.63	180	11.93
0 to 0.5	9944	45.85	979	29.76	333	22.07
-0.5 to 0	10823	49.90	1528	46.44	566	37.51
-1 to -0.5	427	1.97	363	11.03	269	17.83
-1.5 to -1	67	0.31	62	1.88	61	4.04
-2 to -1.5	26	0.12	26	0.79	26	1.72
<-2	17	0.08	16	0.49	16	1.06
Total	21689	1	3290	1	1509	1

5.2 Gene ontology terms selectively represented by the differentially expressed gene set

Selective representation of gene ontology (GO) terms linked to the most differentially expressed set of genes, comprising of 651 genes (3.0 % of total) with an intensity $|\log_2(\text{ratio})| > 0.5$ and $p < 0.05$, was analyzed (see Appendix A.10). The biological process, cellular component and molecular function GO terms that are selectively represented in the differentially expressed subset of genes are listed in Tables 5.7, 5.8, 5.9 and 5.10. GO terms with > 100 hits in the differentially expressed gene set are

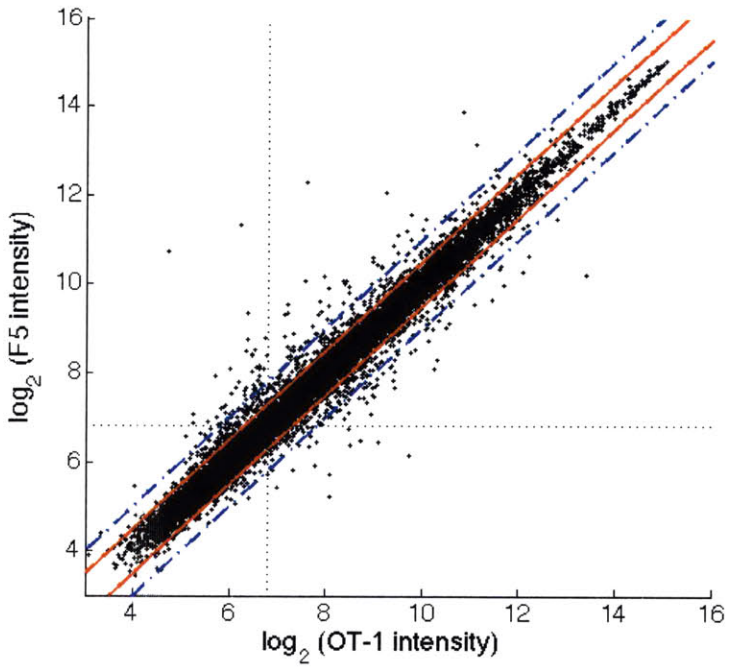

Figure 5-1: **Whole genome comparison of gene expression in OT-1 and F5 cells.** The mean probe intensities in the gene expression arrays for OT-1 and F5 cells (n=3) are depicted. Above background intensity was detectable in probes for 21689 genes in both cell types. The dotted black lines mark the 50^{th} percentiles. The red and blue lines separate genes with an expression $|\log_2(\text{ratio})| > 0.5$ and > 1 respectively.

not included in the above tables as they were not very informative. However, the tables include a number of subsets of the excluded GO terms that point to specific biological functions. Significant over-representation of biological process GO terms related to (i) cell proliferation, (ii) apoptosis, (iii) cell death, (iv) intracellular signaling cascade, and (v) regulation of lymphocyte activation is consistent with the observed intrinsic functional differences in the survival and proliferation capacities between OT-1 and F5 T cells (see Table 5.7 and 5.9). Interestingly, molecular function and cellular component GO terms related to (i) scavenger receptor activity (see Table 5.12, (ii) cytokine binding (see Table 5.13), (iii) chemokine receptor binding (see Table 5.14), (iv) sugar binding (see Table 5.16), (v) innate immune response (see Table 5.15), and (vi) adaptive immune response (see Table 5.15) are enriched in the differentially expressed subset. A number these gene subsets have proven roles in the

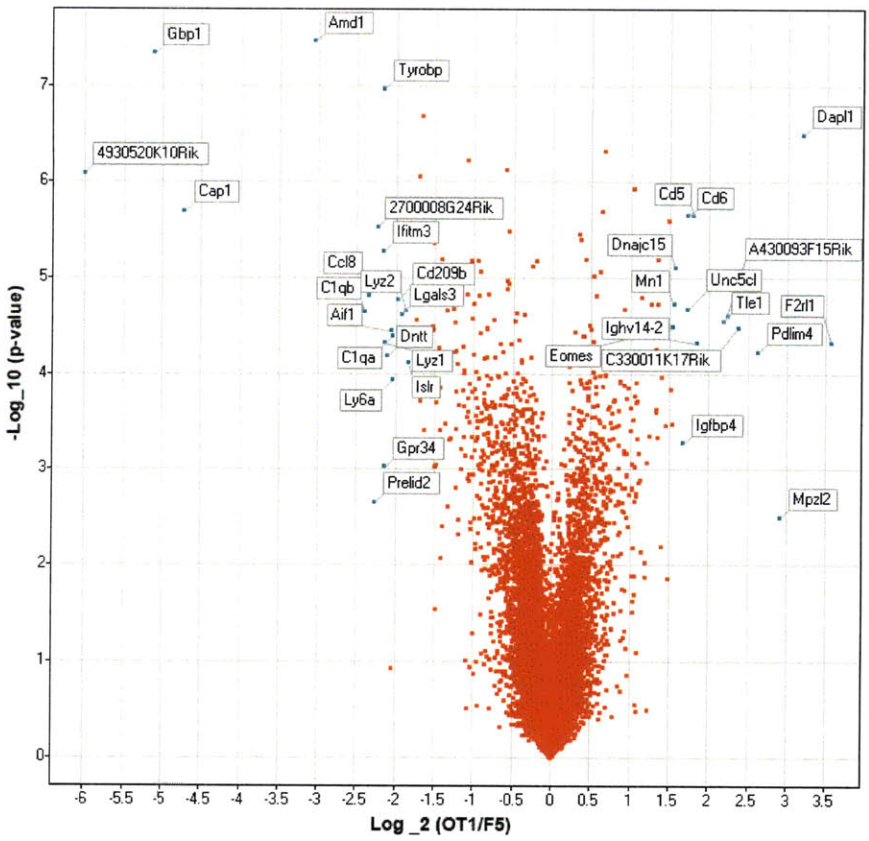

Figure 5-2: **Volcano plot displaying the pattern of differential gene expression between naïve OT-1 and F5 T cells.** The differences in gene expression between naïve OT-1 and F5 cells are shown as a plot of $\log_2$(ratio) vs. $-\log_{10}$(p-value). Selected genes that are most differentially expressed in OT-1 or F5 cells with a p-value < 0.01 are labeled.

immune system and may indicate functional differences in the immunological properties of OT-1 and F5 cells. Table 5.11 lists the differentially expressed list of genes that mapped to the over-represented GO term, 'intracellular signaling cascade', which includes known components of the TCR signaling pathway such as Rasgrp1, Trat1, and Lyn, raising the possibility of intrinsic differences in TCR signaling between OT-1 and F5 T cells. The enrichment of mitochondrial rRNA and mitochondrial outer membrane proteins in F5 cells (see Table 5.9) could imply that F5 T cells have a greater mitochondrial mass per cell and thus may have a higher capacity for oxidative phosphorylation, thereby contributing to the difference in their survival capacity. It could also point to differences in the capacity for autophagy in these cells.

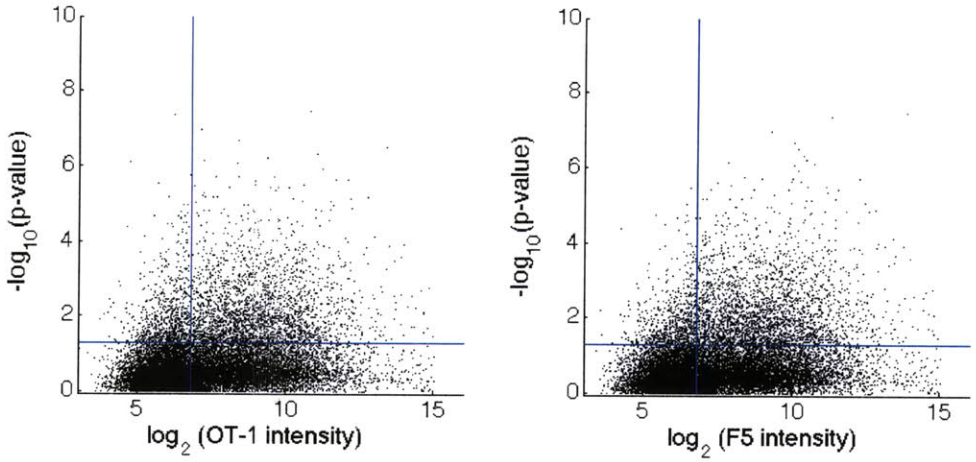

Figure 5-3: **Plot of gene expression intensity *vs* p-value of t-test for differential expression.** The mean intensity of gene expression in naïve OT-1 and F5 cells from gene chip experiments performed in triplicates are plotted against the p-value of Student's t-test for differential expression. The blue lines indicate the 50^{th} percentile intensity and a p-value of 0.05.

Genes of the scavenger receptor family are strongly enriched in the differentially expressed subset (see Table 5.12). Notably, CD5 and CD6 are also among the genes that are most selectively expressed in OT-1 T cells (see Tables 5.2). Both CD5 and CD6 have a similar function in modulating TCR signaling [37, 46, 72]. A430093F15Rik, a gene with unknown function, is also among the top 20 most differentially genes in OT-1 cells, along with CD5 and CD6. Interestingly, CD5, CD6 and A430093F15Rik are transcribed from the same locus in chromosome 19q (see Figure 5-5) and we suspect that these three genes are co-regulated in T cells and may perhaps all be considered to be markers of this intrinsic functional heterogeneity. Expression data from the UCSC genome browser database suggests that the expression pattern of CD5, CD6 and A430093F15Rik is similar and they are expressed at higher levels in $CD4^+$ cells than $CD8^+$ cells, consistent with our hypothesis that they are co-regulated with CD5 [56]. A430093F15Rik is present between CD5 and CD6 in mouse chromosome 19q (see Figure 5-5). Spliced transcripts that lie in the same orientation between CD5 and CD6 are seen in both human and mouse genomes, but the ORFs in these transcripts or their protein translations lack any homology. Furthermore, the translated A430093F15Rik ORF is not homologous to any known protein in Genbank.

Table 5.2: List of genes that are most differentially expressed in OT-1 and F5 cells

Top 20 genes selectively expressed in OT-1 cells with $p < 0.05$			
Gene symbol	Description	log_2(ratio)	p-value
F2rl1	coagulation factor II (thrombin) receptor-like 1	3.56	4.6×10^{-05}
Dapl1	death associated protein-like 1	3.18	3.2×10^{-07}
Mpzl2	myelin protein zero-like 2	2.91	3.1×10^{-03}
Pdlim4	PDZ and LIM domain 4	2.63	5.8×10^{-05}
C330011K17Rik	RIKEN cDNA C330011K17 gene	2.37	3.2×10^{-05}
A430093F15Rik	RIKEN cDNA A430093F15 gene	2.23	2.5×10^{-05}
Tle1	transducin-like enhancer of split 1, homolog of Drosophila E(spl)	2.18	2.8×10^{-05}
Ighv14-2	immunoglobulin heavy variable V14-2	1.84	4.7×10^{-05}
Cd5	CD5 antigen	1.80	2.2×10^{-06}
Unc5cl	unc-5 homolog C (C. elegans)-like	1.72	2.1×10^{-05}
Cd6	CD6 antigen	1.72	2.2×10^{-06}
Igfbp4	insulin-like growth factor binding protein 4	1.68	5.2×10^{-04}
Dnajc15	DnaJ (Hsp40) homolog, subfamily C, member 15	1.56	7.6×10^{-06}
Mn1	meningioma 1	1.55	1.8×10^{-05}
Eomes	eomesodermin homolog (Xenopus laevis)	1.53	3.2×10^{-05}
Plcxd2	phosphatidylinositol-specific phospholipase C, X domain containing 2	1.53	3.3×10^{-04}
Bbs9	Bardet-Biedl syndrome 9 (human)	1.51	1.4×10^{-04}
Esco1	establishment of cohesion 1 homolog 1 (S. cerevisiae)	1.49	1.4×10^{-02}
Bbc3	BCL2 binding component 3	1.48	2.5×10^{-06}
Tlr1	toll-like receptor 1	1.45	3.5×10^{-04}

Top 20 genes selectively expressed in F5 cells with $p < 0.05$			
Gene symbol	Description	log_2(ratio)	p-value
4930520K10Rik	RIKEN cDNA 4930520K10 gene	−6.01	8.1×10^{-07}
Gbp1	guanylate binding protein 1	−5.11	4.5×10^{-08}
Cap1	CAP, adenylate cyclase-associated protein 1 (yeast)	−4.72	2.0×10^{-06}
Amd1	S-adenosylmethionine decarboxylase 1	−3.05	3.3×10^{-08}
C1qb	complement component 1, q subcomponent, beta polypeptide	−2.41	2.2×10^{-05}
Ccl8	chemokine (C-C motif) ligand 8	−2.35	1.5×10^{-05}
Prelid2	PRELI domain containing 2	−2.26	2.2×10^{-03}
2700008G24Rik	RIKEN cDNA 2700008G24 gene	−2.23	2.9×10^{-06}
Tyrobp	TYRO protein tyrosine kinase binding protein	−2.17	1.1×10^{-07}
Ifitm3	interferon induced transmembrane protein 3	−2.17	5.2×10^{-06}
Lyz1	lysozyme 1	−2.15	4.7×10^{-05}
Gpr34	G protein-coupled receptor 34	−2.14	9.4×10^{-04}
Dntt	deoxynucleotidyltransferase, terminal	−2.11	6.4×10^{-05}
Aif1	allograft inflammatory factor 1	−2.07	3.5×10^{-05}
C1qa	complement component 1, q subcomponent, alpha polypeptide	−2.05	4.0×10^{-05}
Ly6a	lymphocyte antigen 6 complex, locus A	−2.04	1.2×10^{-04}
Cd209b	CD209b antigen	−1.98	1.7×10^{-05}
Lgals3	lectin, galactose binding, soluble 3	−1.93	2.4×10^{-05}
Lyz2	lysozyme 2	−1.88	2.1×10^{-05}
Islr	immunoglobulin superfamily containing leucine-rich repeat	−1.83	7.5×10^{-05}

This leads us to suspect that A430093F15Rik is a non-coding gene that functions as a regulatory RNA or participates in the epigenetic regulation of this locus.

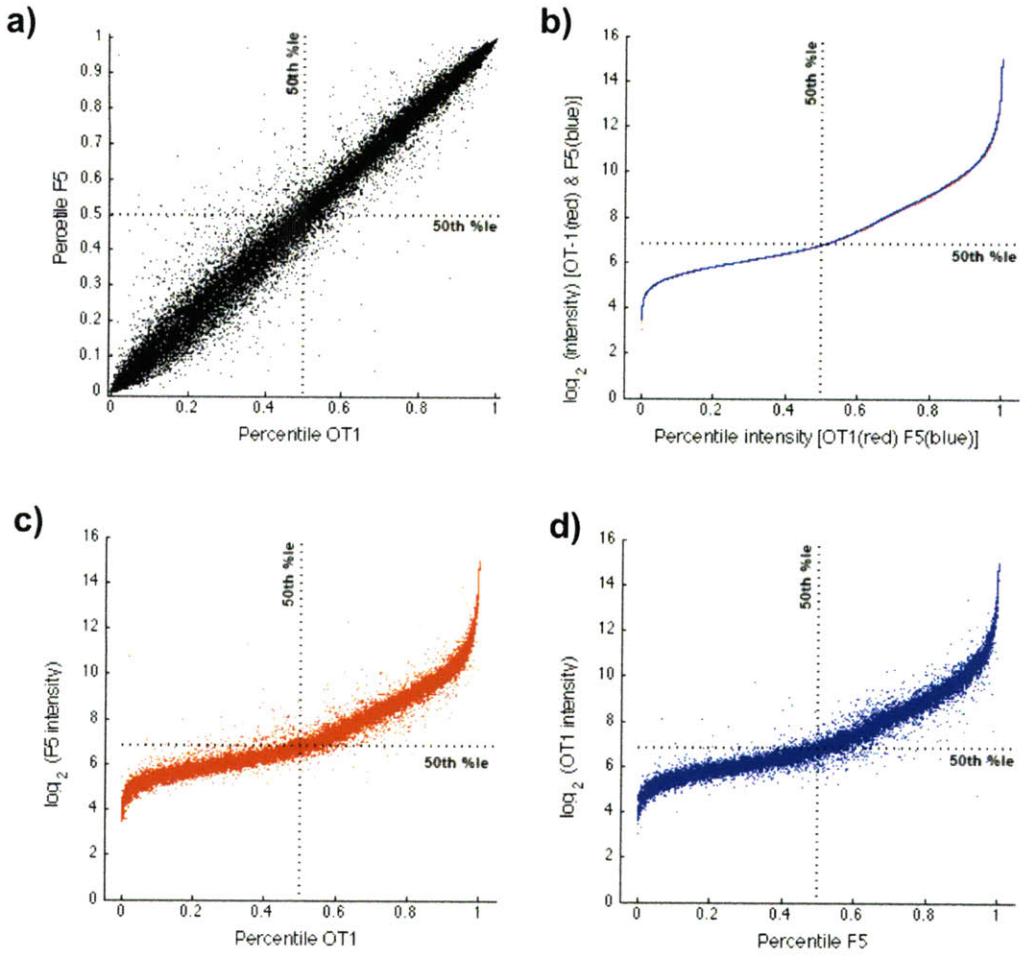

Figure 5-4: **Plots of gene expression intensity *vs* percentile ranks.** (a) Percentile ranks of the mean gene expression intensities in OT-1 vs. F5 cells. (b) Mean gene expression intensities plotted against the percentile rank of gene expression for both OT-1 (red) and F5 (blue) are nearly superimposed. (c) and (d) Mean gene expression intensities of OT-1 cells are plotted against the expression intensity percentile rank for F5 cells and *vice versa*.

5.3 Gene ontology terms under-represented by the differentially expressed gene set

'Transcription factor activity', 'regulation of transcription' or 'DNA binding' are among the few GO terms that are highly under-represented in the differentially expressed subset (see Tables 5.8 and 5.10). Transcription factors tend to have a large

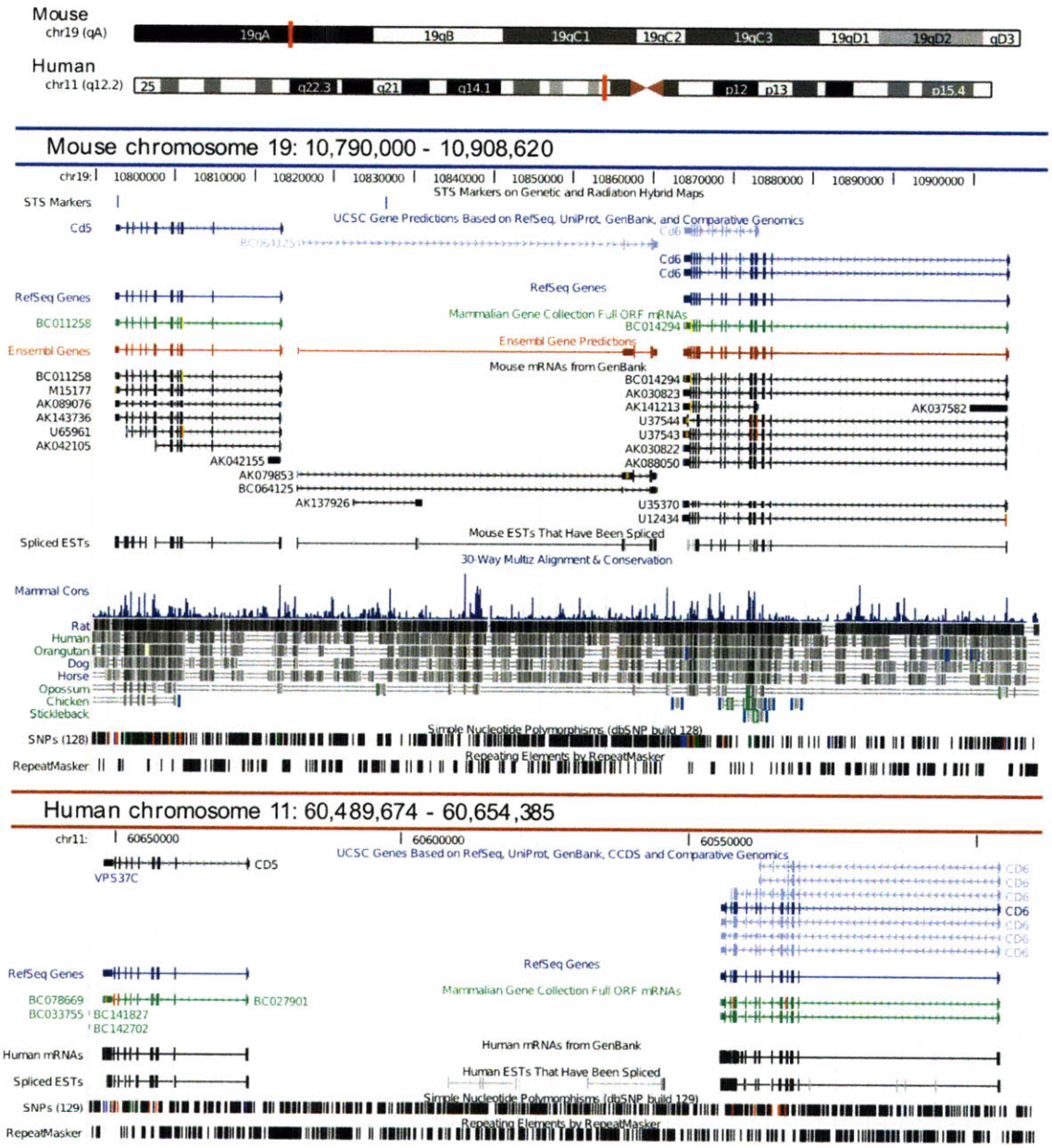

Figure 5-5: **CD5 and CD6 genomic loci.** Syntenic regions on mouse chromosome 19: 10,790,000-10,908,620 and human chromosome 11: 60,489,674-60,654,385 containing the genes for CD5 and CD6 are shown. Putative spliced transcripts originating from the same locus between CD5 and CD6 and the degree of conservation of the entire locus in various vertebrates is also depicted. The Genbank ID BC064125 corresponds to the mouse A430093F15Rik gene.

number of targets and it would be paradoxical if the regulators of transcription are themselves among the most differentially expressed genes. Table 5.3 lists transcription factors that are differentially expressed in OT-1 and F5 cells. It was not possible

to identify single transcription factors as potential 'master regulators' based solely on the degree of differential expression as there was no good way to distinguish between transcription factors that lie upstream or downstream of the critical biological pathways that are responsible for the functional differences in the two cell types. Transcription factors typically require a variety of post-transcriptional modifications or regulated interaction with specific proteins for their activity and such functional changes are not reflected in microarray experiments. Therefore, a pathway analysis approach was applied to identify transcriptionally co-regulated sets of genes that could better explain the biology of the differences.

Table 5.3: Transcription factors that are differentially expressed in OT-1 and F5 cells with an expresion intensity $|\log_2(\text{ratio})|>0.5$

Gene symbol	Description	$\log_2$(ratio)	p-value	percentile	
				OT-1	F5
Eomes	eomesodermin homolog (Xenopus laevis)	1.53	3.16×10^{-05}	80.4	60.7
Pttg1	pituitary tumor-transforming gene 1	1.39	1.06×10^{-04}	96.1	85.9
Hopx	HOP homeobox	1.11	6.77×10^{-04}	91.6	79.9
Irf6	interferon regulatory factor 6	0.92	2.08×10^{-05}	55.5	31.4
Fos	FBJ osteosarcoma oncogene	0.90	1.52×10^{-03}	71.0	59.6
Tbx21	T-box 21	0.52	7.30×10^{-03}	62.7	55.1
Gfi1	growth factor independent 1	−0.51	7.86×10^{-04}	77.6	83.1
Dbp	D site albumin promoter binding protein	−0.53	4.10×10^{-03}	70.6	77.1
Isgf3g	interferon regulatory factor 9	−0.56	5.31×10^{-04}	92.8	95.5
Cebpb	CCAAT/enhancer binding protein beta	−0.58	1.04×10^{-02}	61.5	68.3
Asb2	ankyrin repeat and SOCS box-containing 2	−0.61	6.57×10^{-04}	49.5	59.4
Cebpa	CCAAT/enhancer binding protein alpha	−0.72	6.46×10^{-04}	42.5	57.2
Stat2	signal transducer and activator of transcription 2	−0.73	1.87×10^{-03}	69.5	78.5
Myb	myeloblastosis oncogene	−0.75	1.04×10^{-02}	57.9	66.5
Sfpi1	SFFV proviral integration 1	−0.84	3.28×10^{-05}	50.7	63.0
Irf8	interferon regulatory factor 8	−0.90	3.07×10^{-04}	59.8	70.7
Trafd1	TRAF type zinc finger domain containing 1	−0.98	1.79×10^{-04}	77.6	87.6
Bmyc	brain expressed myelocytomatosis oncogene	−1.13	2.16×10^{-04}	61.1	74.9
Irf7	interferon regulatory factor 7	−1.21	7.79×10^{-05}	90.2	96.4

5.4 Prediction of upstream regulatory transcription factors using F-match

We looked for over-represented transcription factor binding sites (TFBS) in the promoters of differentially expressed genes in OT-1 and F5 cells using the F-match algorithm (see Appendix A.11)). An empirical Bayes test (using a hierarchical Gamma-

Gamma model) was used to identify 500 most differentially as well as 500 most similarly expressed genes between OT-1 and F5 cells. The promoters (-1000 to +100 bases) of these genes were scanned with the P-match algorithm for immune and cell-cycle specific TF binding sites, using position-weight matrices from the TRANSFAC database, which are calculated based on published experimental data [15, 76]. The P-match algorithm combines pattern matching and weight matrix approaches for higher accuracy of recognition than either method alone. Over-representation of the TF binding sites in promoters of differentially expressed genes was compared to a background set of genes with no difference in expression using the F-match algorithm (see Table 5.4). The p-values were calculated assuming a binomial distribution. The TF binding motifs whose frequency in the promoters of the test gene set over background was greater than 1.1 and with $p < 0.05$ were identified for the following comparisons (i) over-expressed in OT-1 vs. unchanged; (ii) over-expressed in F5 vs. unchanged; (iii) over-expressed in OT-1 vs. over-expressed in F5; and (iv) over-expressed in F5 vs. over-expressed in OT-1 (see Table 5.4).

5.5 Gene set enrichment analysis

Gene set enrichment analysis (GSEA) was used to identify candidate transcription factor and miRNAs motifs that may be a part of the upstream regulatory network that is responsible for the difference in gene expression between OT-1 and F5 cells. These motifs are comprised of genes with conserved DNA sequence motifs in their promoters (2kbp upstream and downstream of transcription start site) as well as genes with conserved miRNA target sequences in their 3′ UTRs based on sequence conservation across four mammalian genomes, which are publicly available as a part of the MSigDB v2.5 motif dataset [118]. GSEA analysis was run on the set of differentially expressed genes in OT-1 and F5 cells that were expressed at levels $> 50^{\text{th}}$ percentile expression intensity in either cell type (see Appendix A.12). The transcription factor and miRNA motifs that are enriched in either OT-1 or F5 cells are listed in Table 5.6 and 5.5.

The enriched transcription factor motifs include binding sites for transcription

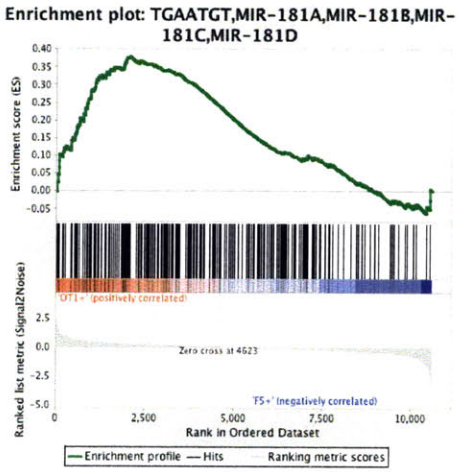

(a) miRNA-181 targets

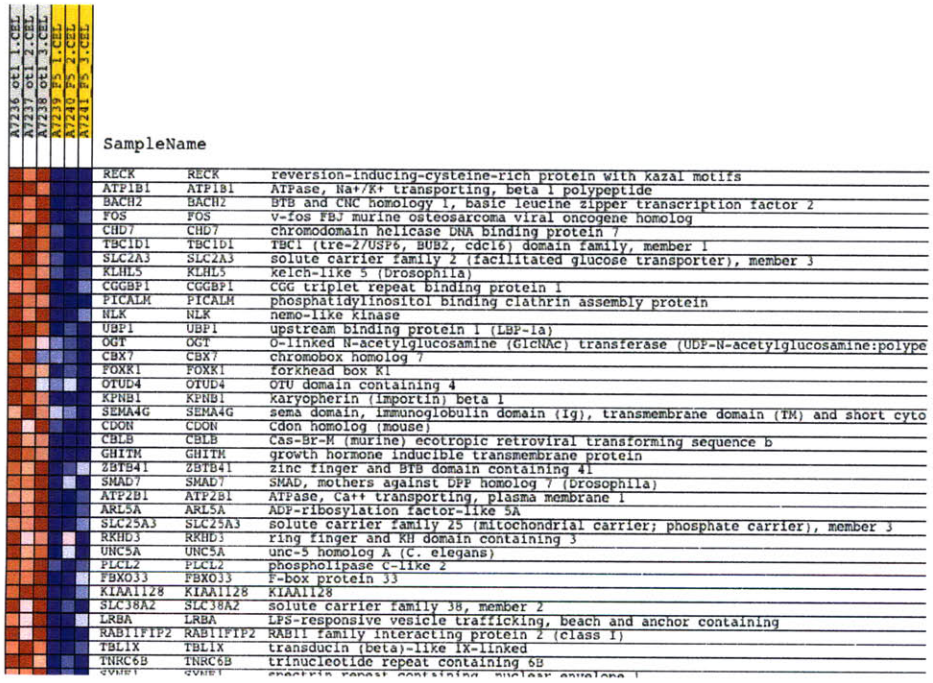

(b) miRNA-181 targets

Figure 5-6: **Gene set enrichment analysis: miRNA target motifs.** GSEA analysis suggests that miRNA-181 could partly explain the profile of differential expression between OT-1 and F5 cells. Genes containing conserved targets of miR-181 in their 3′ UTRs are selectively over-expressed in OT-1 cells. This suggest that miR-181 may be over-expressed in F5 cells. However, this prediction needs to be experimentally tested.

Table 5.4: F-match analysis of over-represented TFBS.

F-match: Promoters of genes over-expressed in OT-1 vs. unchanged (UC)				
	# TF binding sites per promoter			
Matrix name	OT-1	UC	OT-1/UC	p-value
V$SP1_Q2_01	1.8484	1.6678	1.1083	6.21×10^{-04}
V$VDR_Q3	0.2033	0.1573	1.2928	5.60×10^{-03}
V$EGR_Q6	0.2689	0.2178	1.2347	7.60×10^{-03}
V$EBOX_Q6_01	0.5628	0.4895	1.1499	8.60×10^{-03}
V$KROX_Q6	0.7079	0.6274	1.1284	1.01×10^{-02}
V$LMO2COM_01	0.0222	0.0118	1.8838	3.96×10^{-02}

F-match: Promoters of genes over-expressed in OT-1 vs. in F5				
	# TF binding sites per promoter			
Matrix name	OT-1	F5	OT-1/F5	p-value
V$E2F_Q2	4.3965	3.0023	1.4644	0.00
V$E2F1_Q6_01	1.5028	1.0374	1.4486	5.05×10^{-24}
V$E2F1_Q3_01	2.0702	1.5246	1.3579	2.38×10^{-23}
V$SP1_Q6_01	2.0739	1.714	1.21	1.18×10^{-10}
V$SP1_Q4_01	1.2338	0.9758	1.2644	1.39×10^{-09}
V$SP1_Q2_01	1.8484	1.5323	1.2063	1.97×10^{-09}
V$SP1_01	4.2394	3.8122	1.1121	1.28×10^{-07}
V$KROX_Q6	0.7079	0.5791	1.2225	5.34×10^{-05}
V$EGR_Q6	0.2689	0.205	1.312	8.10×10^{-04}
V$E2F1_Q4_01	0.1636	0.12	1.3629	2.90×10^{-03}
V$E2F_Q3_01	0.2024	0.1574	1.2856	5.70×10^{-03}
V$E2F_Q6_01	0.1414	0.1083	1.3052	1.33×10^{-02}
V$VDR_Q3	0.2033	0.1645	1.2363	1.56×10^{-02}
V$CREB_Q2_01	0.414	0.364	1.1375	2.78×10^{-02}
V$XBP1_01	0.1682	0.1395	1.2056	4.23×10^{-02}

F-match: Promoters of genes over-expressed in F5 vs. unchanged (UC)				
	# TF binding sites per promoter			
Matrix name	F5	UC	F5/UC	p-value
V$IRF2_01	0.1193	0.0664	1.7948	1.03×10^{-05}
V$E2A_Q6	1.6617	1.4693	1.131	7.12×10^{-05}
V$EBOX_Q6_01	0.5963	0.4895	1.2181	1.77×10^{-04}
V$EBF_Q6	0.3632	0.2935	1.2374	1.40×10^{-03}
V$HEB_Q6	0.3624	0.3003	1.2071	4.00×10^{-03}
V$NFAT_Q4_01	0.5729	0.4962	1.1545	5.00×10^{-03}
V$BLIMP1_Q6	0.0616	0.0421	1.4642	2.05×10^{-02}
V$NFKAPPAB_01	0.6438	0.5828	1.1046	2.82×10^{-02}

F-match: Promoters of genes over-expressed in F5 vs. in OT-1				
	# TF binding sites per promoter			
Matrix name	F5	OT-1	F5/OT-1	p-value
V$IRF2_01	0.1193	0.0739	1.6129	2.64×10^{-04}
V$EBF_Q6	0.3632	0.2994	1.2129	4.10×10^{-03}
V$LYF1_01	0.3843	0.3207	1.1982	5.30×10^{-03}
V$IRF_Q6	0.06	0.0379	1.5838	1.00×10^{-02}
V$MAF_Q6_01	0.0507	0.0342	1.4815	3.35×10^{-02}

factors such as E2F, E47 and IRF, which are also differentially expressed in OT-1 and F5 T cells (see Table 5.3). To test if E47, which is a splice variant of the E2A gene, was indeed responsible for the differential expression profiles in these cells, GSEA was repeated after including experimentally identified sets of E47 target genes that are

Table 5.5: GSEA: miRNA target motifs

miRNA targets enriched in the 3′ UTRs in genes over-expressed in OT-1 with p < 0.05						
SEQUENCE	NAME	SIZE	ES	NES	NOM p-val	FDR q-val
TGAATGT	miR-181A,-181B,-181C,-181D	249	0.378	1.745	0.000	0.434
ATGCTGC	miR-103,-107	126	0.408	1.695	0.000	0.356
CTAGGAA	miR-384	30	0.523	1.635	0.014	0.405
CCACACA	miR-147	38	0.489	1.621	0.016	0.345
AGGGCCA	miR-328	38	0.473	1.565	0.030	0.426
GTGCAAT	miR-25,-32,-92,-363,-367	163	0.362	1.565	0.000	0.356
GTAGGCA	miR-189	18	0.548	1.550	0.038	0.334
ATGCAGT	miR-217	63	0.417	1.541	0.019	0.315
CACTTTG	miR-520G,-520H	120	0.369	1.525	0.000	0.320
TACTTGA	miR-26A,-26B	154	0.352	1.509	0.000	0.330
TGTATGA	miR-485-3P	68	0.397	1.503	0.013	0.315
AACTGGA	miR-145	126	0.364	1.492	0.007	0.318
TGGTGCT	miR-29A,-29B,-29C	260	0.323	1.470	0.000	0.341
CAATGCA	miR-33	44	0.423	1.459	0.037	0.340
TGCTGCT	miR-15A,-16,-15B,-195,-424,-497	319	0.312	1.456	0.011	0.323
CAAGGAT	miR-362	32	0.443	1.449	0.043	0.319
ACCATTT	miR-522	94	0.362	1.447	0.027	0.303
GTACTGT	miR-101	129	0.350	1.442	0.004	0.298
CTTGTAT	miR-381	113	0.352	1.417	0.018	0.334
ATGTTTC	miR-494	75	0.369	1.400	0.045	0.361

miRNA targets enriched in the 3′ UTRs in genes over-expressed in F5 with p < 0.05						
SEQUENCE	NAME	SIZE	ES	NES	NOM p-val	FDR q-val
CACGTTT	miR-302A	17	-0.598	-1.487	0.047	0.804

either down-regulated or up-regulated after E47 over-expression in an E2A-deficient thymoma cell line (see Appendix A.12) [109]. F5 T cells express marginally higher levels of E47 (FC = 0.80, p = 0.28) and, strikingly, genes that are up-regulated by E47 over-expression in the E2A-deficient thymoma are also over-expressed in F5 T cells and *vice versa* (see Figure 5-7). E47 represses CD5 expression and is known to be involved in regulating cell proliferation [138]. E47 is also predicted to may play a role in inhibiting cytokine signaling by inducing Gfi1 and Socs family members, both of which are also over-expressed in F5 T cells. Thus, given that the biological functions of E47 are consistent with the observed intrinsic differences, and that it is enriched by two different pathway analysis techniques, it appears to be a critical part of the underlying regulatory transcription factor network. Gene set motifs for E2F are enriched in OT-1 cells. The E2F proteins are known to regulate cell cycle in a manner that is consistent with the greater proliferative capacity of OT-1 cells. E2F proteins such as E2F3 (FC = 1.33, p = 0.032) and E2F7 (FC = 1.25, p = 0.028) are indeed over-expressed in OT-1 cells. Similarly, the gene set motifs for IRF are enriched

Table 5.6: GSEA: transcription factor binding motifs

Conserved TFBS enriched in promoters of genes overexpressed in OT-1 with $p < 0.05$					
NAME	SIZE	ES	NES	NOM p-val	FDR q-val
V$AR_03	25	0.606	1.864	0.005	0.144
YNGTTNNNATT_UNKNOWN	112	0.417	1.704	0.000	0.378
V$S8_01	68	0.428	1.636	0.003	0.492
V$CDPCR1_01	37	0.453	1.487	0.039	1.000
V$PR_01	49	0.418	1.476	0.023	0.939
V$GATA1_01	97	0.370	1.475	0.011	0.813
V$E12_Q6	92	0.370	1.470	0.017	0.740
V$E2F_Q4_01	117	0.357	1.460	0.004	0.717
V$E2F1_Q4_01	115	0.357	1.450	0.007	0.694
V$OCT1_05	71	0.388	1.450	0.017	0.631
V$IK2_01	90	0.373	1.444	0.024	0.607
KMCATNNWGGA_UNKNOWN	39	0.423	1.434	0.038	0.606
V$MYOD_Q6	83	0.371	1.411	0.024	0.670
V$E2F_Q3	110	0.345	1.410	0.004	0.632
KTGGYRSGAA_UNKNOWN	42	0.420	1.404	0.035	0.624
V$E2F_Q3_01	114	0.334	1.367	0.019	0.690

Conserved TFBS enriched in promoters of genes overexpressed in F5 with $p < 0.05$					
NAME	SIZE	ES	NES	NOM p-val	FDR q-val
STTTCRNTTT_V$IRF_Q6	92	-0.556	-1.967	0.000	0.006
V$IRF_Q6	108	-0.516	-1.871	0.000	0.020
V$IRF1_01	91	-0.478	-1.716	0.001	0.159
V$IRF2_01	56	-0.522	-1.671	0.006	0.214
V$ISRE_01	97	-0.463	-1.659	0.000	0.201
$E47-2FOLD-UP	60	-0.504	-1.639	0.006	0.216
V$IRF7_01	109	-0.430	-1.573	0.010	0.377
V$LXR_Q3	31	-0.505	-1.488	0.047	0.742
V$MYB_Q5_01	87	-0.423	-1.486	0.022	0.673
V$TATA_C	91	-0.423	-1.485	0.016	0.611
$E47-3FOLD-UP	20	-0.573	-1.481	0.038	0.574
V$TEL2_Q6	121	-0.406	-1.477	0.012	0.503
V$ICSBP_Q6	103	-0.406	-1.453	0.021	0.581
V$IRF1_Q6	110	-0.395	-1.438	0.017	0.619
V$POU3F2_02	78	-0.407	-1.411	0.042	0.730
V$PEA3_Q6	127	-0.376	-1.383	0.036	0.874
V$AML1_Q6	102	-0.374	-1.375	0.041	0.880
V$NFKAPPAB_01	110	-0.374	-1.375	0.042	0.834

in F5 cells and a number of IRF family transcription factors are over-expressed in F5 cells (IRF6, IRF7 and IRF8). Among the miRNA motifs that are enriched in OT-1 cells, miR-181 is particularly interesting as it regulates the sensitivity of TCR signaling, consistent with possible intrinsic differences in the TCR signaling between these two cells. Thus, a regulatory network, that involves transcription factors such as E47, E2F and IRF, and miRNAs such as miR-181, may constitute the intermediary regulators that are responsible for the setting the intrinsic differences in survival and proliferation capacities of OT-1 and F5 cells.

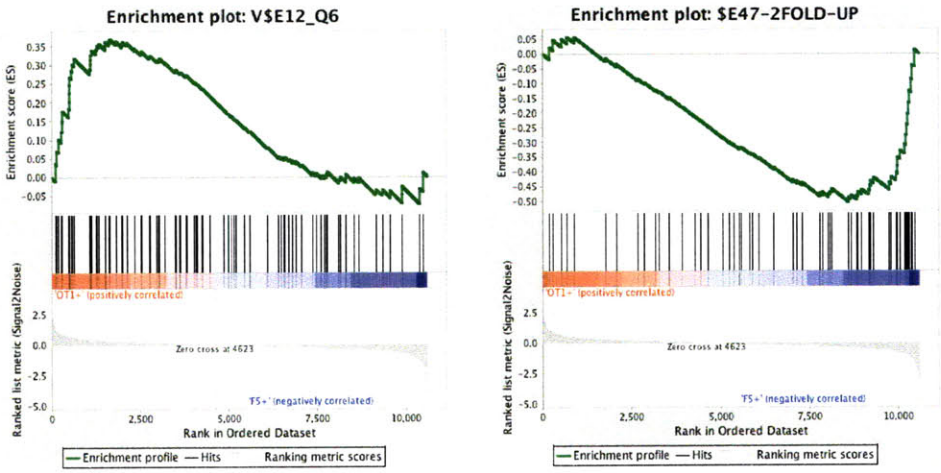

(a) V$E12_Q6_24 (b) V$E47-2-FOLD-UP

Figure 5-7: **Gene set enrichment analysis: E47.** (a) V$E12_Q6_24: Set of genes with promoter regions [-2kb,2kb] around transcription start site containing the motif RRCAGGTGNCV which matches annotation for TCF3: transcription factor 3 (E2A immunoglobulin enhancer binding factors E12/E47) (b) V$E47-2-FOLD-UP: Set of genes up-regulated by 2-fold upon transgenic expression of E47 in a E47 deficient lymphoma cell line [109].

Table 5.7: Biological process gene ontology terms over-represented in the differentially expressed subset of genes with $|\log_2(\text{ratio})| > 0.5$.

GO Identifier	GO Term (top 50 over-represented with $p < 0.05$)	# Hits/Expected, (Group size)	p-value
GO:0006952	immune response	97/26, (961)	4.18×10^{-28}
GO:0051707	defense response	64/26, (964)	2.35×10^{-09}
GO:0009607	response to other organism	35/10, (352)	3.46×10^{-09}
GO:0045087	response to biotic stimulus	39/13, (479)	8.16×10^{-08}
GO:0045321	leukocyte activation	33/11, (390)	6.00×10^{-07}
GO:0050776	cell activation	35/12, (435)	6.57×10^{-07}
GO:0001775	regulation of immune response	22/6, (197)	1.23×10^{-06}
GO:0006954	antigen processing and presentation of peptide or	8/1, (19)	1.30×10^{-06}
GO:0050778	positive regulation of immune response	20/5, (170)	2.11×10^{-06}
GO:0009611	innate immune response	19/5, (163)	5.01×10^{-06}
GO:0002504	positive regulation of immune system process	20/5, (183)	5.36×10^{-06}
GO:0009615	immune response-regulating cell surface receptor s	11/2, (52)	5.73×10^{-06}
GO:0001816	lymphocyte activation	28/9, (334)	5.88×10^{-06}
GO:0002684	response to virus	17/4, (137)	6.95×10^{-06}
GO:0046649	antigen processing and presentation of exogenous a	9/1, (33)	7.16×10^{-06}
GO:0009605	antigen processing and presentation of exogenous p	7/1, (18)	1.05×10^{-05}
GO:0008283	cytokine production	21/6, (213)	1.18×10^{-05}
GO:0002768	activation of immune response	16/4, (128)	1.24×10^{-05}
GO:0019884	immune response-activating cell surface receptor s	10/2, (49)	2.11×10^{-05}
GO:0019886	cell proliferation	59/33, (1222)	2.29×10^{-04}
GO:0002429	T cell activation	19/6, (219)	2.43×10^{-04}
GO:0002253	antigen processing and presentation of peptide ant	10/2, (65)	2.75×10^{-04}
GO:0051249	cell death	61/35, (1302)	3.51×10^{-04}
GO:0002443	induction of programmed cell death	25/10, (360)	3.80×10^{-04}
GO:0008219	induction of apoptosis	25/10, (359)	3.89×10^{-04}
GO:0042221	antigen processing and presentation	13/4, (116)	3.89×10^{-04}
GO:0016265	death	61/35, (1309)	3.97×10^{-04}
GO:0042110	adaptive immune response	19/7, (236)	5.06×10^{-04}
GO:0002250	stimulatory C-type lectin receptor signaling pathw	3/1, (3)	5.15×10^{-04}
GO:0042107	programmed cell death	58/33, (1241)	5.30×10^{-04}
GO:0009617	inflammatory response	32/15, (543)	6.15×10^{-04}
GO:0051251	leukocyte mediated immunity	20/7, (263)	6.42×10^{-04}
GO:0042089	apoptosis	57/33, (1226)	6.44×10^{-04}
GO:0012501	regulation of lymphocyte activation	14/4, (143)	6.68×10^{-04}
GO:0006915	regulation of innate immune response	6/1, (24)	7.07×10^{-04}
GO:0019882	response to wounding	42/23, (836)	1.32×10^{-03}
GO:0042127	response to bacterium	17/6, (219)	1.78×10^{-03}
GO:0006950	positive regulation of tumor necrosis factor biosy	4/1, (10)	1.95×10^{-03}
GO:0006917	positive regulation of phagocytosis	5/1, (19)	2.31×10^{-03}
GO:0012502	cytokine biosynthetic process	11/3, (106)	2.42×10^{-03}
GO:0042221	response to chemical stimulus	61/38, (1424)	2.57×10^{-03}
GO:0042107	cytokine metabolic process	11/3, (107)	2.58×10^{-03}
GO:0007242	intracellular signaling cascade	80/54, (2008)	2.58×10^{-03}
GO:0009605	response to external stimulus	56/34, (1274)	2.60×10^{-03}
GO:0050863	regulation of T cell activation	11/3, (109)	2.78×10^{-03}
GO:0051251	positive regulation of lymphocyte activation	10/3, (92)	2.92×10^{-03}
GO:0045089	positive regulation of innate immune response	5/1, (21)	3.18×10^{-03}
GO:0042127	regulation of cell proliferation	40/22, (826)	3.20×10^{-03}
GO:0045582	positive regulation of T cell differentiation	5/1, (21)	3.24×10^{-03}
GO:0050764	regulation of phagocytosis	5/1, (22)	3.87×10^{-03}

Table 5.8: Biological process gene ontology terms under-represented in the differentially expressed subset of genes with $|\log_2(\text{ratio})| > 0.5$.

GO Identifier	GO Term (all under-represented with $p < 0.05$)	# Hits/Expected, (Group size)	p-value
GO:0007600	sensory perception	14/46, (1717)	1.76×10^{-06}
GO:0010467	gene expression	74/119, (4462)	3.24×10^{-05}
GO:0050877	neurological system process	29/61, (2274)	7.87×10^{-05}
GO:0007186	G-protein coupled receptor protein signaling pathw	36/69, (2587)	1.01×10^{-04}
GO:0006139	nucleobase, nucleoside, nucleotide and nucleic aci	95/128, (4810)	2.55×10^{-04}
GO:0016070	RNA metabolic process	58/93, (3497)	3.99×10^{-04}
GO:0006350	transcription	52/83, (3110)	1.52×10^{-03}
GO:0045449	regulation of transcription	50/80, (2997)	1.74×10^{-03}
GO:0006351	transcription, DNA-dependent	48/76, (2851)	3.07×10^{-03}
GO:0006355	regulation of transcription, DNA-dependent	47/74, (2783)	3.62×10^{-03}
GO:0010468	regulation of gene expression	59/88, (3279)	4.89×10^{-03}
GO:0019222	regulation of metabolic process	74/99, (3691)	4.44×10^{-02}
GO:0031323	regulation of cellular metabolic process	69/92, (3462)	4.89×10^{-02}

Table 5.9: Cellular compoent gene ontology terms over- and under-represented in the differentially expressed subset of genes with $|\log_2(\text{ratio})| > 0.5$.

GO Identifier	GO Term	# Hits/Expected, (Group size)	p-value
GO:0009897	external side of plasma membrane	28/6, (207)	2.16×10^{-10}
GO:0009986	cell surface	32/11, (402)	2.64×10^{-06}
GO:0005615	extracellular space	97/62, (2301)	1.23×10^{-04}
GO:0042613	MHC class II protein complex	5/1, (11)	1.63×10^{-04}
GO:0042824	MHC class I peptide loading complex	5/1, (13)	2.90×10^{-04}
GO:0044421	extracellular region part	99/67, (2482)	4.22×10^{-04}
GO:0042825	TAP complex	4/1, (11)	1.92×10^{-03}
GO:0005770	late endosome	9/3, (76)	2.29×10^{-03}
GO:0031094	platelet dense tubular network	2/1, (2)	6.60×10^{-03}
GO:0005955	calcineurin complex	3/1, (7)	6.72×10^{-03}
GO:0005602	complement component C1 complex	2/1, (2)	7.15×10^{-03}
GO:0031307	integral to mitochondrial outer membrane	3/1, (8)	8.28×10^{-03}
GO:0005794	Golgi apparatus	42/27, (976)	1.36×10^{-02}
GO:0031306	intrinsic to mitochondrial outer membrane	3/1, (10)	1.49×10^{-02}
GO:0005887	integral to plasma membrane	59/42, (1545)	2.49×10^{-02}
GO:0032592	integral to mitochondrial membrane	3/1, (13)	2.98×10^{-02}
GO:0001772	immunological synapse	4/1, (27)	2.98×10^{-02}
GO:0005741	mitochondrial outer membrane	8/3, (100)	3.09×10^{-02}
GO:0031226	intrinsic to plasma membrane	59/43, (1576)	3.23×10^{-02}
GO:0019897	extrinsic to plasma membrane	7/3, (79)	3.29×10^{-02}
GO:0001726	ruffle	6/2, (66)	4.18×10^{-02}
GO:0005771	multivesicular body	3/1, (16)	4.30×10^{-02}

GO Identifier	GO Term (all under-represented with $p < 0.05$)	# Hits/Expected, (Group size)	p-value
—	—No under-represented terms—	—	—

Table 5.10: Molecular function gene ontology terms over- and under-represented in the differentially expressed subset of genes with $|\log_2(\text{ratio})| > 0.5$.

GO Identifier	GO Term (top 40 over-represented with $p < 0.05$)	# Hits/Expected, (Group size)	p-value
GO:0042287	MHC protein binding	8/1, (30)	2.08×10^{-04}
GO:0005529	sugar binding	25/9, (334)	3.96×10^{-04}
GO:0005044	scavenger receptor activity	8/2, (46)	2.14×10^{-03}
GO:0016814	hydrolase activity, acting on carbon-nitrogen (but	7/1, (36)	2.46×10^{-03}
GO:0042288	MHC class I protein binding	6/1, (26)	2.59×10^{-03}
GO:0008179	adenylate cyclase binding	3/1, (4)	2.80×10^{-03}
GO:0030246	carbohydrate binding	29/14, (503)	3.18×10^{-03}
GO:0019955	cytokine binding	14/5, (166)	4.39×10^{-03}
GO:0042379	chemokine receptor binding	8/2, (59)	4.49×10^{-03}
GO:0019864	IgG binding	3/1, (5)	4.80×10^{-03}
GO:0019865	immunoglobulin binding	4/1, (12)	4.96×10^{-03}
GO:0016298	lipase activity	11/4, (126)	1.13×10^{-02}
GO:0045233	natural killer cell receptor activity	3/1, (7)	1.15×10^{-02}
GO:0008009	chemokine activity	7/2, (57)	1.21×10^{-02}
GO:0048029	monosaccharide binding	6/2, (42)	1.22×10^{-02}
GO:0019763	immunoglobulin receptor activity	3/1, (7)	1.24×10^{-02}
GO:0008125	pancreatic elastase I activity	2/1, (2)	1.27×10^{-02}
GO:0019239	deaminase activity	5/1, (29)	1.33×10^{-02}
GO:0015057	thrombin receptor activity	6/2, (46)	1.78×10^{-02}
GO:0005537	mannose binding	4/1, (20)	2.15×10^{-02}
GO:0003876	AMP deaminase activity	2/1, (3)	2.35×10^{-02}
GO:0004720	protein-lysine 6-oxidase activity	3/1, (10)	2.37×10^{-02}
GO:0003924	GTPase activity	17/8, (295)	2.37×10^{-02}
GO:0001872	zymosan binding	2/1, (3)	2.45×10^{-02}
GO:0005102	receptor binding	47/31, (1167)	2.48×10^{-02}
GO:0016462	pyrophosphatase activity	39/25, (927)	2.65×10^{-02}
GO:0016818	hydrolase activity, acting on acid anhydrides, in	39/25, (937)	3.08×10^{-02}
GO:0008034	lipoprotein binding	5/2, (39)	3.12×10^{-02}
GO:0017111	nucleoside-triphosphatase activity	37/24, (891)	3.14×10^{-02}
GO:0016208	AMP binding	4/1, (26)	3.16×10^{-02}
GO:0048154	S100 beta binding	2/1, (4)	3.16×10^{-02}
GO:0042803	protein homodimerization activity	18/9, (342)	3.17×10^{-02}
GO:0008329	pattern recognition receptor activity	3/1, (12)	3.17×10^{-02}
GO:0016494	C-X-C chemokine receptor activity	5/2, (42)	3.24×10^{-02}
GO:0048306	calcium-dependent protein binding	4/1, (26)	3.24×10^{-02}
GO:0019770	IgG receptor activity	2/1, (4)	3.25×10^{-02}
GO:0016211	ammonia ligase activity	2/1, (4)	3.35×10^{-02}
GO:0019965	interleukin binding	7/3, (80)	3.40×10^{-02}
GO:0016641	oxidoreductase activity, acting on the CH-NH2 grou	4/1, (25)	3.43×10^{-02}
GO:0008132	pancreatic elastase activity	2/1, (4)	3.46×10^{-02}

GO Identifier	GO Term (all under-represented with $p < 0.05$)	# Hits/Expected, (Group size)	p-value
GO:0001584	rhodopsin-like receptor activity	18/56, (2097)	7.32×10^{-09}
GO:0004930	G-protein coupled receptor activity	22/60, (2283)	9.18×10^{-09}
GO:0003677	DNA binding	44/78, (2939)	4.98×10^{-05}
GO:0003676	nucleic acid binding	79/115, (4350)	2.00×10^{-04}
GO:0004872	receptor activity	72/101, (3814)	1.61×10^{-03}
GO:0004888	transmembrane receptor activity	51/74, (2814)	3.89×10^{-03}
GO:0030528	transcription regulator activity	32/49, (1859)	9.09×10^{-03}
GO:0004871	signal transducer activity	93/114, (4312	3.01×10^{-02}

Table 5.11: Differentially expressed genes linked to the GO term: 'Intracellular signaling cascade'

Gene symbol	Description	$log_2(ratio)$	p-value	percentile	
				OT-1	F5
Pdlim4	PDZ and LIM domain 4	2.63	5.77×10^{-05}	81.2	41.6
Igfbp4	insulin-like growth factor binding protein 4	1.68	5.25×10^{-04}	97.2	86.7
Plcxd2	phosphatidylinositol-specific phospholipase C	1.53	3.33×10^{-04}	93.7	81.4
Bbc3	BCL2 binding component 3	1.48	2.49×10^{-06}	80.0	61.0
Tlr1	toll-like receptor 1	1.45	3.46×10^{-04}	93.4	80.4
Eps8l1	EPS8-like 1	1.35	1.86×10^{-05}	65.4	42.0
Cxcr3	chemokine (C-X-C motif) receptor 3	1.27	1.81×10^{-05}	76.8	60.3
Sgk1	serum/glucocorticoid regulated kinase 1	1.20	1.13×10^{-05}	97.6	92.7
Depdc1b	DEP domain containing 1B	1.13	1.26×10^{-03}	71.2	56.8
Gimap7	GTPase, IMAP family member 7	1.05	1.69×10^{-04}	92.9	84.8
Cd96	CD96 antigen	1.04	1.15×10^{-06}	96.7	91.3
Racgap1	Rac GTPase-activating protein 1	1.04	3.05×10^{-02}	78.6	63.8
Tnk2	tyrosine kinase, non-receptor, 2	0.98	3.87×10^{-03}	92.5	82.2
Pmaip1	phorbol-12-myristate-13-acetate-induced protein 1	0.96	1.12×10^{-03}	73.1	60.7
Gna15	guanine nucleotide binding protein, alpha 15	0.85	2.29×10^{-03}	68.1	57.1
Rapgef4	Rap guanine nucleotide exchange factor (GEF) 4	0.84	4.74×10^{-03}	80.8	69.8
Vipr1	vasoactive intestinal peptide receptor 1	0.81	2.31×10^{-03}	69.0	54.6
Malt1	MALT lymphoma translocation gene 1	0.80	2.47×10^{-02}	90.2	83.1
Rgs11	regulator of G-protein signaling 11	0.75	3.19×10^{-04}	68.3	58.7
Mfhas1	malignant fibrous histiocytoma amplified seq 1	0.70	2.48×10^{-03}	93.1	87.7
Rasgrp1	RAS guanyl releasing protein 1	0.69	3.70×10^{-02}	92.0	85.2
Dennd4c	DENN/MADD domain containing 4C	0.69	2.76×10^{-05}	88.7	81.3
Pim2	proviral integration site 2	0.68	1.59×10^{-03}	94.4	89.8
Cdc42bpg	CDC42 binding protein kinase gamma	0.68	3.77×10^{-03}	65.1	55.9
Rhoq	ras homolog gene family, member Q	0.68	3.80×10^{-03}	73.4	64.6
Asb13	ankyrin repeat and SOCS box-containing 13	−0.66	1.13×10^{-03}	73.6	81.2
Igf1	insulin-like growth factor 1	−0.66	8.65×10^{-03}	31.3	50.5
Stat2	signal transducer and activator of transcription 2	−0.73	1.87×10^{-03}	69.5	78.5
Coro2a	coronin, actin binding protein 2A	−0.74	2.25×10^{-04}	58.9	67.9
Trat1	TCR-associated transmembrane adaptor 1	−0.74	2.14×10^{-04}	78.0	85.8
Rab37	RAB37, member of RAS oncogene family	−0.75	5.63×10^{-04}	83.2	90.0
Hmox1	heme oxygenase (decycling) 1	−0.76	8.85×10^{-04}	52.6	63.1
Lyn	v-yes-1 oncogene homolog	−0.77	6.65×10^{-04}	55.0	64.9
Ccr2	chemokine (C-C motif) receptor 2	−0.77	3.43×10^{-02}	44.7	57.4
Cd81	CD81 antigen	−0.77	9.56×10^{-04}	60.0	69.2
Abca1	ATP-binding cassette, sub-family A, member 1	−0.78	1.34×10^{-03}	67.5	77.9
Plek	pleckstrin	−0.80	1.12×10^{-02}	41.2	57.5
Prkar2b	protein kinase, cAMP dependent regulatory, IIb	−0.82	3.66×10^{-03}	33.1	54
Clec7a	C-type lectin domain family 7, member a	−0.84	3.35×10^{-05}	45.3	59.9
Lgals1	lectin, galactose binding, soluble 1	−0.84	1.04×10^{-04}	98.4	99.2
Cish	cytokine inducible SH2-containing protein	−0.88	4.23×10^{-04}	66.5	77.4
Hck	hemopoietic cell kinase	−0.88	2.01×10^{-04}	46.1	60.8
Il4i1	interleukin 4 induced 1	−0.89	2.38×10^{-03}	55.3	66.6
Eya2	eyes absent 2 homolog (Drosophila)	−0.96	3.08×10^{-04}	66.1	78
Aldh1a2	aldehyde dehydrogenase family 1, subfamily A2	−0.96	4.54×10^{-04}	59.7	71.2
Ldhb	lactate dehydrogenase B	−1.00	6.21×10^{-05}	66.4	78.1
F2r	coagulation factor II (thrombin) receptor	−1.02	7.46×10^{-04}	89	95.1
Cap2	CAP, adenylate cyclase-associated protein, 2	−1.32	4.82×10^{-04}	24.6	58.2
P2ry6	pyrimidinergic receptor P2Y, G-protein coupled, 6	−1.37	3.36×10^{-04}	12.3	52.5
Gzma	granzyme A	−1.55	3.25×10^{-06}	80	93.3
Cd74	CD74 antigen	−1.64	1.70×10^{-05}	79.9	93.8
Apoe	apolipoprotein E	−1.68	3.78×10^{-05}	56.6	77.8
Aif1	allograft inflammatory factor 1	−2.07	3.53×10^{-05}	27.9	68.4
Tyrobp	TYRO protein tyrosine kinase binding protein	−2.17	1.10×10^{-07}	56.6	83.4
Cap1	CAP, adenylate cyclase-associated protein 1	−4.72	2.02×10^{-06}	63	98.6

Note: Genes with $|\log_2(\text{ratio})| < 0.65$ are not shown in this table

Table 5.12: Differentially expressed genes linked to the GO term: 'Scavenger receptor activity'

Gene symbol	Description	$log_2(ratio)$	p-value	percentile	
				OT-1	F5
Cd5	CD5 antigen	1.80	2.24×10^{-06}	98.4	91.8
Cd6	CD6 antigen	1.72	2.24×10^{-06}	97.7	89.7
5830411N06Rik	RIKEN cDNA 5830411N06 gene	1.40	8.79×10^{-05}	72.7	53.9
Cd163l1	CD163 molecule-like 1	1.06	7.38×10^{-03}	67.35	53.05
Zmynd15	zinc finger, MYND-type containing 15	−0.63	3.48×10^{-03}	34.2	51.2
Cxcl16	chemokine (C-X-C motif) ligand 16	−0.69	3.44×10^{-03}	56.9	63.4
Cd5l	CD5 antigen-like	−1.16	9.98×10^{-04}	43.8	63.3
Marco	macrophage receptor with collagenous structure	−1.55	1.12×10^{-05}	45.4	69.1

Table 5.13: Differentially expressed genes linked to the GO term: 'Cytokine binding'

Gene symbol	Description	$log_2(ratio)$	p-value	percentile	
				OT-1	F5
F2rl1	coagulation factor II (thrombin) receptor-like 1	3.56	4.62×10^{-05}	88	32.4
Cxcr3	chemokine (C-X-C motif) receptor 3	1.27	1.81×10^{-05}	76.8	60.3
Ebi2	G protein-coupled receptor 183	1.04	3.03×10^{-04}	85	71
Tnfrsf25	tumor necrosis factor receptor superfamily, 25	0.82	3.76×10^{-06}	68.9	58.3
Il6ra	interleukin 6 receptor, alpha	0.79	7.86×10^{-03}	76.8	64.1
Il7r	interleukin 7 receptor	0.57	4.42×10^{-04}	98.1	96.6
Il12rb1	interleukin 12 receptor, beta 1	−0.54	1.07×10^{-03}	59.9	66.2
Cdk5rap1	CDK5 regulatory subunit associated protein 1	−0.67	4.86×10^{-05}	81.2	87.6
Il18bp	interleukin 18 binding protein	−0.73	5.13×10^{-04}	56.1	65.2
Ccr2	chemokine (C-C motif) receptor 2	−0.77	3.43×10^{-02}	44.7	57.4
Ccrl2	chemokine (C-C motif) receptor-like 2	−0.79	1.11×10^{-04}	37.7	55.8
Csf2rb	colony stimulating factor 2 receptor, beta	−0.81	1.12×10^{-03}	37.3	56.5
P2ry6	pyrimidinergic receptor P2Y, G-protein coupled, 6	−1.37	3.36×10^{-04}	12.3	52.5
Cd74	CD74 antigen	−1.64	1.70×10^{-05}	79.9	93.8

Table 5.14: Differentially expressed genes linked to the GO term: 'Chemokine receptor binding'

Gene symbol	Description	$log_2(ratio)$	p-value	percentile	
				OT-1	F5
Xcl1	chemokine (C motif) ligand 1	−0.51	1.78×10^{-02}	40.7	52.8
Ccl22	chemokine (C-C motif) ligand 22	−0.56	4.18×10^{-03}	60.4	66.9
Zmynd15	zinc finger, MYND-type containing 15	−0.63	3.48×10^{-03}	34.2	51.2
Cxcl16	chemokine (C-X-C motif) ligand 16	−0.69	3.44×10^{-03}	56.9	63.4
Ccr2	chemokine (C-C motif) receptor 2	−0.77	3.43×10^{-02}	44.7	57.4
Ccl5	chemokine (C-C motif) ligand 5	−1.39	8.29×10^{-05}	81.1	92.9
Cxcl10	chemokine (C-X-C motif) ligand 10	−1.57	1.18×10^{-04}	42.3	67.8
Ccl8	chemokine (C-C motif) ligand 8	−2.35	1.50×10^{-05}	57.6	85.9

Table 5.15: Genes linked to the GO terms:'adaptive and innate immune response', that are over-represented in the differentially expressed subset.

Adaptive Immune Response					
Gene symbol	Description	$\log_2$(ratio)	p-value	percentile	
				OT-1	F5
Eomes	eomesodermin homolog (Xenopus laevis)	1.53	3.16×10^{-05}	80.4	60.7
Malt1	MALT lymphoma translocation gene 1	0.80	2.47×10^{-02}	90.2	83.1
Il7r	interleukin 7 receptor	0.57	4.42×10^{-04}	98.1	96.6
Tbx21	T-box 21	0.52	7.30×10^{-03}	62.7	55.1
Cd86	CD86 antigen	−0.53	6.08×10^{-03}	40.9	52.7
Cd1d2	CD1d2 antigen	−0.59	5.45×10^{-04}	46.0	57.0
C3	complement component 3	−0.69	2.51×10^{-03}	31.9	51.1
Il18bp	interleukin 18 binding protein	−0.73	5.13×10^{-04}	56.1	65.2
H2-DMa	histocompatibility 2, class II, locus DMa	−0.80	1.06×10^{-03}	74.7	86.0
Ada	adenosine deaminase	−0.84	2.35×10^{-04}	63.0	72.8
Fcer1g	Fc receptor, IgE, high affinity I, gamma	−1.20	3.37×10^{-03}	57.3	72.0
Irf7	interferon regulatory factor 7	−1.21	7.79×10^{-05}	90.2	96.4
Fcgr3	Fc receptor, IgG, low affinity III	−1.24	5.86×10^{-05}	42.9	64.0
C1qc	complement component 1, q subcomponent, C	−1.49	1.38×10^{-03}	46.5	68.6
Il18	interleukin 18	−1.51	9.11×10^{-04}	28.2	61.7
Cd74	CD74 antigen	−1.64	1.70×10^{-05}	79.9	93.8
H2-Aa	histocompatibility 2, class II antigen A, alpha	−1.69	1.90×10^{-04}	65.9	86.5
C1qa	complement component 1, q subcomponent, alpha	−2.05	4.00×10^{-05}	49.2	77.3
C1qb	complement component 1, q subcomponent, beta	−2.41	2.21×10^{-05}	39.4	76.9

Innate Immune Response					
Gene symbol	Description	$\log_2$(ratio)	p-value	percentile	
				OT-1	F5
Tlr1	toll-like receptor 1	1.45	3.46×10^{-04}	93.4	80.4
Klrd1	killer cell lectin-like receptor, subfamily D 1	1.34	6.47×10^{-06}	99.1	97.1
Pglyrp1	peptidoglycan recognition protein 1	0.92	6.24×10^{-04}	64.2	50.2
Malt1	MALT translocation gene 1	0.80	2.47×10^{-02}	90.2	83.1
Brca2	breast cancer 2	0.60	2.87×10^{-03}	62.3	53.4
Cd1d2	CD1d2 antigen	−0.59	5.45×10^{-04}	46.0	57.0
C3	complement component 3	−0.69	2.51×10^{-03}	31.9	51.1
Clec7a	C-type lectin domain family 7, member a	−0.84	3.35×10^{-05}	45.3	59.9
Ncr1	natural cytotoxicity triggering receptor 1	−0.87	6.96×10^{-05}	39.5	57.9
Cfp	complement factor properdin	−0.90	2.58×10^{-04}	51.4	64.2
Ifih1	interferon induced with helicase C domain 1	−0.97	4.98×10^{-04}	81.8	90.7
Klre1	killer cell lectin-like receptor family E 1	−1.05	1.31×10^{-03}	29.8	56.3
Klrk1	killer cell lectin-like receptor subfamily K 1	−1.08	1.81×10^{-04}	47.3	64.0
Mx1	myxovirus (influenza virus) resistance 1	−1.12	4.60×10^{-04}	62.4	76.0
Unc93b1	unc-93 homolog B1 (C. elegans)	−1.14	1.47×10^{-04}	58.2	72.2
Mx2	myxovirus (influenza virus) resistance 2	−1.22	5.73×10^{-05}	59.1	74.2
C1qc	complement component 1, q subcomponent, C	−1.49	1.38×10^{-03}	46.5	68.6
C1qa	complement component 1, q subcomponent, alpha	−2.05	4.00×10^{-05}	49.2	77.3
C1qb	complement component 1, q subcomponent, beta	−2.41	2.21×10^{-05}	39.4	76.9

Table 5.16: Differentially expressed genes linked to the GO term: 'Sugar binding'

Gene symbol	Description	$log_2(ratio)$	p-value	percentile	
				OT-1	F5
Klrd1	killer cell lectin-like receptor, subfamily D 1	1.34	6.47×10^{-06}	99.1	97.1
Ly75	lymphocyte antigen 75	1.06	2.03×10^{-02}	90.8	80.3
Aim1	absent in melanoma 1	1.06	2.12×10^{-03}	85.7	72.7
Aim1l	absent in melanoma 1-like	1.05	9.24×10^{-04}	60.7	39.6
Fcgrt	Fc receptor, IgG, alpha chain transporter	0.67	4.34×10^{-03}	80.8	71.9
Galnt10	N-acetylgalactosaminyltransferase 10	0.65	3.63×10^{-03}	79.8	70.7
Fgd6	FYVE, RhoGEF and PH domain containing 6	0.62	1.33×10^{-03}	56.4	43
Sell	selectin, lymphocyte	0.52	5.26×10^{-04}	99.4	99.2
Cel	carboxyl ester lipase	−0.55	1.03×10^{-03}	42.6	54.5
Lman2l	lectin, mannose-binding 2-like	−0.57	1.81×10^{-03}	68.3	77.2
Bsg	basigin	−0.58	1.20×10^{-02}	92.4	95.3
AW821953	protein phosphatase 1, regulatory subunit 3B	−0.60	2.95×10^{-03}	61	68
Asb2	ankyrin repeat and SOCS box-containing 2	−0.61	6.57×10^{-04}	49.5	59.4
Reg1	regenerating islet-derived 1	−0.80	1.05×10^{-03}	40.4	57.3
Mgl1	macrophage galactose specific lectin 1	−0.81	5.13×10^{-04}	38.6	56.6
Pygl	liver glycogen phosphorylase	−0.83	4.18×10^{-04}	28.1	51.5
Clec7a	C-type lectin domain family 7, member a	−0.84	3.35×10^{-05}	45.3	59.9
Lgals1	lectin, galactose binding, soluble 1	−0.84	1.04×10^{-04}	98.4	99.2
Reg2	regenerating islet-derived 2	−0.88	8.16×10^{-04}	61.8	72.2
Fcna	ficolin A	−0.93	9.95×10^{-04}	46.7	61.8
Klre1	killer cell lectin-like receptor family E member 1	−1.05	1.31×10^{-03}	29.8	56.3
Klrk1	killer cell lectin-like receptor subfamily K 1	−1.08	1.81×10^{-04}	47.3	64
Clec4n	C-type lectin domain family 4, member n	−1.36	2.15×10^{-05}	12.9	52.5
Mrc1	mannose receptor, C type 1	−1.38	8.94×10^{-05}	21.4	57.6
Pap	regenerating islet-derived 3 beta	−1.40	3.87×10^{-03}	23.2	57.7
Apoe	apolipoprotein E	−1.68	3.78×10^{-05}	56.6	77.8
Lgals3	lectin, galactose binding, soluble 3	−1.93	2.39×10^{-05}	42.3	72.3
Cd209b	CD209b antigen	−1.98	1.70×10^{-05}	42.2	72.9
Ccl8	chemokine (C-C motif) ligand 8	−2.35	1.50×10^{-05}	57.6	85.9

Chapter 6

Pathophysiologic implications

Lymphocyte homeostasis is maintained by competition for limiting resources. However, if the ability of lymphocytes to compete for these resources varies, lymphocytes that are better at competing for limiting resources can be expected to eventually dominate the repertoire. This suggestion has been called the 'competition-diversity paradox' and is discussed in section 2.7. This thesis suggests that the variability in the rates of LIP among T cells bearing different TCRs is caused by intrinsic differences in their proliferation capacity in response to IL7 rather than differential responsiveness to spMHC. Thus, the 'competition-diversity paradox' would need to be considered in the context of IL7 rather than spMHC. This chapter explores this consideration in further detail.

6.1 Competition-diversity paradox

We have shown that $CD5^{hi}$ cells have a greater capacity for proliferation at higher levels of IL7. In contrast, we found that $CD5^{lo}$ cells have a higher capacity for survival at low concentrations of IL7. Naïve T cells are quiescent *in vivo* and are not in cell cycle. The amount of IL7 *in vivo* has been described to be 'limiting' by various authors, which is thought to prevent spontaneous LIP of naïve cells in lymphoreplete animals. However, if IL7 levels were indeed limiting in lymphoreplete mice, one would expect that $CD5^{lo}$ cells would have a relative survival advantage. To test this, we

transferred a polyclonal population of 2.5×10^6 naïve B6.Thy1.2$^+$ CD8$^+$ T cells into age- and sex-matched B6.Thy1.1 mice and followed their CD5 profile over three weeks. There was no change in the CD5 profile of the transferred CD8$^+$ cells compared to the naïve CD8$^+$ T cells in the recipient. Although the numbers of the transferred cells declined steadily, their CD5 profile did not change. This suggested that the death kinetics of CD5^{hi} and CD5^{lo} cells may be equivalent *in vivo* in lymphoreplete mice. Additionally, this would also suggest that CD5^{hi} and CD5^{lo} cells are replenished by the thymus at equivalent rates *in vivo*. Thus, it appears that the level of IL7 *in vivo* is sufficiently high to prevent the preferential survival of CD5^{lo} cells, thereby avoiding the 'competition-diversity paradox'.

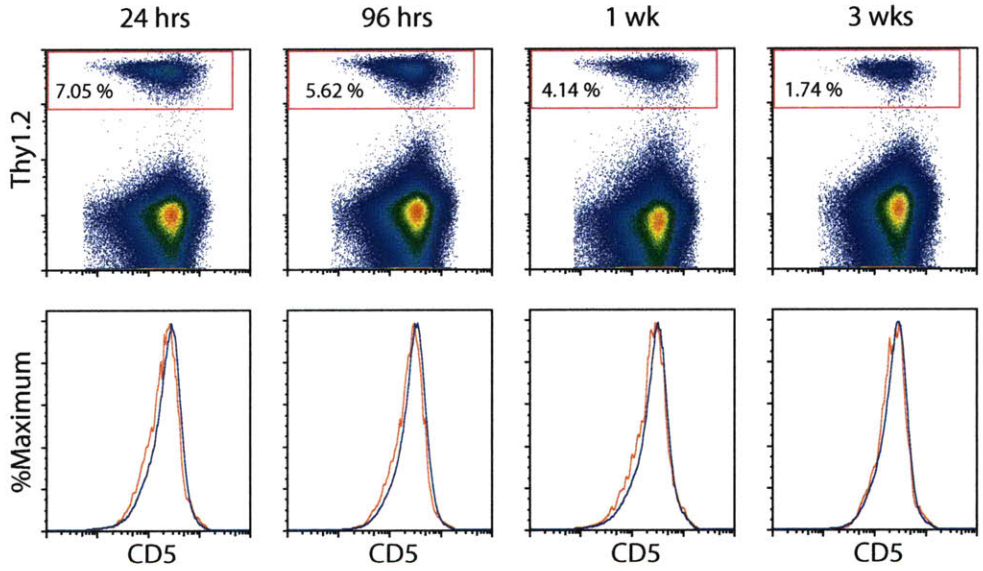

Figure 6-1: **CD5 profile of adoptively transferred of polyclonal naïve CD8$^+$ T cells.** 2.5×10^6 B6.Thy1.2$^+$ CD8$^+$ CD44^{lo} T cells were transferred into age and sex-matched B6.Thy1.1$^+$ recipients. The percentage of donor cells is shown in the upper panel. The lower panel contrasts the profile of CD5 levels of transferred cells (red) with the naïve CD8$^+$ T cells in the recipient mice (blue) at each time point.

6.2 Effect of increasing the level of IL7 in vivo

IL7-induced proliferation of T cells occurs *in vivo* when there is an excess of IL7 even in the absence of foreign antigen, e.g. lymphopenia or exogenous IL7 therapy. $CD5^{hi}$ cells have a greater rate of LIP than $CD5^{lo}$ cells under lymphopenic conditions. While this has been previously attributed to the greater responsiveness of $CD5^{hi}$ cells to presumably excess cognate spMHC seen during lymphopenia, we have demonstrated that this phenomenon is largely due to the greater intrinsic proliferation capacity of $CD5^{hi}$ cells in response to IL7. We tested if the selective proliferation of $CD5^{hi}$ cells in response to IL7 is also manifest *in vivo* under lymphoreplete conditions by transferring CFSE labeled T cells into mice with sub-cutaneous implants of IL7-releasing miniosmotic pumps that released 5 μg of IL7 over one week (see Figure 6-2a). Proliferation of both $CD8^+$ and $CD4^+$ T cells was seen in mice implanted with IL7-releasing pumps as previously reported[82]. No proliferation was seen in the control mice that received PBS only. Indeed, there was a greater proliferation of $CD5^{hi}$ cells among both $CD8^+$ and $CD4^+$ T cells. In order to exclude the possibility that CD5 levels change during proliferation, we sorted naïve $Thy1.2^+$ $CD8^+$ T cells into $CD5^{hi}$ and $CD5^{lo}$ fractions and transferred them individually into lymphoreplete $Thy1.1^+$ congenic mice bearing IL7-releasing pumps (see Figure 6-2b). $CD5^{hi}$ cells showed substantially higher proliferation in mice implanted with IL7 miniosmotic pumps. These results suggest that exogenous IL7 therapy has the potential to skew the existing naïve T cell repertoire by inducing a selective proliferation of IL7-responsive $CD5^{hi}$ cells.

6.3 Effect of decreasing the level of IL7 in vivo

We have shown that $CD5^{hi}$ cells have a reduced ability to survive *in vitro* compared to $CD5^{lo}$ cells at lower concentrations of IL7. To test if differential survival of $CD5^{hi}$ and $CD5^{lo}$ cells is manifest *in vivo* under conditions of IL7 deficiency, we adoptively transferred with B6.CD45.2 naïve $CD8^+$ $Thy1.1^+$ $CD5^{hi}$ and $Thy1.2^+$ $CD5^{lo}$ T cells into B6.CD45.1 mice and injected 1 mg of an IL7 depleting antibody (M25) i.p. ev-

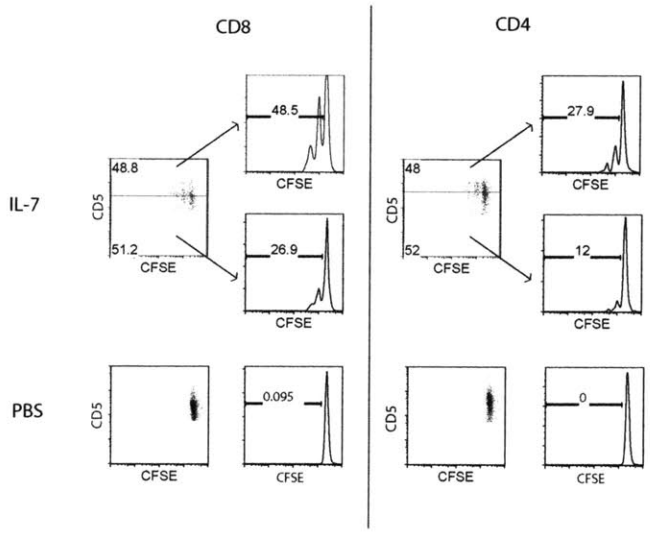

(a) Adoptive transfer of unsorted naïve $CD8^+$ T cells

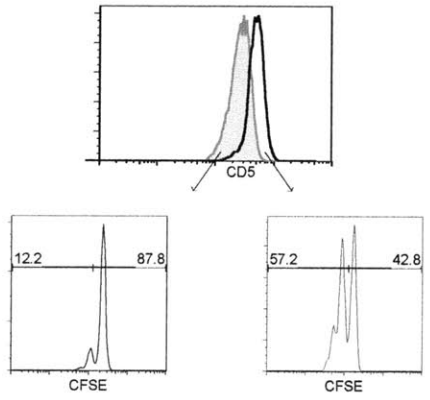

(b) Adoptive transfer of naïve $CD5^{hi\ or\ lo}$ $CD8^+$ T cells

Figure 6-2: **Effect of exogenous IL7 on lymphoreplete mice.** (a) $CD5^{hi}$ cells selectively proliferate following exogenous IL7 treatment in lymphoreplete mice. 2×10^6 CFSE labeled cells from the lymph nodes of B6.Thy1.2 mice were transferred into congenic Thy1.1 mice implanted with miniosmotic pumps that released IL7 or PBS only. CFSE dilution of the transferred $CD5^{hi}$ and $CD5^{lo}$ cells in the lymphoid organs of recipient mice was measured after seven days. (b) Naïve $CD8^+$ Thy1.2 T cells were sorted into $CD5^{hi}$ cells and $CD5^{lo}$ fractions and adoptively transferred into lymphoreplete congenic Thy1.1 mice implanted with miniosmotic pumps that released 5 μg IL7 over seven days. CFSE dilution of transferred cells was measured at seven days.

ery alternate day for one week and measured its impact on the $CD5^{hi}$:$CD5^{lo}$ (i.e. Thy1.1:Thy1.2) ratio of the adoptively transferred cell population and *vice versa* (see

Figure 6-3). The M25 antibody treatment was also found to result in the skewing of the CD5 profiles of naïve $CD8^+$ T cells in the treated animals towards $CD5^{lo}$ phenotype by one week (see Figure 6-3). As IL7 does not affect the CD5 levels, at least in vitro, this could be due to selective survival of $CD5^{lo}$ cells under conditions of IL7 deprivation.

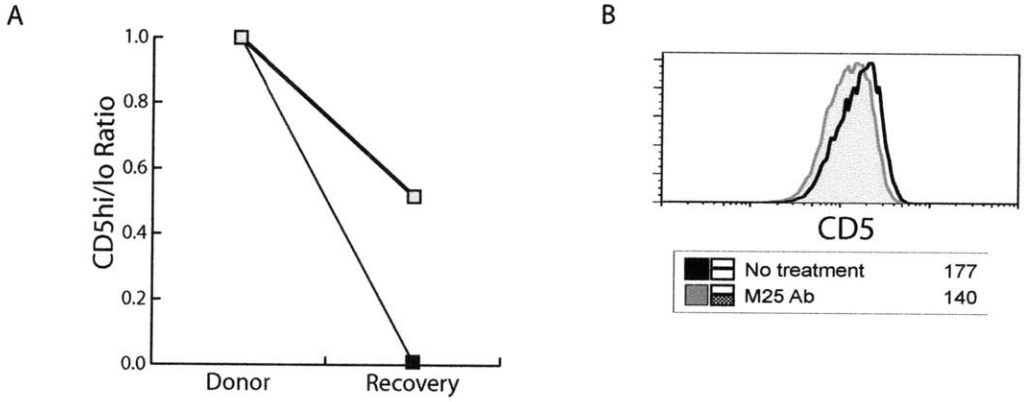

Figure 6-3: **Effect of IL7 depletion in lymphoreplete mice.** (a) Congenically marked $CD45.2^+$ $CD5^{hi}$ and $CD5^{lo}$ cells ($Thy1.1^+$ and $Thy1.2^+$) were transferred into CD45.1 mice and treated with 1 mg of anti-IL7 (M25) antibody i.p. every two days. The lymphoid organs were analyzed after one week. The ratio of the transferred $CD5^{hi}$:$CD5^{lo}$ cells is shown at the time of transfer and recovery in two mice. (b) The profile of CD5 levels on naïve $CD8^+$ T cells in a mouse treated with M25 for seven days as above (filled histogram) is compared with that of an untreated mouse (open histogram). The mean values of CD5 MFI are indicated in the legend.

6.4 Estimation of the physiological levels of IL7

The level of IL7 present *in vivo* is likely to be in the range that avoids the competition-diversity paradox in terms of selective survival or proliferation of $CD5^{lo}$ or $CD5^{hi}$ cells respectively (see Figure 6-1). Direct estimation of the amount of IL7 present in lymphoreplete mice is technically challenging because it is close to the lower limit of detection by ELISA. Furthermore, as IL7 is known to bind glycosaminoglycans in the extracellular matrix, the levels of serum IL7 may not reflect the amount of IL7 available to lymphocytes in lymphoid organs. Therefore, we have tried to indirectly

estimate the levels of IL7 in vivo using bioassays based on the observation that IL7R is transcriptionally repressed by IL7[93].

The change in IL7R level of freshly isolated naïve $CD8^+$ T cells from OT-1, 2C, F5 and B6 mice upon overnight culture in medium with varying concentrations of IL7 *in vitro* was measured. The inverse relationship between IL7R level on $CD8^+$ T cells and IL7 concentration in culture medium can be used to get a rough estimate the physiological level of IL7. Naïve $CD8^+$ T cells from all these mice need between 0.1 and 1 ng/mL of IL7 to maintain their surface IL7R at levels comparable to those on freshly isolated T cells (see Figure 6-4a). At this range of IL7, we do not see preferential survival or proliferation of $CD5^{hi}$ and $CD5^{lo}$ cells at least *in vitro*. However, OT-1, 2C and F5 cells have intrinsic differences in their IL7 signaling cascades. They also have different baseline levels of IL7R, which could result in differential ligand consumption, making such an assay harder to interpret. If IL7 is indeed consumed at different rates by cells with different levels of IL7R, a bioassay based upon $CD8^+$ cells with different baseline levels of IL7R would be unreliable. Thus, to get a better estimate of the IL7 levels in lymphoid organs, we used identical 2C.Thy1.1 cells as reporters of *in vivo* IL7 levels (see Figure 6-4b). 2×10^6 $2C^+$ $Thy1.1^+$ $Rag^{-/-}$ mice were transferred into $Thy1.2^+$ OT-1, 2C, F5 and B6 mice. The transferred $2C^+$ $Thy1.1^+$ cells were recovered from the spleens of recipient mice after 18 hrs and IL7R levels were measured. Analysis of IL7R levels on the recovered reporter cells suggest that the level of IL7 *in vivo* follows the order: $Rag1^{-/-}$ > F5 > 2C > OT-1 mice. These results are consistent with the observation that the total number of CD8 cells follows the opposite order: $Rag1^{-/-}$ < F5 < 2C < OT-1 mice.

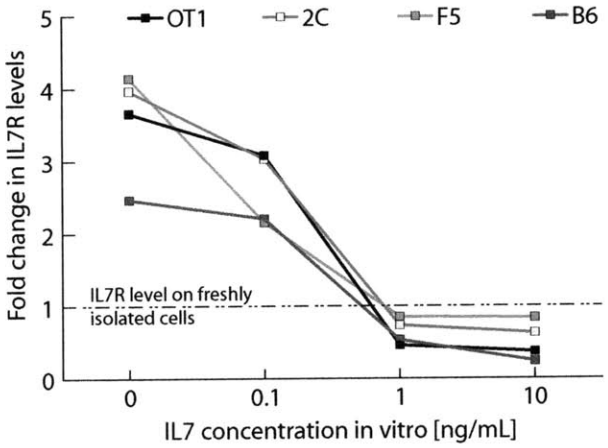

(a) Estimation of IL7 concentration in vivo

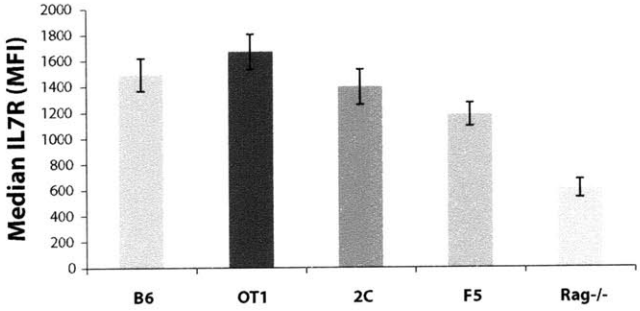

(b) Reporter cell assay

Figure 6-4: **Estimation of IL7 concentration in vivo.** (a) The amount of IL7 concentration needed in vitro to equilibrate the IL7R level to a level that is comparable with that of freshly isolated cells after overnight culture (18 hrs) was used as a bioassay to estimate the relative levels of IL7 in vivo in various mice. (b) 2C $Rag1^{-/-}$ $Thy1.1^{+}$ cells were used as reporter cells and their IL7R level 24 hrs after adoptive transfer was used as a readout of *in vivo* levels of IL7 in OT-1, 2C, F5, B6 $Thy1.2^{+}$ recipient mice.

Chapter 7

Conclusions

7.1 Single cell analysis of spMHC-mediated signaling in T cells

A direct comparison of cognate spMHC-induced signaling among mature T cells of different specificities has not been undertaken before. We used OT-1 and F5 cells for this comparison, which were expected to have a different spMHC-responsiveness based on their CD5 levels. Indeed, we confirmed that the strength of thymic selection is dramatically different in OT-1 and F5 cells, which suggests that their TCRs probably have a genuine biochemical difference in interaction with their cognate spMHC. However, we did not see any obvious difference in the spMHC-induced Ca^{2+} flux between naïve OT-1 and F5 cells interacting with DCs. Despite the lack of observable differences in proximal TCR signaling as measured by Ca^{2+} influx in OT-1 and F5 cells, there is a dramatic difference in proliferation induced by spMHC on the same dendritic cells. While it is possible that there are differences in spMHC-mediated signals in OT-1 and F5 cells that involve mediators other than cytosolic Ca^{2+} flux, they may be hard to define given that the specific molecular components involved in spMHC-mediated survival of naïve T cells or their LIP are still poorly understood, unlike agonist pMHC-mediated TCR signaling. It is also possible that OT-1 and F5 cells respond differentially to accessory molecules presented on DCs, which modulate the

same spMHC-mediated signal, that are necessary but not sufficient for maintaining T cell survival or LIP [29, 19]. Nevertheless, CD5 is a negative regulator of proximal TCR signaling and we have demonstrated that the CD5 level is an intrinsic property of T cells, implying that the TCR signaling cascades of OT-1 and F5 cells are intrinsically different. Indeed, this is supported by the microarray data which shows that a number of mediators of the TCR signaling pathway are also differentially expressed (see Table 5.11). For instance, Rasgrp1, which is a critical component of a feedback amplification loop in proximal TCR signaling, is over-expressed in OT-1 cells (FC = 1.62, p = 0.037). Such intrinsic differences in TCR signaling networks in these two T cell types could explain how the proximal TCR signal induced by the same spMHC repertoire, as defined by Ca^{2+} influx, may be similar although the avidity of the two TCRs for the same spMHC repertoire may differ.

It has been proposed that the developmental regulation of intrinsic differences in CD5 levels helps to dynamically dampen excessive spMHC signals in an attempt to maximize the T cell repertoire that is selected [6]. This allows TCRs with a broader range of self-specificities to pass the stringency of thymic selection than would otherwise be possible. This thesis suggests that the TCR-specific tuning of CD5 levels during thymic development gets imprinted as an intrinsic feature of mature T cells and it may have a role in preventing autoimmunity in the periphery regardless of the biochemical interaction strength of a TCR with its cognate spMHC. It may also contribute to the avoidance of the competition-diversity paradox in the periphery. From this perspective, it would make sense that naïve OT-1 and F5 T cells exhibit equivalent spMHC-induced Ca^{2+} influx. Indeed, such differentially imprinted intrinsic differences may also seen with other components in the TCR signaling cascade, in addition to CD5.

Our analysis of spMHC-mediated signaling in naïve $CD8^+$ T cells of two defined specificities in response to the same spMHC at the single cell level using Ca^{2+} influx video microscopy also confirms the asynchronous and stochastic nature of spMHC-induced signals as previously reported with polyclonal T cells [106]. The lack of any Ca^{2+} reponse in a significant fraction of T cells could be due to the spatiotemporal

variability in the presentation of cognate spMHC by dendritic cells and is consistent with the stochastic model of cell division during LIP presented by Yates et al [140]. An additional source of this variablilty could arise from within the T cell itself. Triggering of the TCR cascade has a significant stochastic component [97] and the intrinsic noise in the sensitivity of the detection system [26] could become particularly apparent during spMHC-mediated signaling given the biochemically weak nature of spMHC-TCR interactions.

7.2 Intrinsic functional heterogeneity in the naïve $CD8^+$ T cell repertoire

We have identified a novel 'layer' of intrinsic functional heterogeneiety in the survival and proliferation capacities within the seemingly homogeneous naïve $CD8^+$ T cell repertoire that is predictably marked by surface CD5 expression. The range of this heterogeneity is summarized in Table 7.1. This functional heterogeneity is distinct from non-genetic cell-to-cell variability within a cell population that has been recently quantified in both eukaryotic and prokaryotic systems [114, 121, 26]. While stochastic fluctuations in protein state can transmitted from mother to daughter [114], they result in transient heritability in cell fate. In contrast, we have shown that this seemingly *continuous* 'layer' functional heterogeneity is robustly heritable even after several rounds of cell division. Elucidation of the mechanisms underlying the robust transmission of these subtly different characteristics during T cell proliferation networks may lead to interesting biological insights.

Naïve $CD8^+$ T cells that are also $CD5^{hi}$ have a greater intrinsic capacity for proliferation than $CD5^{lo}$ cells. The increased capacity for proliferation of $CD5^{hi}$ cells is manifest with the same degree of stimulation of the TCR signaling cascade with the same dose of PMA/ionomycin as well as at identical but high (supra-physiological) doses of IL7. Differences in metabolic capacities are also evident from the larger cell size, lower mitochondrial mass and reduced glucose uptake in naive $CD5^{hi}$ cells.

Functional characteristic	$CD5^{hi}$	$CD5^{lo}$
Proliferation capacity (same TCR or IL7 stimulus)	High	Low
Survival capacity in the absence of cytokine	Low	High
Baseline IL7R level	High	Low
CD5 and CD6 levels (regulators of the TCR cascade)	High	Low
pStat5, Bcl2, CD8α, pGsk3 induction by IL7	High	Low
Gfi1, Socs1	Low	High
Cell size	High	Low
Mitochondrial mass	Low	High
Glucose uptake	Low	High

Table 7.1: **Intrinsic heterogeneity naive $CD8^+$ T cells.** Intrinsic heterogeneity in naive $CD8^+$ T cells is predictably marked by surface levels of CD5.

Differences in mitochondrial mass may also reflect differences in the capacity for autophagy in $CD5^{hi}$ and $CD5^{lo}$ cells which is critical for maintaining T cell survival in the periphery [98, 99]. Additionally, differences in glucose uptake could also explain why $CD5^{lo}$ cells survive better in reduced amounts of pro-survival cytokines both in vitro and in vivo. As T cell size is maintained by IL-7 signaling [103], it is possible that the differences in cell size between $CD5^{hi}$ and $CD5^{lo}$ cells are a consequence of corresponding demonstrated differences in their responsiveness to IL7. The differential responsiveness to IL7 is also likely to be imprinted because it persists even after activation and several rounds of cell division.

7.3 CD5 level as a lineage marker rather than a surrogate for spMHC signal strength

Based on the requirement of spMHC for maintaining CD5 levels *in vivo* [113], a number of studies have directly interpreted the CD5 level on naïve T cells as a surrgoate measure for the strength of spMHC-induced T cell signal [33, 60]. However, we have presented many lines of evidence that the *baseline* CD5 level is an intrinsic feature of a T cell. Relative differences in CD5 levels in OT-1 and F5 cells, or polyclonal $CD5^{hi}$ and $CD5^{lo}$ T cells, persist in vitro even after withdrawal from spMHC signals although the absolute levels of CD5 decrease in all cases. Furthermore, the differences

in CD5 levels persist even after many rounds of activation-induced proliferation and conversion into memory-like cells in vitro and can survive dramatic changes in cell physiology as well as multiple rounds of cell division that occur during T cell activation. Strikingly, the above results can be reproduced even with T cells from the *same* TCR transgenic mouse but with high or low levels of CD5, strongly suggesting that the relative baseline CD5 levels are intrinsic or imprinted. These findings suggest that the observed differences in CD5 levels are maintained by both extrinsic and intrinsic mechanisms, thus reconciling the observations on developmental regulation of CD5 levels by varying strengths of selection in the thymus [7] with the requirement for spMHC signals to maintain CD5 levels in the periphery [113]. Thus, the *baseline* CD5 level may be better viewed as a lineage 'marker' of subtle but predictable differences in T cell survival and proliferation capacities. The degree of induction of CD5 level above baseline may better reflect the TCR:spMHC signal received by a particular TCR in the periphery. We have also found that CD5 and CD6 are co-regulated in OT-1 and F5 T cells and suspect that it could also be used as an additional marker of this functional heterogeneity. Like CD5, CD6 is also upregulated during positive selection. The levels of CD6 are low in female HY and DO.11 T cells which are also known to express low levels of CD5 compared to other T cells from other TCR transgenic mice [112].

The level of CD5 is believed to be upregulated during positive selection in DP cells in a manner that is proportional to the avidity of the TCR for its cognate spMHC. However, a direct comparison of CD5 levels in the thymi of OT-1 and F5 mice is not possible due to dramatic differences in the progression from DP to SP stage between OT-1 and F5 mice. However, both OT-1 and F5 $Rag^{-/-}$ T cells that emerge into the periphery acquire complete immunological competence. Indeed, numerous studies have shown that OT-1 and F5 T cells can protect against tumors and pathogens [20, 86, 143]. Azzam et al have shown how the developmental regulation of CD5 levels can dynamically impact the efficiency of TCR selection in multiple TCR transgenic systems by negatively modulating the TCR signal [6]. It has been proposed but not explicity demonstrated that $CD5^{hi}$ and $CD5^{lo}$ T cells undergo different strengths

of thymic selection and result in different efficiencies of positive selection [7]. This question is difficult to address with wild-type mice as it is not possible to follow the same TCR through different stages of development. Therefore we have addressed this question using OT-1 and F5 mice. The thymic output is significantly higher in OT-1 cells than in F5 cells. A majority of the cells undergo death by neglect in the latter. The higher efficiency of positive selection in OT-1 cells is also supported by mixed hematopoietic chimera experiments. This confirms the prediction that OT-1 cells are indeed selected by a stronger signal in the thymus and the CD5 level may be developmentally imprinted to be higher in OT-1 cells than in F5 cells. Pathway analysis of microarray data points to a possible role for E47 in this process, which is consistent with its known involvement in lymphoid differentiation lineage decisions as well as in the regulation of CD5 transcription during lymphoid development [138]. It is thus possible that the degree of cognate spMHC-mediated induction of CD5 levels that occurs in the thymus persists in the periphery in the form of differentially imprinted 'baseline' CD5 levels.

Studies with CD5 transgenic and CD5 knockout animals have focussed on T cell selection [6]. Germline over-expression of CD5 by a transgene can reduce positive selection of TCRs with a low avidity for spMHC and germline deletion of CD5 can increase the rate of negative selection. These phenotypes are thought to result from the dysregulation of the dynamic regulation of TCR signaling by CD5 during T cell development. Similarly, based on our findings of different baseline levels of CD5 in the periphery, we would predict that inducible over-expression of CD5 in mature T cells may result in cell death due to inadequate spMHC-induced survival signals or anergy to foreign pMHC. Similarly, inducible knockout of CD5 could cause autoimmunity or increased reactivity to foreign pMHC.

7.4 Intraclonal heterogeneity in T cells

The strongest evidence for the intrinsic and non-genetic nature of these differences comes from the observation that T cells from the same TCR transgenic mouse have

subtle but analogous differences that are predicted by CD5 levels. Our previous work has shown that it is possible for T cells bearing the same TCR to be selected in multiple lineages within the *same* TCR transgenic mouse [35]. This has been investigated thoroughly in case of the 2C TCR, which we now know can be selected in the $CD4^+$, $CD8^+$ or DN lineage, within the same background [35, 64]. The percentage of T cells selected in any given lineage can be modulated by changing the relative amounts of MHC-I and II using MHC-deficient backgrounds [35, 64]. Additionally, 2C T cells can also be selected into the CD8$\alpha\alpha$ lineage of intra-eptithelial T cells in the H2-b $K^bD^{b-/-}$ background [77]. The phenomenon of heterogeneous lineage selection is not peculiar to the 2C TCR, and indeed, almost all the TCR transgenics that we have examined so far can be selected in both the $CD4^+$ and $CD8^+$ lineages [35]. This is summarized in a table based on published flow cytometry data of the thymi of TCR transgenic mice in the $Rag1^{-/-}$ or $Rag2^{-/-}$ background that we were able to identify (see Table 7.2). Competition for spMHC between TCRs in the thymus can also affect lineage choice [14]. These data suggest that heterogeneity in thymic selection of the same TCR into different lineages in the same mouse is the outcome of spatiotemporal variability in the spMHC repertoire. The asynchronous and unpredictable nature of calcium influx detected in our T:DC co-culture experiments with mature naïve T cells is also consistent with a spatio-temporally variable spMHC repertoire and spMHC-mediated signals in the thymus. Our demonstration of functional intra-clonal heterogeneity further bolsters this view as selection on a heterogeneous spMHC repertoire in the thymus could explain how T cells with the same TCR can receive varying strengths of selection in the thymus and be selected into a functionally variable population of cells within the same lineage. The heterogeneity in the spMHC repertoire within the thymus and the consequent variability in the strengths of selection is also supported by our studies of T cell selection in OT-1 and F5 mice. For instance, in the F5 $Rag^{-/-}$ thymus, a majority of the DP F5 cells die by neglect, presumably due to an inability to receive a selecting signal, while only a few cells expressing the same F5 TCR get a selecting signal that allows them to mature and emerge into the periphery.

Table 7.2: Contra-nominal lineage selection in various TCR transgenic $Rag^{-/-}$ mice. The numbers indicate the percentage of cells selected into the specified lineage based on published flow cytometry profiles of the thymi from various TCR transgenic mice in the $Rag^{-/-}$ background.

TCR	agonist pMHC	Haplotype	Predominant lineage		Minor lineage		Ref
			CD8	MHC	CD4	MHC	
2C	SIYRYYGL/K^b	H-2^b	80	K^b	5	I-A^b, K^b	[35]
HY	SMCY738-764/D^b	H-2^b	10	D^b	3.5	I-A^b	[71, 112]
OT1	OVA257-264/K^b	H-2^b	80	K^b	0.4	I-A^b	[79]
BM3.3	pBM1/K^b	H-2^k	87 [1]	Class I	0 [1]	-	[5, 105]
N15	VSV52-59/K^b	H-2^b	28	K^b	1	I-A^b	[108]
P14	LCMV GP33/D^b	H-2^b	25 [2]	D^b	1 [2]	I-A^b	[32]
Clone 4	HA518-526/K^d	H-2^d	61	K^d	3	Class II	[85]
F5	NP366-374/D^b	H-2^b	9.3	D^b	0	-	[130]
TCR	agonist pMHC	Haplotype	Predominant lineage		Minor lineage		Ref
			CD4	MHC	CD8	MHC	
AND	PCC88-104/I-A^b	H-2^b	61	I-A^b	2.1	Class I	[75]
5B6	PLP139-151/I-A^s	H-2^s	22	I-A^s	3	Class I	[132]
TAZ10	TPO536-547/I-A^k	H-2^k	++ [3]	I-A^k	++ [3]	Class I	[101]
		H-2^k	16 [1]	I-A^k	20 [1]	Class I	[101]
A18	C5107-121/I-E^k	H-2^k	9.4	I-E^k	1.4	Class I	[8]
		H-$2^{q/k}$	55	Class II	23.5	Class I	[8]
HA	HA107-119/I-E^d	H-2^d	7.7	I-E^d	2.5	Class I, I-E^d	[2, 61]
3.L2	Hb65-74/I-E^k	H-2^k	7.7	I-E^k	1.5	Class I	[58]
2.102	Hb64-76/I-E^k	H-2^k	5	I-E^k	6	Class I	[41]
		H-2^b	3	I-A^b	2	Class I	[41]
DO11.10	Ova323-339/I-A^d	H-2^d	10	I-A^d	3.5	Class I	[112]
B5	MSp1151-1171/I-E^d	H-2^d	<1	I-E^d	0.4	Class I	[117]
TCli	CLIP81-104/I-A^b	H-2^b	8	I-A^b	1	Class I	[135]
Tea	I-Ea52-68/I-A^b	H-2^b	57	I-A^b	2	Class I	[10]
OT-II	Ova323-339/I-A^b	H-2^b	48	I-A^b	1	Class I	[135]
2D2	MOG35-55/I-A^b	H-2^b	37	I-A^b	1	Class I	[10]
5C.C7	MCC88-104/I-E^k	H-2^k	++ [3]	I-E^k	+ [3]	Class I	[133]
KB	hC4675-686/I-E^s	H-2^s	++ [3]	I-E^s	+ [3]	Class I	[48]
N3.L2	Hb65-74/I-E^k	H-2^k	++ [3]	I-E^k	+ [3]	Class I	[55]

[1] Percentage of CD4 or CD8 T cells in the lymph nodes
[2] Percentage of CD4 or CD8 T cells in the spleen
[3] + and ++ indicate the relative percentages of CD4 and CD8 T cells as estimated from published FACS plots.

7.5 Implications for extrinsic models of functional T cell diversity

Two recent studies have explained observations of functional T cell diversity in the levels of CD5, CD8α, and IL7R, solely in the context of heterogeneous extrinsic signals, which include both spMHC and IL7 (see Figure 2-8) [93, 94]. We have re-interpreted the data from these studies in the light of our identification of intrinsic diversity in T cell signaling networks, as discussed below.

In what they have termed the 'co-receptor tuning' model, Park *et al* have proposed that T cells that receive a strong signal from spMHC have a reduced responsiveness to IL7 due to cross-wiring of the TCR and IL7 signaling cascades [94]. They found that spMHC-mediated TCR signaling can inhibit IL7 signaling and that IL7 can increase the strength of TCR signaling by inducing the transcription of CD8α. Male HY TCR transgenic mice, which express high levels of CD5, completely lack the ability to phosphorylate Stat5 in response to IL7 until the TCR-induced inhibitory signal dissipates by resting the cells overnight. Their conclusions are in apparent contradiction to our findings. However, we did not see comparable defect in the ability of freshly isolated OT-1 cells to phosphorylate Stat5. As male HY T cells are selected on agonist ligands, this phenomenon may not be applicable to the rest of the $CD8^+$ T cell population. The inverse correlation between surface levels of CD5 and CD8α in a panel of TCR transgenic mice selected in the same background (2C, F5 and female HY) has also been presented in support of the 'co-receptor tuning' model, and indeed we find a similar inverse correlation in OT-1, 2C and F5 cells. However, OT-1, 2C and F5 mice have decreasing numbers of $CD8^+$ cells and as a consequence they have conversely increasing levels of IL7 (see Figure 6-4). There is also a very strong correlation between baseline IL7R levels and the degree of IL7 consumption per $CD8^+$ T cell[1]. This likely further exacerbates the differences in IL7 consumption in OT-1, 2C and F5 mice as 'baseline' IL7R levels in $CD8^+$ cells from these mice follow the order: OT-1 > 2C > F5.

We also find that the 'baseline' levels of IL7R are higher in OT-1 and polyclonal $CD5^{hi}$ cells than F5 or polyclonal $CD5^{lo}$ cells, and that the IL7R levels are strongly correlated with IL7-induced signal transduction in these cells. We believe that the differences in the baseline levels of IL7R are due to imprinted differences in the T cells as they are apparent after the dissipation of both IL7 and TCR signals by resting cells overnight in culture medium. This result is also in apparent contradiction to the results of Park *et al.* However, IL7R levels are downregulated by IL7 and the IL7R levels in $CD8^+$ T cells from HY male, HY female and B6 mice as reported by Park *et*

[1]Personal communication from Megan Palmer of the Lauffenburger lab

al may also be affected by differences in the levels of IL7 in these mice, arising from possible variations in the total numbers of total $CD8^+$ T cells, as discussed above. IL7R has a broad pattern of expression on polyclonal $CD8^+$ T cells. It is speculated that it reflects localized 'altruistic' downregulation of IL7R in response to extrinsic levels of IL7, particularly in close proximity to cytokine-rich areas around the sites of IL7 production [78]. However, our results suggest that the intrinsic heterogeneity in IL7R levels among $CD8^+$ T cells could also contribute to the variation in IL7R levels in vivo. Unlike other gamma-chain cytokine receptors, IL7R is under tight transcriptional control by way of an inhibitory feedback loop, and the cell type and stage-specific regulation of IL7R is thought to ensure optimal utilization of limited cytokine stores. Furthermore, such negative feedback control of IL7R transcription, in response to spatially heterogeneous IL7 levels, is believed to maximize the size of the T cell population in the presence of limiting amounts of IL7. This hypothesis is based on the observation that enforced expression of IL7R in DN cells results in a paradoxical decrease in the number of DN cells believed to be due the depletion of the ligand in the thymus, where IL7 is produced by the thymic stromal and epithelial cells in very limited amounts [87]. Similar results are seen with enforced expression of IL7R in mature cells, resulting a decrease in the size of the mature T cell pool. However, enforced expression of IL7R by a transgene is not quantitatively equivalent to the lack of an 'altruistic' feedback transcriptional inhibition loop. In particular, enforced transgenic expression of IL7R by a strong promoter like hu-CD2 is very likely to result in significantly higher 'baseline' levels of IL7R compared to IL7R transcribed solely off the native gene. Instead, an IL7R transgene construct that drives IL7R expression with an IL7R promoter which is insensitive to IL7-mediated feedback inhibition would be necessary to make the case for 'altruistic' regulation of IL7R. Therefore, reduced cell numbers in IL7R transgenic mice may be more simply explained by greater IL7R-mediated consumption of IL7 as originally proposed by Munitic et al [87] rather than the lack of putatively 'altruistic' IL7-mediated feedback inhibition of IL7R transcription.

7.6 Transcriptional networks that underlie differential imprinting

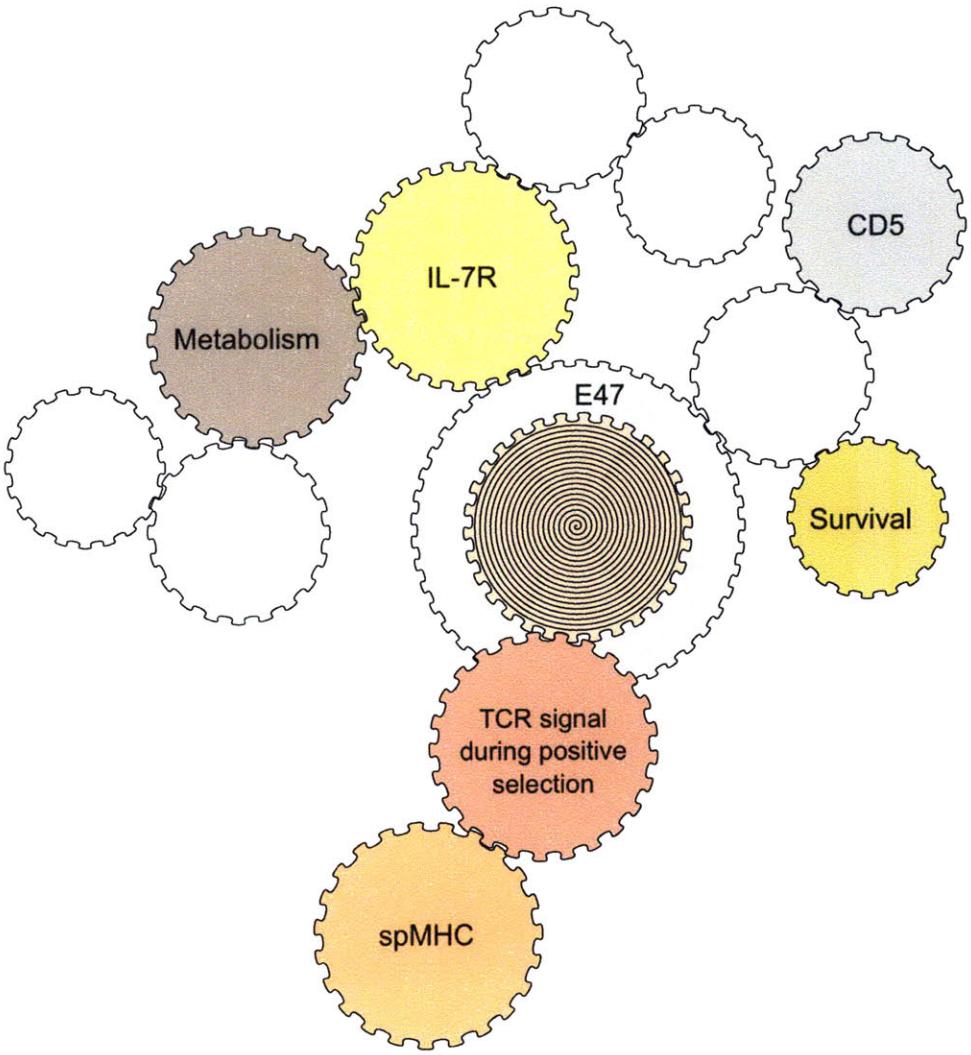

Figure 7-1: **Upstream master regulatory networks.** The intrinsic differences in survival and proliferation capacities as well as CD5 levels among T cells are ultimately linked to the TCR, likely through various intermediary regulators. Microarray analysis suggests that transcription factors of the E2A and IRF family and miRNAs of the miR-181 family may determine these functional differences. It is likely that this master regulatory network is differentially imprinted during thymic development itself, when these factors are first expressed in T cells.

The whole genome expression profiles of OT-1 and F5 cells were analyzed for

upstream regulatory transcription factors (see Figure 7-1). Transcription factors like E47, E2F and IRF are predicted to underlie the differential expression patterns in these cells. E47 was of particular interest as it inihibits the transcription of CD5 [138] and was also validated independently using cDNA array data from previous studies with E47-deficient and over-expressing T cell lymphoma lines [109]. E47 is known to be critical for regulating T cell development and is therefore a likely candidate for being a part of the transcription network that regulates these intrinsic differences in T cell signaling networks. Our analysis also suggests that the targets of miR-181 family of miRNAs are significantly enriched in OT-1 cells. As miRNAs can regulate both mRNA translation [91] and stability [141], differential expression of a miRNA can affect the transcription profiles of its target mRNAs. This suggests that miR-181 is functionally over-expressed in F5 cells. This is particularly interesting as miR-181a is an intrinsic modulator of T cell sensitivity and selection [67], and it increases sensitivity of the TCR to antigen. This further supports the possibility that there are intrinsic differences in the TCR cascade in F5 T cells and that changes in T cell signaling networks that are initiated in the thymus persist in the periphery. Given our observation that F5 cells are weakly selected and are imprinted with lower levels of CD5, it is possible that miR-181a is developmentally imprinted in a manner analogous to CD5, such that it increases the range of the selected TCR repertoire.

Lineage determining transcription networks (T vs. B, Myeloid vs. Lymphoid, CD4 vs. CD8, Th1 vs. Th2) tend to have network motifs comprising of cross-inhibiting loops and self-amplifying positive feedback loops resulting in bistable behavior and differentiation into one of two lineages. However, it is interesting to speculate on the likely features of a putative transcriptional network that regulates subtle differences within a particular lineage, like we have described. However, a majority of epigenetic changes that have been investigated so far focus on all-or-none type of regulation. This is especially true of DNA methylation. One would anticipate 'tunable' marks of both heterochromatin and euchromatin associated with such a network. Epigenetic encoding of a seemingly continuous or graded response may possibly emerge from discrete epigenetic regulation of multiple genes encoding the regulatory nodes of the

underlying signaling networks. The study of regulatory nodes in $CD8^+$ T cell signaling networks could provide a model system to study such phenomena. Another possibility could be that systematic epigenetic regulation of enhancer regions rather than the core promoters themselves could allow for a certain baseline activity that is stably but subtly modified.

7.7 Competition-diversity paradox

It has often been stated that T cells compete for spMHC. Given that this process involves a diverse repertoire of T cells competing for access to their cognate self-peptides within a diverse repertoire of spMHC, this statement merits further clarification. For reasons that I have laid out in detail in sections 2.3 and 2.4, T cells with TCRs of different specificities are unlikely to compete for the same cognate spMHC unless their specificities are closely related. Surprisingly, adoptive transfer experiments using T cells from different TCR transgenic mice suggest that T cells of dramatically different specificities do compete for access to 'homeostatic' factors in a hierarchal manner that is closely correlated with their CD5 levels [33]. For instance, OT-1 cells proliferate upon transfer into 2C mice, but 2C cells do not proliferate when transferred into OT-1 mice. This demonstration of seemingly hierarchical interclonal competition between T cells of different specificities for spMHC has remained a puzzling result without a satisfying mechanistic explanation. However, in light of the new findings of this thesis, we present an alternate interpretation of the result. We have identified that the amount of IL7 varies in different TCR transgenic mice and is inversely correlated with the total number of T cells in the TCR transgenic animals (OT-1 > 2C > F5). Thus, what seemed like hierarchical competition may be, more simply, a consequence of differences in the IL7 availability between different TCR transgenic mice.

Variable rates of LIP among T cells with different TCRs have been attributed to their variable strengths of interaction with spMHC. If T cells had different spMHC-dependent survival signals in the physiological steady state, it would raise the problem of 'competition-diversity paradox' (see Section 2.7). While clonal loss due to the trade-

off between diversity and the competition for spMHC or IL7 has been proposed, it hasn't been tested in practice. Knowing that the relative CD5 level acts as a lineage marker for a heterogeneous population of $CD8^+$ T cells, we could address this question by tracking CD5 profiles of polyclonal $CD8^+$ T cells upon transfer into congenic lymphoreplete mice and found that they were steadily maintained. This study also suggests that proximal spMHC-induced TCR signals in the periphery may not be very different even among T cells bearing TCRs that were selected with dramatically different strengths in the thymus, possibly due to the compensatory effects of 'TCR tuning' by differential imprinting of regulatory molecules such as CD5 and CD6, which may together act as a 'rheostat' for the TCR cascade, giving an equal opportunity to all T cells to receive a spMHC-based survival signal, regardless of the specificity of their TCRs. However, this merely shifts the focus of the competition-diversity paradox to the heterogeneous intrinsic responsiveness to IL7 among $CD8^+$ T cells.

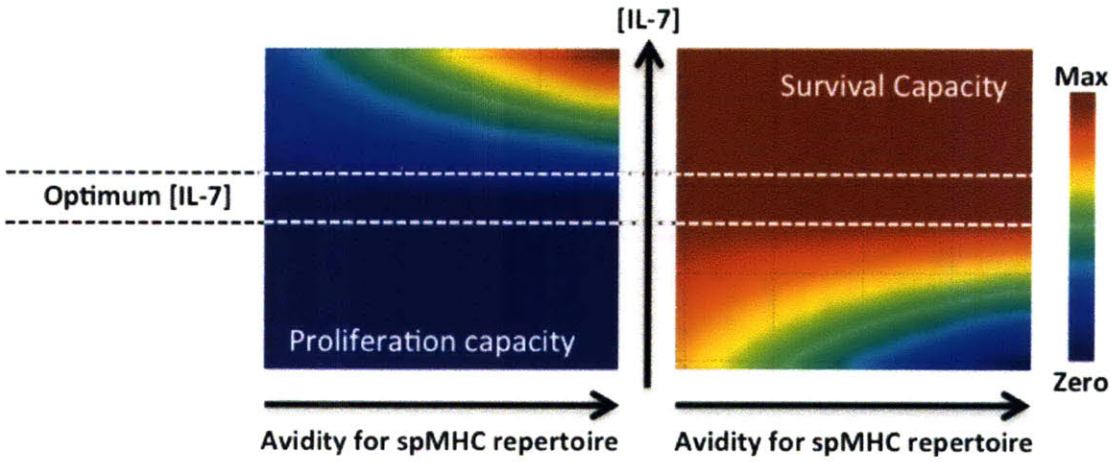

Figure 7-2: **Optimal level of IL7 to maintain diversity.** These heatmaps represent the proliferation and survival capacities of the naïve $CD8^+$ repertoire in response to IL7. Skewed responses to IL7 occur at both high and low levels of IL7 and the physiological level of IL7 likely corresponds to an 'optimum' at which all the T cells respond equally to IL7, regardless of their CD5 levels or strength of selection.

Our in vitro studies show that T cells have different baseline levels of IL7R and that a stronger IL7 signal is transduced in $CD5^{hi}$ than in $CD5^{lo}$ cells even at the same dose of IL7. Thus, based on the 'competition-diversity' argument, one would expect that $CD5^{hi}$ cells would dominate the repertoire due to their better ability to

signal in response to IL7. However, $CD5^{lo}$ cells have a greater capacity to survive under conditions of IL7 deprivation, both in vitro as well as in vivo. Furthermore, it is believed that the levels of IL7 are 'limiting', which restricts the population of T cells. But if they were limiting enough to result in preferential survival of $CD5^{lo}$ cells, the 'competition-diversity argument' would suggest the repertoire would be gradually skewed towards $CD5^{lo}$ cells. This may suggest that the physiological level of IL7 is at an 'optimum' where the IL7-induced survival and proliferation responses of T cells are equal irrespective of their CD5 levels (see Figure 7-2). Indeed, our estimate of the level of IL7 in vivo using a bioassay based on the ability of IL7 to cause downregulation of IL7R supports this possibility and offers an explanation why the 'competition-diversity parodox' is avoided despite intrinsic differences in IL7 responsiveness among $CD8^+$ T cells. Exogenous IL7 therapy is being intensively investigated as a potential immunotherapy [66]. We have shown that IL7 therapy could result in the skewing of the repertoire towards a $CD5^{hi}$ phenotype. Conversely, reduction in the levels of IL7 with depleting antibodies caused skewing of the repertoire towards the $CD5^{lo}$ phenotype. The functional consequences of such qualitative shifts in the T cell repertoire in response to modulating IL7 levels away from the physiological optimum remain to be investigated. Preliminary results suggest that such effects may also be seen with $CD4^+$ cells as well but further characterization is necessary.

7.8 Future directions

This thesis presents evidence for intrinsic but subtle differences in the TCR and IL7 signaling networks among naïve $CD8^+$ T cells. These differences are likely differentially imprinted during development and are marked by the levels of CD5 and possibly CD6. The identification of a lineage marker for this functional intrinsic heterogeneity will make it possible to track T cells during development or activation-induced differentiation and it provides a model system to look for putative non-genetic mechanisms that have the potential to robustly imprint subtle differences in gene expression in contrast to the commonly studied 'all-or-none' type of epigenetic regulatory mecha-

nisms.

Our microarray analysis is consistent with the possibility that $CD8^+$ T cells in the periphery are differentially wired and points to possible underlying regulatory mechanisms. Identifying the key network nodes that are different will require systematic network perturbation of key regulatory nodes, combined with high-throughput signaling analysis. In the absence of such analysis, in this study, we have used the 'baseline' expression profiles of these signaling mediators as a surrogate measure for the intrinsic differences. However, the complete withdrawal of extrinsic signals may itself be a cell-specific extrinsic signal that may elicit a cell-type specific response in these two cells. This is especially a concern for T cells that rapidly execute a specific cell death pathway upon growth factor withdrawal. This would make the estimation of the true 'baseline' state of all the nodes of the TCR signaling network hard to assess in these cell types using our simplified approach. Therefore, an accurate description of the differences in intrinsic parameters of a signaling network can perhaps only be achieved through systematic perturbation of key signaling network nodes. New multiplex technologies have made such an approach feasible and it could yield novel insights into understanding how central tolerance is achieved by differential imprinting of signaling networks.

Our analysis of the microarray profiles in naïve OT-1 and F5 cells predicts the role of an underlying regulatory network involving transcription factors of the E2A family, as well as miRNAs of the miR-181 family. Direct validation of these predictions will be necessary to elucidate the contribution of these factors to the underlying intrinsic differences. Development of a mouse model that allows inducible knockdown of CD5 or other negative mediators of the TCR pathway could be a better approach to studying the interaction of naïve T cells with their cognate spMHC as this will would increase the sensitivity of detection. A number of differentially expressed genes have been identified using two well-defined populations of naïve $CD8^+$ T cells from two different TCR transgenic mice of defined specificities. It will be interesting to see if these differences can are also seen with polyclonal $CD5^{hi}$ and $CD5^{lo}$ cells as this will allow further validation of the microarray data and also help confirm the predictions

from the analysis of upstream regulatory factors.

Given the increasing interest in IL7 and anti-IL7 based therapies, further investigation of the intrinsic differences in the signaling networks in $CD8^+$ T cells will help us understand the clinical impact of skewing the T cell repertoire toward a $CD5^{hi}$ or $CD5^{lo}$ phenotype while modulating the IL7 levels. Such studies will also help elucidate how the developmental tuning of T cell signaling networks may be critical for the homeostasis of T cell diversity as well as the avoidance of autoimmunity.

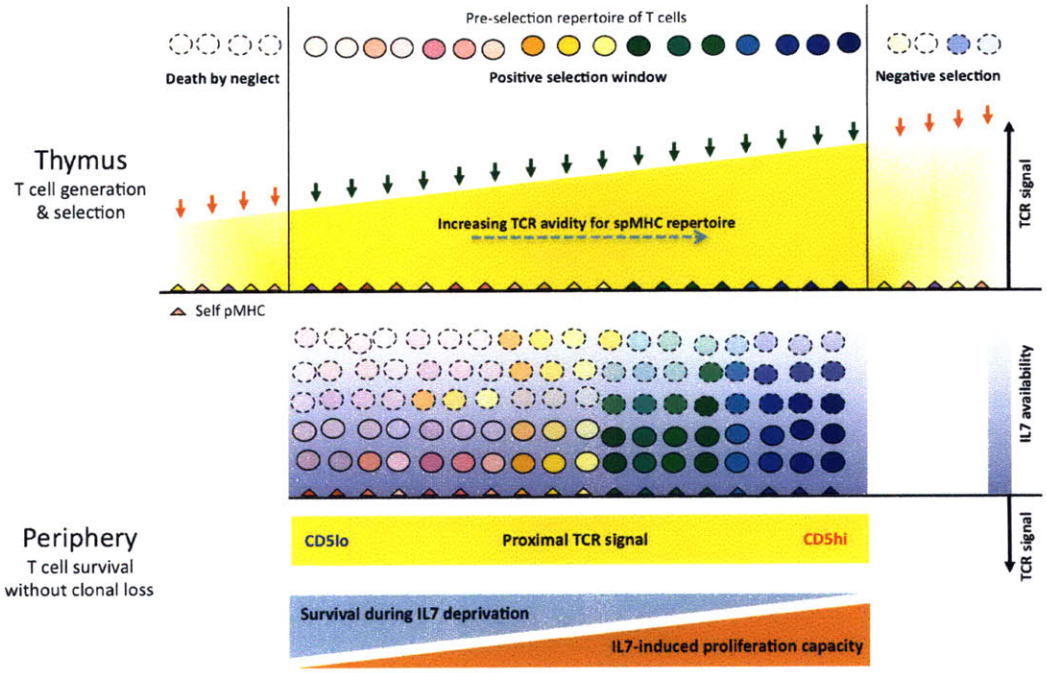

Figure 7-3: **Updated model for the homeostasis of T cell diversity.** This thesis presents an updated model for the homeostasis of T cell diversity. A broad range of TCRs with a wide range of avidities for spMHC is selected in the thymus. This is made possible by the developmental upregulation of CD5, a negative regulator of TCR signaling, in the thymus which parallels TCR avidity for spMHC. The induction in CD5 level is imprinted and thus, cells selected with a strong signal in the thymus differentiate into $CD5^{hi}$ cells and T cells that are weakly selected in the thymus differentiate into $CD5^{lo}$ cells. The $CD8^{+}$ T cells have correlated intrinsic functional differences in their TCR and IL7 signaling networks, which are marked by 'baseline' CD5 levels. $CD5^{hi}$ cells also have a greater capacity for proliferation *at supra-physiological doses* of IL7 but a lower capacity for survival under conditions of IL7 depletion. T cells bearing TCRs with different avidities for their cognate spMHC within the same spMHC background receive broadly equivalent proximal TCR signals from spMHC in the periphery, possibly because of differential imprinting of T cell signaling networks. Thus, at physiological levels of IL7 and spMHC, the homeostasis of T cell diversity is maintained due to the absence of T cells that have a selective advantage in access to or signaling in response to either IL7 or spMHC.

Appendix A

Experimental procedures

A.1 Mice

C57BL/6 (B6) mice and congenic mice expressing the CD90.1/Thy1.1 allele (B6.PL-Thy1a/Cy) were obtained from the Jackson laboratory. OT-1, 2C and F5 TCR transgenic mice were backcrossed on to the B6.RAG1$^{-/-}$ background for over twenty generations. The mice were maintained at the MIT animal facilities and used according to the guidelines of the Institutional Committee on Animal Care. All mice used were between 6-20 weeks of age unless otherwise indicated.

A.2 Generation of Dendritic cells

BMDCs were generated as described by Inaba *et al* [49] with minor modifications. Briefly, bone marrow was isolated from the tibias and femurs of B6, β_2m$^{-/-}$ or TAP$^{-/-}$ mice, filtered through a 70 μm nylon mesh, and resuspended in complete medium with conditioned media from J5 cells, which secrete GMCSF. Aliqouts of 1×10^6 cells were plated into 24-well plates (Beckton Dickinson) and two-thirds of the medium was replaced on day 3 and 6. The non-adherent cells were harvested on day 8, and CD11c$^+$ cells were enriched using anti-CD11c magnetic meads (Miltenyi MACS) to $> 95\%$ purity. To prepare splenic dendritic cells, 2×10^6 B16 melanoma cells, which were transduced with a GMCSF expression vector, were injected s.c. into B6 or β_2m$^{-/-}$

mice. Ten days later, dendritic cells were isolated from the spleens using anti-CD11c magnetic beads to > 95% purity [34].

A.3 Cell proliferation assays

Cells were labeled with 5 μM carboxy-fluorescein succinimidyl ester (CFSE) in serum free RPMI for 5 minutes at 37 °C and washed twice with RPMI containing 10 % FBS. Cell proliferation was measured by flow cytometry at least 24 hrs after CFSE labeling. FlowJo software (v8.8.4) was used for cell proliferation analysis.

A.4 Calcium flux analysis by epifluorescence microscopy

2×10^5 T cells were incubated for 20 min at 37 °C with 1 μM Fura 2-AM ester (Molecular Probes). After washing twice, they were mixed with an equal number of DCs and resuspended in 250 μL of RPMI imaging medium and loaded onto a 6-well Lab-Tek chambered coverglass slide. T cells and DCs were rapidly brought into contact at the bottom of the slide by a brief spin for two minutes and immediately placed in an environment chamber with circulating humidified air containing 5 % CO_2 at 37 °C. Epifluorescence images (560 nm emission) were recorded at 340 and 380 nm excitation every 15 seconds using an inverted epifluorescence microscope (Zeiss) and a Xenon arc illumination source at 400 × magnification for upto 60 minutes. In a dense co-culture like this, dendritic cells and T cells are highly migratory and move in all three dimensions. Therefore, data was recorded in 4 horizontal planes encompassing 20 μm in the z-axis . The 340 and 380 nm excitation images for each timepoint were projected into the xy-plane and ratiometric analysis was performed using Metamorph software. Finally, Volocity software (Improvision) was used for deconvolution and cell-tracking, yielding time-series of cytosolic calcium measurements in individual T cells.

A.5 Antibodies and flow cytometry

Fluorescent marker-conjugated antibodies against murine CD5 (53-7.3), CD8α (53-6.7), CD4 (L3T4), CD44 (IM7), Thy1.1 (OX-7), Thy1.2 (53-2.1), IL-7Rα (A7R34), Vα2 (B20.1), Vβ5 (MR9-4) and CD45.1 (A20) were obtained from BD Biosciences or eBioscience. Briefly, titrated amount of antibody was incubated with the 10^4 to 10^6 cells in PBS containing 0.5% BSA and 0.1% NaN_3 and washed twice before flow cytometry analysis on a BD FACSCalibur or LSRII. Cell survival was assayed using flow cytometry by measuring propidium iodide dye exclusion. For BrdU incorporation studies, mice were injected with 100 µg of BrdU i.p., and and BrdU staining was performed in cells isolated from the lymphoid organs after 48 hrs using a BrdU Flow kit (BD Biosciences). Glucose uptake was measured using a fluoresecent glucoase analog, 2-(N-(7-nitrobenz-2-oxa-1,3-diazol-4-yl)amino)-2-deoxyglucose (NBDG), from Invitrogen. Cells were incubated in glucose-free medium containing 100 µM NBDG for 1 hr at 37 °C and washed 3 × with ice-cold FACS buffer just prior to analysis by flow cytometry.

A.6 Microarray expression profiling

Single cell suspensions were prepared from the lymph nodes of female OT-1 $Rag^{-/-}$ or F5 $Rag^{-/-}$ mice at 6-8 wks of age. $CD44^{hi}$ cells were depleted by MACS (Miltenyi) using CD44-biotin antibody and streptavidin-coated magnetic beads according to manufacturer's instructions. A small number of cells were saved to confirm purity by FACS. Extraction of total RNA was performed using Qiagen RNeasy Mini kit according to manufacturer's instructions. The fraction of naïve $CD8^+$ $CD44^{lo}$ cells was greater than 95% in all samples. The quality of RNA was assessed using agarose gel electrophoresis (Agilent Bioanalyzer) and samples with RNA degradation were excluded. Unlike OT-1 mice, the RNA yield from none of F5 mice was sufficient to run one gene chip, necessating the pooling for RNA from multiple mice. As we expected the differences in the gene expression profiles between naïve OT-1 and F5 T cells to

be very subtle, we relied solely upon technical replicates to calculate statistical significance of the data and RNA from 5 OT-1 and 8 F5 mice was pooled for expression profiling in three technical replicates for each cell type. Standard Affymetrix protocols detailed in the 'Genechip Expression Analysis Technical Manual' was followed at the MIT BioMicro Center for all labeling, fragmentation, hybridization and scanning. Briefly, biotinylated cRNA was prepared according to the standard Affymetrix protocol from 6 μg total RNA. Following fragmentation, 10 μg of cRNA were hybridized for 16 hr at 45 °C on the Affymetrix Array, washed and stained in the Affymetrix Fluidics Station 450. GeneChips were scanned using the Affymetrix Genechip Scanner 7G. GCOS v1.4 Software was used for quality checking and initial data extraction, with Affymetrix default parameters.

A.7 Generation of bone marrow chimeras

Bone marrow was obtained from the femurs and tibias of OT-1 and F5 donor mice and filtered through a SI70μm mesh. The cells were resuspended in HBSS, mixed in a 1:1 ratio and 5×10^6 cells were injected i.v. into 6-8 wk old recipient B6.Rag$^{-/-}$ mice irradiated with 600 Rads. B6 mice were injected with 100 μg anti-NK1.1 antibody 24 hrs prior to irradiation (1000 Rads) and reconstitution with bone marrow from TAP$^{-/-}$ mice.

A.8 Implantation of drug-release pumps

The mice were anesthetized in a veterinary anesthesia flow chamber with 2.5 % isoflurane and 0.5 Lpm O_2. Prior to implantation, the miniosmotic pumps were filled with 100 μL of PBS containing a total of 5 ng of IL7. Using aseptic techniques, a 0.5 mm midscapular incision was made and a blunt hemostat was used to create a 2 cm long subcutaneous pocket over the right flank for the implantation of a miniosmotic pump with a hemostat. The pumps were gently slid into the flank and the incision was closed with upto two wound clips. Betadine antiseptic was applied on the incision

site and the wound site was monitored daily in the animals.

A.9 Preprocessing of Data

The probe intensities were calculated from .CEL files using MAS5.0 normalization. Significant gene expression was was assessed using Student's t-test. The raw microarray data as well as processed data is available at the NCBI GEO database.

A.10 Functional analysis using GO terms

GO terms are hierarchically organized groups of genes in three categories: biological process, cellular compartment or molecular function. Over- or under-representation of GO classification groups in the differentially expressed subset of genes for all the categories was analyzed using the Biobase Explain 4.1 platform. Briefly, two p-values are computed for each set of hits or matches to a GO category group: an over-representation p-value, p(+), and an under-representation p-value, p(−), assuming a hyper-geometric distribution as follows, and a Benjamini-Hochberg correction is applied to control the false-discovery rate [137].

$$k_{max} = min(n, D); \qquad k_{min} = max(0, n - (N - D))$$

$$p(+) = \sum_{i=k}^{k_{max}} \frac{\binom{N}{n}}{\binom{N-D}{n-i}}; \qquad p(-) = \sum_{i=k_{min}}^{k} \frac{\binom{N}{n}}{\binom{N-D}{n-i}}$$

where

N = number of genes linked to any group of the chosen GO category

D = number of genes in the given group of the GO category

n = size of the input list

k = number of genes that matched a gene in the group of the category

A.11 F-match

The F-Match algorithm compares the number of sites found in a query sequence set against the background set[1]. It is assumed, if a certain TF (or factor family) plays a significant role in the regulation of the considered set of promoters, then the frequency of the corresponding sites found in these sequences should be significantly higher than expected by random chance. F-Match evaluates the set of promoters, and for each matrix, tries to find two thresholds: (i) th_{max}, which provides maximum ratio between the frequency of matches in the promoters in focus (main set) and background promoters (background set) (over-represented sites); and (ii) th_{min}, that minimizes the same ratio (under-represented sites) . As a result, for each weight matrix, a set of predicted K sites and M sites in the both promoter sets with the corresponding matrix scores are obtained. The F-Match algorithm makes an exhaustive search through the space of all scores observed in the sequence sets. Each observed score is taken as a threshold th and the program computes the number of sites k found in the main promoter set and number of sites m found in the background promoter set. Then, the expected number of sites in the main set to be observed in the case of even distribution of sites between two sets will be:

$$k_{exp} = n.f, \qquad n = k + m, \qquad f = \frac{|main\,set|}{|main\,set| + |background\,set|}$$

and assuming a binomial distribution of the sites between two sets, we can calculate the p-value of finding the observed number of sites and higher, for over-represented matches, or lower, in the case of under-represented matches

$$\text{if } k \geq k_{exp}, \quad \text{p-value}(+) = \sum_{i=k}^{n} C_i^n.f^i.(i-f)^{(n-i)}$$

$$\text{if } k < k_{exp}, \quad \text{p-value}(-) = \sum_{i=1}^{k} C_i^n.f^i.(i-f)^{(n-i)}$$

giving the p-value of over- and under-representation of matches in the main pro-

[1]The F-match methods section is reproduced from Biobase Explain v4.1 documentation

moter set. For a given significance level p (e.g. p = 0.001), F-Match finds such thresholds th-max and th-min that maximizes and minimizes, respectively, the ratio k/k_{exp} provided that the p-value < p. If the required significance level cannot be reached for a given matrix, this matrix will not be considered.

A.12 Gene Set Enrichment Analysis

Gene Set Enrichment Analysis was performed using the Desktop software tool [118]. All the genes with probe intensity ranks > 50^{th} percentile in both OT-1 and F5 cells, i.e. a total of 10588 genes, were ranked using a signal-to-noise ratio (SNR) as defined below and used for GSEA analysis with the following parameters. Given the small number of classes, 1000 permutations of gene sets were performed to estimate the statistical significance.

$$\text{Signal-to-Noise Ratio (SNR)} = \frac{\mu_{\text{OT-1}} - \mu_{\text{F5}}}{\sigma_{\text{OT-1}} + \sigma_{\text{F5}}}$$

```
producer_class xtools.gsea.Gsea
param collapse true
param cls /Users/vinay/GSEA/OT1F5.cls#OT1+_versus_F5+
param plot_top_x 20
param norm meandiv
param save_rnd_lists false
param median false
param num 100
param scoring_scheme weighted
param make_sets true
param mode Max_probe
param gui false
param chip gseaftp.broad.mit.edu://pub/gsea/annotations/Mouse430_2.chip
```

```
param metric Signal2Noise
param help false
param order descending
param out /Users/vinay/GSEA/results
param permute gene_set
param rnd_type no_balance
param set_min 15
param include_only_symbols true
param sort real
param rnd_seed timestamp
param nperm 1000
param zip_report true
param set_max 500
```

Bibliography

[1] A N Akbar, N J Borthwick, R G Wickremasinghe, P Panayoitidis, D Pilling, M Bofill, S Krajewski, J C Reed, and M Salmon. Interleukin-2 receptor common gamma-chain signaling cytokines regulate activated T cell apoptosis in response to growth factor withdrawal: selective induction of anti-apoptotic (bcl-2, bcl-xL) but not pro-apoptotic (bax, bcl-xS) gene expression. *Eur J Immunol*, 26(2):294–299, Feb 1996.

[2] Irina Apostolou, Adelaida Sarukhan, Ludger Klein, and Harald von Boehmer. Origin of regulatory T cells with known specificity for antigen. *Nat Immunol*, 3(8):756–763, Aug 2002.

[3] Monica Arman, Javier Calvo, Maria E Trojanowska, Peter N Cockerill, Monica Santana, Manuel Lopez-Cabrera, Jordi Vives, and Francisco Lozano. Transcriptional regulation of human CD5: important role of Ets transcription factors in CD5 expression in T cells. *J Immunol*, 172(12):7519–7529, Jun 2004.

[4] T. P. Arstila, A. Casrouge, V. Baron, J. Even, J. Kanellopoulos, and P. Kourilsky. A direct estimate of the human alphabeta T cell receptor diversity. *Science*, 286(5441):958 – 961, 1999.

[5] H Asnagli, A M Schmitt-Verhulst, and A Guimezanes. Class I- and class II-reactive TCRs coexpressed on CD4+ T cells both trigger CD4/CD8-shared and CD4-unique functions. *J Immunol*, 158(10):4533–4542, May 1997.

[6] H S Azzam, J B DeJarnette, K Huang, R Emmons, C S Park, C L Sommers, D El-Khoury, E W Shores, and P E Love. Fine tuning of TCR signaling by CD5. *J Immunol*, 166(9):5464–5472, May 2001.

[7] H S Azzam, A Grinberg, K Lui, H Shen, E W Shores, and P E Love. CD5 expression is developmentally regulated by T cell receptor (TCR) signals and TCR avidity. *J Exp Med*, 188(12):2301–2311, Dec 1998.

[8] T Barthlott, R J Wright, and B Stockinger. Normal thymic selection of TCR transgenic CD4 T cells, but impaired survival in the periphery despite the presence of selecting MHC molecules. *J Immunol*, 161(8):3992–3999, Oct 1998.

[9] J. Bender, T. Mitchell, J. Kappler, and P. Marrack. CD4+ T cell division in irradiated mice requires peptides distinct from those responsible for thymic selection. *J Exp Med*, 190(3):367 – 374, 1999.

[10] Estelle Bettelli, Maria Pagany, Howard L Weiner, Christopher Linington, Raymond A Sobel, and Vijay K Kuchroo. Myelin oligodendrocyte glycoprotein-specific T cell receptor transgenic mice develop spontaneous autoimmune optic neuritis. *J Exp Med*, 197(9):1073–1081, May 2003.

[11] Joseph N Blattman, Rustom Antia, David J D Sourdive, Xiaochi Wang, Susan M Kaech, Kaja Murali-Krishna, John D Altman, and Rafi Ahmed. Estimating the precursor frequency of naive antigen-specific CD8 T cells. *J Exp Med*, 195(5):657–664, Mar 2002.

[12] P Bongrand and B Malissen. Quantitative aspects of T-cell recognition: from within the antigen-presenting cell to within the T cell. *Bioessays*, 20(5):412–422, May 1998.

[13] Cedric Brossard, Monique Semichon, Alain Trautmann, and Georges Bismuth. CD5 inhibits signaling at the immunological synapse without impairing its formation. *J Immunol*, 170(9):4623–4629, May 2003.

[14] Matilde Canelles, Melissa L Park, Owen M Schwartz, and B J Fowlkes. The influence of the thymic environment on the CD4-versus-CD8 T lineage decision. *Nat Immunol*, 4(8):756–764, Aug 2003.

[15] D S Chekmenev, C Haid, and A E Kel. P-Match: transcription factor binding site search by combining patterns and weight matrices. *Nucleic Acids Res*, 33(Web Server issue):W432–7, Jul 2005.

[16] Tian H Chi, Mimi Wan, Keji Zhao, Ichiro Taniuchi, Lei Chen, Dan R Littman, and Gerald R Crabtree. Reciprocal regulation of CD4/CD8 expression by SWI/SNF-like BAF complexes. *Nature*, 418(6894):195–199, Jul 2002.

[17] Jerry E Chipuk and Douglas R Green. How do BCL-2 proteins induce mitochondrial outer membrane permeabilization? *Trends Cell Biol*, 18(4):157–164, Apr 2008.

[18] B. K. Cho, V. P. Rao, Q. Ge, H. N. Eisen, and J. Chen. Homeostasis-stimulated proliferation drives naive T cells to differentiate directly into memory T cells. *J Exp Med*, 192(4):549 – 556, 2000.

[19] Claire Conche, Genevieve Boulla, Alain Trautmann, and Clotilde Randriamampita. T cell adhesion primes antigen receptor-induced calcium responses through a transient rise in adenosine 3',5'-cyclic monophosphate. *Immunity*, 30(1):33–43, Jan 2009.

[20] T A Cordaro, K E de Visser, F H Tirion, Y M Graus, J B Haanen, D Kioussis, and A M Kruisbeek. Tumor size at the time of adoptive transfer determines whether tumor rejection occurs. *Eur J Immunol*, 30(5):1297–1307, May 2000.

[21] Z Dai and F G Lakkis. Cutting edge: Secondary lymphoid organs are essential for maintaining the CD4, but not CD8, naive T cell pool. *J Immunol*, 167(12):6711–6715, Dec 2001.

[22] M M Davis and P J Bjorkman. T-cell antigen receptor genes and T-cell recognition. *Nature*, 334(6181):395–402, Aug 1988.

[23] R J De Boer and A S Perelson. T cell repertoires and competitive exclusion. *J Theor Biol*, 169(4):375–390, Aug 1994.

[24] J Delon, N Bercovici, G Raposo, R Liblau, and A Trautmann. Antigen-dependent and -independent Ca2+ responses triggered in T cells by dendritic cells compared with B cells. *J Exp Med*, 188(8):1473–1484, Oct 1998.

[25] P C Doherty, J M Riberdy, and G T Belz. Quantitative analysis of the CD8+ T-cell response to readily eliminated and persistent viruses. *Philos Trans R Soc Lond B Biol Sci*, 355(1400):1093–1101, Aug 2000.

[26] Michael B Elowitz, Arnold J Levine, Eric D Siggia, and Peter S Swain. Stochastic gene expression in a single cell. *Science*, 297(5584):1183–1186, Aug 2002.

[27] V H Engelhard. Structure of peptides associated with class I and class II MHC molecules. *Annu Rev Immunol*, 12:181–207, 1994.

[28] B. Ernst, D. S. Lee, J. M. Chang, J. Sprent, and C. D. Surh. The peptide ligands mediating positive selection in the thymus control T cell survival and homeostatic proliferation in the periphery. *Immunity*, 11(2):173 – 181, 1999.

[29] Vincent Feuillet, Bruno Lucas, James P Di Santo, Georges Bismuth, and Alain Trautmann. Multiple survival signals are delivered by dendritic cells to naive CD4+ T cells. *Eur J Immunol*, 35(9):2563–2572, Sep 2005.

[30] A A Freitas and B Rocha. Population biology of lymphocytes: the flight for survival. *Annu Rev Immunol*, 18:83–111, 2000.

[31] Antonio Freitas and Jianzhu Chen. Introduction: regulation of lymphocyte homeostasis. *Microbes Infect*, 4(5):529–530, Apr 2002.

[32] Kristine M Garza, Kim J McKall-Faienza, Tashiaki Otheki, Arsen Zakarian, Bernhard Odermatt, and Pamela S Ohashi. Enhanced T cell responses contribute to the genetic predisposition of CD8-mediated spontaneous autoimmunity. *Eur J Immunol*, 32(3):885–894, Mar 2002.

[33] Q. Ge, A. Bai, B. Jones, H. N. Eisen, and J. Chen. Competition for self-peptide-MHC complexes and cytokines between naive and memory CD8+ T cells expressing the same or different T cell receptors. *Proc. Natl. Acad. Sci. USA*, 101(9):3041 – 3046, 2004.

[34] Q. Ge, H. Hu, H. N. Eisen, and J. Chen. Different contributions of thymopoiesis and homeostasis-driven proliferation to the reconstitution of naive and memory T cell compartments. *Proc. Natl. Acad. Sci. USA*, 99(5):2989 – 2994, 2002.

[35] Qing Ge, Phillip D Holler, Vinay S Mahajan, Tam Nuygen, Herman N Eisen, and Jianzhu Chen. Development of CD4+ T cells expressing a nominally MHC class I-restricted T cell receptor by two different mechanisms. *Proc Natl Acad Sci U S A*, 103(6):1822–1827, 2006.

[36] Qing Ge, Hui Hu, Herman N Eisen, and Jianzhu Chen. Naive to memory T-cell differentiation during homeostasis-driven proliferation. *Microbes Infect*, 4(5):555–558, Apr 2002.

[37] Idoia Gimferrer, Montse Farnos, Maria Calvo, Maria Mittelbrunn, Carlos Enrich, Francisco Sanchez-Madrid, Jordi Vives, and Francisco Lozano. The accessory molecules CD5 and CD6 associate on the membrane of lymphoid T cells. *J Biol Chem*, 278(10):8564–8571, Mar 2003.

[38] A. W. Goldrath, C. J. Luckey, R. Park, C. Benoist, and D. Mathis. The molecular program induced in T cells undergoing homeostatic proliferation. *Proc. Natl. Acad. Sci. USA*, 101(48):16885 – 16890, 2004.

[39] A. W. Goldrath, P. V. Sivakumar, M. Glaccum, M. K. Kennedy, M. J. Bevan, C. Benoist, D. Mathis, and E. A. Butz. Cytokine requirements for acute and Basal homeostatic proliferation of naive and memory CD8+ T cells. *J Exp Med*, 195(12):1515 – 1522, 2002.

[40] K H Grabstein, J Eisenman, K Shanebeck, C Rauch, S Srinivasan, V Fung, C Beers, J Richardson, M A Schoenborn, and M Ahdieh. Cloning of a T cell growth factor that interacts with the beta chain of the interleukin-2 receptor. *Science*, 264(5161):965–968, May 1994.

[41] A Grakoui, S K Bromley, C Sumen, M M Davis, A S Shaw, P M Allen, and M L Dustin. The immunological synapse: a molecular machine controlling T cell activation. *Science*, 285(5425):221–227, Jul 1999.

[42] J M Grayson, A J Zajac, J D Altman, and R Ahmed. Cutting edge: increased expression of Bcl-2 in antigen-specific memory CD8+ T cells. *J Immunol*, 164(8):3950–3954, Apr 2000.

[43] Zvi Grossman, Booki Min, Martin Meier-Schellersheim, and William E Paul. Concomitant regulation of T-cell activation and homeostasis. *Nat Rev Immunol*, 4(5):387–395, May 2004.

[44] J B Gurdon. A community effect in animal development. *Nature*, 336(6201):772–774, Dec 1988.

[45] J B Gurdon, P Lemaire, and K Kato. Community effects and related phenomena in development. *Cell*, 75(5):831–834, Dec 1993.

[46] Namir J Hassan, Stephen J Simmonds, Nicholas G Clarkson, Sarah Hanrahan, Michael J Puklavec, Martine Bomb, A Neil Barclay, and Marion H Brown. CD6 regulates T-cell responses through activation-dependent recruitment of the positive regulator SLP-76. *Mol Cell Biol*, 26(17):6727–6738, Sep 2006.

[47] Jason Hataye, James J Moon, Alexander Khoruts, Cavan Reilly, and Marc K Jenkins. Naive and memory CD4+ T cell survival controlled by clonal abundance. *Science*, 312(5770):114–116, Apr 2006.

[48] Xin He, Charles A Jr Janeway, Matthew Levine, Eve Robinson, Paula Preston-Hurlburt, Christophe Viret, and Kim Bottomly. Dual receptor T cells extend the immune repertoire for foreign antigens. *Nat Immunol*, 3(2):127–134, Feb 2002.

[49] K Inaba, M Inaba, N Romani, H Aya, M Deguchi, S Ikehara, S Muramatsu, and R M Steinman. Generation of large numbers of dendritic cells from mouse bone marrow cultures supplemented with granulocyte/macrophage colony-stimulating factor. *J Exp Med*, 176(6):1693–1702, Dec 1992.

[50] Darrell J Irvine, Marco A Purbhoo, Michelle Krogsgaard, and Mark M Davis. Direct observation of ligand recognition by T cells. *Nature*, 419(6909):845–849, Oct 2002.

[51] D E Isaksen, H Baumann, P A Trobridge, A G Farr, S D Levin, and S F Ziegler. Requirement for stat5 in thymic stromal lymphopoietin-mediated signal transduction. *J Immunol*, 163(11):5971–5977, Dec 1999.

[52] T. S. Jardetzky, W. S. Lane, R. A. Robinson, D. R. Madden, and D. C. Wiley. Identification of self peptides bound to purified HLA-B27. *Nature*, 353(6342):326 – 329, 1991.

[53] Qiong Jiang, Wen Qing Li, Francesca B Aiello, Renata Mazzucchelli, Benyam Asefa, Annette R Khaled, and Scott K Durum. Cell biology of IL-7, a key lymphotrophin. *Cytokine Growth Factor Rev*, 16(4-5):513–533, Aug-Oct 2005.

[54] Paul Jorgensen and Mike Tyers. How cells coordinate growth and division. *Curr Biol*, 14(23):R1014–27, Dec 2004.

[55] Henry Kao and Paul M Allen. An antagonist peptide mediates positive selection and CD4 lineage commitment of MHC class II-restricted T cells in the absence of CD4. *J Exp Med*, 201(1):149–158, Jan 2005.

[56] D Karolchik, R Baertsch, M Diekhans, T S Furey, A Hinrichs, Y T Lu, K M Roskin, M Schwartz, C W Sugnet, D J Thomas, R J Weber, D Haussler, and W J Kent. The UCSC Genome Browser Database. *Nucleic Acids Res*, 31(1):51–54, Jan 2003.

[57] George Kassiotis, Sylvie Garcia, Elizabeth Simpson, and Brigitta Stockinger. Impairment of immunological memory in the absence of MHC despite survival of memory T cells. *Nat Immunol*, 3(3):244–250, Mar 2002.

[58] G J Kersh, D L Donermeyer, K E Frederick, J M White, B L Hsu, and P M Allen. TCR transgenic mice in which usage of transgenic alpha- and beta-chains is highly dependent on the level of selecting ligand. *J Immunol*, 161(2):585–593, Jul 1998.

[59] Annette R Khaled and Scott K Durum. Lymphocide: cytokines and the control of lymphoid homeostasis. *Nat Rev Immunol*, 2(11):817–830, Nov 2002.

[60] W. C. Kieper, J. T. Burghardt, and C. D. Surh. A role for TCR affinity in regulating naive T cell homeostasis. *J Immunol*, 172(1):40 – 44, 2004.

[61] J Kirberg, A Baron, S Jakob, A Rolink, K Karjalainen, and H von Boehmer. Thymic selection of CD8+ single positive cells with a class II major histocompatibility complex-restricted receptor. *J Exp Med*, 180(1):25–34, Jul 1994.

[62] J. Kirberg, A. Berns, and H. von Boehmer. Peripheral T cell survival requires continual ligation of the T cell receptor to major histocompatibility complex-encoded molecules. *J Exp Med*, 186(8):1269 – 1275, 1997.

[63] J O Koopmann, G J Hammerling, and F Momburg. Generation, intracellular transport and loading of peptides associated with MHC class I molecules. *Curr Opin Immunol*, 9(1):80–88, Feb 1997.

[64] Qibin Leng, Qing Ge, Tam Nguyen, Herman N Eisen, and Jianzhu Chen. Stage-dependent reactivity of thymocytes to self-peptide–MHC complexes. *Proc Natl Acad Sci U S A*, 104(12):5038–5043, Mar 2007.

[65] W J Leonard. Cytokines and immunodeficiency diseases. *Nat Rev Immunol*, 1(3):200–208, Dec 2001.

[66] Yves Levy, Christine Lacabaratz, Laurence Weiss, Jean-Paul Viard, Cecile Goujard, Jean-Daniel Lelievre, Francois Boue, Jean-Michel Molina, Christine Rouzioux, Veronique Avettand-Fenoel, Therese Croughs, Stephanie Beq, Rodolphe Thiebaut, Genevieve Chene, Michel Morre, and Jean-Francois Delfraissy. Enhanced T cell recovery in HIV-1-infected adults through IL-7 treatment. *J Clin Invest*, 119(4):997–1007, Apr 2009.

[67] Qi-Jing Li, Jacqueline Chau, Peter J R Ebert, Giselle Sylvester, Hyeyoung Min, Gwen Liu, Ravi Braich, Muthiah Manoharan, Juergen Soutschek, Petra Skare, Lawrence O Klein, Mark M Davis, and Chang-Zheng Chen. miR-181a is an intrinsic modulator of T cell sensitivity and selection. *Cell*, 129(1):147–161, Apr 2007.

[68] J Lin and A Weiss. T cell receptor signalling. *J Cell Sci*, 114(Pt 2):243–244, Jan 2001.

[69] Alexander Link, Tobias K Vogt, Stephanie Favre, Mirjam R Britschgi, Hans Acha-Orbea, Boris Hinz, Jason G Cyster, and Sanjiv A Luther. Fibroblastic reticular cells in lymph nodes regulate the homeostasis of naive T cells. *Nat Immunol*, 8(11):1255–1265, Nov 2007.

[70] Yong-Jun Liu, Vasilli Soumelis, Norihiko Watanabe, Tomoki Ito, Yui-Hsi Wang, Rene de Waal Malefyt, Miyuki Omori, Baohua Zhou, and Steven F Ziegler. TSLP: an epithelial cell cytokine that regulates T cell differentiation by conditioning dendritic cell maturation. *Annu Rev Immunol*, 25:193–219, 2007.

[71] P E Love, J Lee, and E W Shores. Critical relationship between TCR signaling potential and TCR affinity during thymocyte selection. *J Immunol*, 165(6):3080–3087, Sep 2000.

[72] F Lozano, M Simarro, J Calvo, J M Vila, O Padilla, M A Bowen, and K S Campbell. CD5 signal transduction: positive or negative modulation of antigen receptor signaling. *Crit Rev Immunol*, 20(4):347–358, 2000.

[73] Julian J Lum, Daniel E Bauer, Mei Kong, Marian H Harris, Chi Li, Tullia Lindsten, and Craig B Thompson. Growth factor regulation of autophagy and cell survival in the absence of apoptosis. *Cell*, 120(2):237–248, Jan 2005.

[74] Vinay S Mahajan, Ilya B Leskov, and Jian Zhu Chen. Homeostasis of T cell diversity. *Cell Mol Immunol*, 2(1):1–10, 2005.

[75] E O Matechak, N Killeen, S M Hedrick, and B J Fowlkes. MHC class II-specific T cells can develop in the CD8 lineage when CD4 is absent. *Immunity*, 4(4):337–347, Apr 1996.

[76] V Matys, O V Kel-Margoulis, E Fricke, I Liebich, S Land, A Barre-Dirrie, I Reuter, D Chekmenev, M Krull, K Hornischer, N Voss, P Stegmaier, B Lewicki-Potapov, H Saxel, A E Kel, and E Wingender. TRANSFAC and its module TRANSCompel: transcriptional gene regulation in eukaryotes. *Nucleic Acids Res*, 34(Database issue):D108–10, Jan 2006.

[77] M M Maurice, D S Gould, J Carroll, Y Vugmeyster, and H L Ploegh. Positive selection of an MHC class-I restricted TCR in the absence of classical MHC class I molecules. *Proc Natl Acad Sci U S A*, 98(13):7437–7442, Jun 2001.

[78] Renata Mazzucchelli and Scott K Durum. Interleukin-7 receptor expression: intelligent design. *Nat Rev Immunol*, 7(2):144–154, Feb 2007.

[79] Maureen A McGargill, Dita Mayerova, Heather E Stefanski, Brent Koehn, Evan A Parke, Stephen C Jameson, Angela Panoskaltsis-Mortari, and Kristin A Hogquist. A spontaneous CD8 T cell-dependent autoimmune disease to an antigen expressed under the human keratin 14 promoter. *J Immunol*, 169(4):2141–2147, Aug 2002.

[80] M B Miller and B L Bassler. Quorum sensing in bacteria. *Annu Rev Microbiol*, 55:165–199, 2001.

[81] Booki Min, Rebecca McHugh, Gregory D Sempowski, Crystal Mackall, Gilles Foucras, and William E Paul. Neonates support lymphopenia-induced proliferation. *Immunity*, 18(1):131–140, Jan 2003.

[82] Booki Min, Hidehiro Yamane, Jane Hu-Li, and William E Paul. Spontaneous and homeostatic proliferation of CD4 T cells are regulated by different mechanisms. *J Immunol*, 174(10):6039–6044, 2005 May 15.

[83] C R Monks, B A Freiberg, H Kupfer, N Sciaky, and A Kupfer. Three-dimensional segregation of supramolecular activation clusters in T cells. *Nature*, 395(6697):82–86, Sep 1998.

[84] James J Moon, H Hamlet Chu, Marion Pepper, Stephen J McSorley, Stephen C Jameson, Ross M Kedl, and Marc K Jenkins. Naive CD4(+) T cell frequency varies for different epitopes and predicts repertoire diversity and response magnitude. *Immunity*, 27(2):203–213, Aug 2007.

[85] David J Morgan, C Thomas Nugent, Benjamin J E Raveney, and Linda A Sherman. In a transgenic model of spontaneous autoimmune diabetes, expression of a protective class II MHC molecule results in thymic deletion of diabetogenic CD8+ T cells. *J Immunol*, 172(2):1000–1008, Jan 2004.

[86] D Moskophidis and D Kioussis. Contribution of virus-specific CD8+ cytotoxic T cells to virus clearance or pathologic manifestations of influenza virus infection in a T cell receptor transgenic mouse model. *J Exp Med*, 188(2):223–232, Jul 1998.

[87] Ivana Munitic, Joy A Williams, Yili Yang, Bei Dong, Philip J Lucas, Nahed El Kassar, Ronald E Gress, and Jonathan D Ashwell. Dynamic regulation of IL-7 receptor expression is required for normal thymopoiesis. *Blood*, 104(13):4165–4172, Dec 2004.

[88] K Murali-Krishna, L L Lau, S Sambhara, F Lemonnier, J Altman, and R Ahmed. Persistence of memory CD8 T cells in MHC class I-deficient mice. *Science*, 286(5443):1377–1381, Nov 1999.

[89] Janko Nikolich-Zugich, Mark K Slifka, and Ilhem Messaoudi. The many important facets of T-cell repertoire diversity. *Nat Rev Immunol*, 4(2):123–132, Feb 2004.

[90] Joshua J Obar, Kamal M Khanna, and Leo Lefrancois. Endogenous naive CD8+ T cell precursor frequency regulates primary and memory responses to infection. *Immunity*, 28(6):859–869, Jun 2008.

[91] P H Olsen and V Ambros. The lin-4 regulatory RNA controls developmental timing in Caenorhabditis elegans by blocking LIN-14 protein synthesis after the initiation of translation. *Dev Biol*, 216(2):671–680, Dec 1999.

[92] Megan J Palmer, Vinay S Mahajan, Lily C Trajman, Darrell J Irvine, Douglas A Lauffenburger, and Jianzhu Chen. Interleukin-7 receptor signaling network: an integrated systems perspective. *Cell Mol Immunol*, 5(2):79–89, 2008.

[93] J.-H. Park, Q. Yu, B. Erman, J. S. Appelbaum, D. Montoya-Durango, H. L. Grimes, and A. Singer. Suppression of IL7Ralpha transcription by IL-7 and other prosurvival cytokines: a novel mechanism for maximizing IL-7-dependent T cell survival. *Immunity*, (2):289 – 302.

[94] Jung-Hyun Park, Stanley Adoro, Philip J Lucas, Sophia D Sarafova, Amala S Alag, Loretta L Doan, Batu Erman, Xiaolong Liu, Wilfried Ellmeier, Remy Bosselut, Lionel Feigenbaum, and Alfred Singer. 'Coreceptor tuning': cytokine signals transcriptionally tailor CD8 coreceptor expression to the self-specificity of the TCR. *Nat Immunol*, 8(10):1049–1059, Oct 2007.

[95] J J Peschon, P J Morrissey, K H Grabstein, F J Ramsdell, E Maraskovsky, B C Gliniak, L S Park, S F Ziegler, D E Williams, C B Ware, J D Meyer, and B L Davison. Early lymphocyte expansion is severely impaired in interleukin 7 receptor-deficient mice. *J Exp Med*, 180(5):1955–1960, Nov 1994.

[96] Ciriaco A Piccirillo and Angela M Thornton. Cornerstone of peripheral tolerance: naturally occurring CD4+CD25+ regulatory T cells. *Trends Immunol*, 25(7):374–380, Jul 2004.

[97] Ashok Prasad, Julie Zikherman, Jayajit Das, Jeroen P Roose, Arthur Weiss, and Arup K Chakraborty. Origin of the sharp boundary that discriminates positive and negative selection of thymocytes. *Proc Natl Acad Sci U S A*, 106(2):528–533, Jan 2009.

[98] Heather H Pua, Ivan Dzhagalov, Mariana Chuck, Noboru Mizushima, and You-Wen He. A critical role for the autophagy gene Atg5 in T cell survival and proliferation. *J Exp Med*, 204(1):25–31, Jan 2007.

[99] Heather H Pua, Jian Guo, Masaaki Komatsu, and You-Wen He. Autophagy is essential for mitochondrial clearance in mature T lymphocytes. *J Immunol*, 182(7):4046–4055, Apr 2009.

[100] Heather H Pua and You-Wen He. Maintaining T lymphocyte homeostasis: another duty of autophagy. *Autophagy*, 3(3):266–267, May-Jun 2007.

[101] Sonia Quaratino, Ester Badami, Yun Yun Pang, Istvan Bartok, Julian Dyson, Dimitris Kioussis, Marco Londei, and Luigi Maiuri. Degenerate self-reactive human T-cell receptor causes spontaneous autoimmune disease in mice. *Nat Med*, 10(9):920–926, Sep 2004.

[102] H G Rammensee, K Falk, and O Rotzschke. Peptides naturally presented by MHC class I molecules. *Annu Rev Immunol*, 11:213–244, 1993.

[103] J C Rathmell, E A Farkash, W Gao, and C B Thompson. IL-7 enhances the survival and maintains the size of naive T cells. *J Immunol*, 167(12):6869–6876, Dec 2001.

[104] P A Reche, V Soumelis, D M Gorman, T Clifford, M Travis, S M Zurawski, J Johnston, Y J Liu, H Spits, R de Waal Malefyt, R A Kastelein, and J F Bazan. Human thymic stromal lymphopoietin preferentially stimulates myeloid cells. *J Immunol*, 167(1):336–343, Jul 2001.

[105] J B Reiser, C Darnault, A Guimezanes, C Gregoire, T Mosser, A M Schmitt-Verhulst, J C Fontecilla-Camps, B Malissen, D Housset, and G Mazza. Crystal structure of a T cell receptor bound to an allogeneic MHC molecule. *Nat Immunol*, 1(4):291–297, Oct 2000.

[106] P Revy, M Sospedra, B Barbour, and A Trautmann. Functional antigen-independent synapses formed between T cells and dendritic cells. *Nat Immunol*, 2(10):925–931, Oct 2001.

[107] Fabio R Santori, William C Kieper, Stuart M Brown, Yun Lu, Thomas A Neubert, Kenneth L Johnson, Stephen Naylor, Stanislav Vukmanovic, Kristin A Hogquist, and Stephen C Jameson. Rare, structurally homologous self-peptides promote thymocyte positive selection. *Immunity*, 17(2):131–142, Aug 2002.

[108] T Sasada and E L Reinherz. A critical role for CD2 in both thymic selection events and mature T cell function. *J Immunol*, 166(4):2394–2403, Feb 2001.

[109] Ruth Schwartz, Isaac Engel, Mohammad Fallahi-Sichani, Howard T Petrie, and Cornelis Murre. Gene expression patterns define novel roles for E47 in cell cycle progression, cytokine-mediated signaling, and T lineage development. *Proc Natl Acad Sci U S A*, 103(26):9976–9981, Jun 2006.

[110] B. Seddon, P. Tomlinson, and R. Zamoyska. Interleukin 7 and T cell receptor signals regulate homeostasis of CD4 memory cells. *Nat Immunol*, 4(7):680 – 686, 2003.

[111] Z Shen, G Reznikoff, G Dranoff, and K L Rock. Cloned dendritic cells can present exogenous antigens on both MHC class I and class II molecules. *J Immunol*, 158(6):2723–2730, Mar 1997.

[112] Nora G Singer, David A Fox, Tariq M Haqqi, Laura Beretta, Judith S Endres, Susan Prohaska, Jane R Parnes, Jonathan Bromberg, and R Michael Sramkoski. CD6: expression during development, apoptosis and selection of human and mouse thymocytes. *Int Immunol*, 14(6):585–597, Jun 2002.

[113] K Smith, B Seddon, M A Purbhoo, R Zamoyska, A G Fisher, and M Merkenschlager. Sensory adaptation in naive peripheral CD4 T cells. *J Exp Med*, 194(9):1253–1261, Nov 2001.

[114] SL Spencer, S Gaudet, JG Albeck, JM Burke, and PK Sorger. Non-genetic origins of cell-to-cell variability in TRAIL-induced apoptosis. *Nature*, Apr 2009.

[115] Jonathan Sprent and Charles D Surh. Cytokines and T cell homeostasis. *Immunol Lett*, 85(2):145–149, Jan 2003.

[116] Irena Stefanova, Jeffrey R Dorfman, and Ronald N Germain. Self-recognition promotes the foreign antigen sensitivity of naive T lymphocytes. *Nature*, 420(6914):429–434, Nov 2002.

[117] Robin Stephens, Frank R Albano, Stuart Quin, Benjamin J Pascal, Vicky Harrison, Brigitta Stockinger, Dimitris Kioussis, Hans-Ulrich Weltzien, and Jean Langhorne. Malaria-specific transgenic CD4(+) T cells protect immunodeficient mice from lethal infection and demonstrate requirement for a protective threshold of antibody production for parasite clearance. *Blood*, 106(5):1676–1684, Sep 2005.

[118] Aravind Subramanian, Heidi Kuehn, Joshua Gould, Pablo Tamayo, and Jill P Mesirov. GSEA-P: a desktop application for Gene Set Enrichment Analysis. *Bioinformatics*, 23(23):3251–3253, Dec 2007.

[119] C D Surh, D S Lee, W P Fung-Leung, L Karlsson, and J Sprent. Thymic selection by a single MHC/peptide ligand produces a semidiverse repertoire of CD4+ T cells. *Immunity*, 7(2):209–219, Aug 1997.

[120] Charles D Surh and Jonathan Sprent. Homeostasis of naive and memory T cells. *Immunity*, 29(6):848–862, Dec 2008.

[121] Peter S Swain, Michael B Elowitz, and Eric D Siggia. Intrinsic and extrinsic contributions to stochasticity in gene expression. *Proc Natl Acad Sci U S A*, 99(20):12795–12800, Oct 2002.

[122] S Takeda, H R Rodewald, H Arakawa, H Bluethmann, and T Shimizu. MHC class II molecules are not required for survival of newly generated CD4+ T cells, but affect their long-term life span. *Immunity*, 5(3):217–228, Sep 1996.

[123] J. T. Tan, E. Dudl, E. LeRoy, R. Murray, J. Sprent, K. I. Weinberg, and C. D. Surh. IL-7 is critical for homeostatic proliferation and survival of naive T cells. *Proc. Natl. Acad. Sci. USA*, 98(15):8732 – 8737, 2001.

[124] C Tanchot, F A Lemonnier, B Perarnau, A A Freitas, and B Rocha. Differential requirements for survival and proliferation of CD8 naive or memory T cells. *Science*, 276(5321):2057–2062, Jun 1997.

[125] C Tanchot, M M Rosado, F Agenes, A A Freitas, and B Rocha. Lymphocyte homeostasis. *Semin Immunol*, 9(6):331–337, Dec 1997.

[126] Ichiro Taniuchi, Motomi Osato, Takeshi Egawa, Mary Jean Sunshine, Suk Chul Bae, Toshihisa Komori, Yoshiaki Ito, and Dan R Littman. Differential requirements for Runx proteins in CD4 repression and epigenetic silencing during T lymphocyte development. *Cell*, 111(5):621–633, Nov 2002.

[127] A Tarakhovsky, S B Kanner, J Hombach, J A Ledbetter, W Muller, N Killeen, and K Rajewsky. A role for CD5 in TCR-mediated signal transduction and thymocyte selection. *Science*, 269(5223):535–537, Jul 1995.

[128] Jorge Vera, Rafael Fenutria, Olga Canadas, Maite Figueras, Ruben Mota, Maria-Rosa Sarrias, David L Williams, Cristina Casals, Jose Yelamos, and Francisco Lozano. The CD5 ectodomain interacts with conserved fungal cell wall components and protects from zymosan-induced septic shock-like syndrome. *Proc Natl Acad Sci U S A*, 106(5):1506–1511, Feb 2009.

[129] U von Freeden-Jeffry, P Vieira, L A Lucian, T McNeil, S E Burdach, and R Murray. Lymphopenia in interleukin (IL)-7 gene-deleted mice identifies IL-7 as a nonredundant cytokine. *J Exp Med*, 181(4):1519–1526, Apr 1995.

[130] A Wack, M Coles, T Norton, A Hostert, and D Kioussis. Early onset of CD8 transgene expression inhibits the transition from DN3 to DP thymocytes. *J Immunol*, 165(3):1236–1242, Aug 2000.

[131] T Waldmann, Y Tagaya, and R Bamford. Interleukin-2, interleukin-15, and their receptors. *Int Rev Immunol*, 16(3-4):205–226, 1998.

[132] H Waldner, M J Whitters, R A Sobel, M Collins, and V K Kuchroo. Fulminant spontaneous autoimmunity of the central nervous system in mice transgenic for the myelin proteolipid protein-specific T cell receptor. *Proc Natl Acad Sci U S A*, 97(7):3412–3417, Mar 2000.

[133] Taconic website. http://www.taconic.com/emerging/004094.htm .

[134] Sara Wojciechowski, Pulak Tripathi, Tristan Bourdeau, Luis Acero, H Leighton Grimes, Jonathan D Katz, Fred D Finkelman, and David A Hildeman. Bim/Bcl-2 balance is critical for maintaining naive and memory T cell homeostasis. *J Exp Med*, 204(7):1665–1675, Jul 2007.

[135] P Wong, A W Goldrath, and A Y Rudensky. Competition for specific intrathymic ligands limits positive selection in a TCR transgenic model of CD4+ T cell development. *J Immunol*, 164(12):6252–6259, Jun 2000.

[136] L. E. Wrenshall and J. L. Platt. Regulation of T cell homeostasis by heparan sulfate-bound IL-2. *J Immunol*, 163(7):3793 – 3800, 1999.

[137] Benjamini Y. and Hochberg Y. Controlling the False Discovery Rate: a Practical and Powerful Approach to Multiple Testing. *Journal of the Royal Statistical Society Series B-Methodological*, 57(1):289–300, 1995.

[138] Yang Yang, Christopher H Contag, Dean Felsher, Catherine M Shachaf, Yuan Cao, Leonard A Herzenberg, Leonore A Herzenberg, and James W Tung. The E47 transcription factor negatively regulates CD5 expression during thymocyte development. *Proc Natl Acad Sci U S A*, 101(11):3898–3902, Mar 2004.

[139] Zhengju Yao, Yongzhi Cui, Wendy T Watford, Jay H Bream, Kunihiro Yamaoka, Bruce D Hissong, Denise Li, Scott K Durum, Qiong Jiang, Avinash Bhandoola, Lothar Hennighausen, and John J O'Shea. Stat5a/b are essential for normal lymphoid development and differentiation. *Proc Natl Acad Sci U S A*, 103(4):1000–1005, Jan 2006.

[140] Andrew Yates, Manoj Saini, Anne Mathiot, and Benedict Seddon. Mathematical modeling reveals the biological program regulating lymphopenia-induced proliferation. *J Immunol*, 180(3):1414–1422, Feb 2008.

[141] Soraya Yekta, I-Hung Shih, and David P Bartel. MicroRNA-directed cleavage of HOXB8 mRNA. *Science*, 304(5670):594–596, Apr 2004.

[142] Jonathan W Yewdell, Eric Reits, and Jacques Neefjes. Making sense of mass destruction: quantitating MHC class I antigen presentation. *Nat Rev Immunol*, 3(12):952–961, Dec 2003.

[143] Kyung H Yi, Hovav Nechushtan, William J Bowers, Gail R Walker, Yu Zhang, Dien G Pham, Eckhard R Podack, Howard J Federoff, Khaled A Tolba, and Joseph D Rosenblatt. Adoptively transferred tumor-specific T cells stimulated ex vivo using herpes simplex virus amplicons encoding 4-1BBL persist in the host and show antitumor activity in vivo. *Cancer Res*, 67(20):10027–10037, Oct 2007.